Productivity Evaluation Model of Binder-Jetting Additive Manufacturing Processes

Yuhaowei Zhou

Mechanical Engineering

McGill University, Montreal

June 2015

A thesis submitted to McGill University in partial fulfillment of the requirements of the degree of MSc (Thesis)

Productivity Assessment model of Binder-Jetting Additive Manufacturing Processes

By

Yuhaowei Zhou

Abstract

The interests towards Additive Manufacturing (AM) technologies are rapidly rising due to their great potential in new product design possibilities and the reduction of environmental impacts. Currently AM technologies are largely investigated in automotive, aerospace and medical equipment industries on design, production quality and manufacturability aspects. Due to its inherited layer by layer fabrication process, there is a concern regarding to the manufacturing efficiency of AM processes. However, there is very limited research on productivity of AM, which includes the time consumption, raw material consumption and the production efficiency. This paper presents a simulation method to assess the productivity of AM. Based on this method, a productivity model of Binder-Jetting AM technology is created. Binder-Jetting AM (BJAM) is one of the commercialized AM technologies which can process a variety of materials including stainless steel, ceramic, sand and polymer. Process decomposition is performed to analyze the BJAM printing process. Curing and sintering process as well as manual processing procedure are also included as part of a complete production system of BJAM. Life Cycle Assessment (LCA) model is developed in order to evaluate the whole production process and the production-consumption relation. Experiments are conducted in order to collect data on operation and manipulation time of the machine and actual material consumption. Based on experimental data, an evaluation algorithm has been developed in estimating the time and material consumption as a function of part geometry and process parameters. Several process parameters are taken into account, including the layer thickness, spreading speed, drying time, binder saturation, drying power and curing and sintering profiles. Furthermore, the production efficiency is assessed on adapted Key Performance

Indicator (KPI). Machine Availability, Machine Efficiency, Material Efficiency, Material Consumption Ratio, Waste Ratio and Machine Preparation degree are considered. An estimation of the production time, material consumption as well as the KPIs from the given STL design file and the recommended process parameters is given as the output of the productivity model. Finally, A Case study is performed to validate the BJAM algorithms and productivity model. The result shows that the Productivity Model can provide reliable estimation of the time and material consumption of the BJAM production system.

Thesis supervisor: Prof. Fiona Zhao

Résumé

Les intérêts vers les technologies de fabrication additive (AM) augmentent rapidement en raison de leur grand potentiel dans la flexibilité de conception de produits et la réduction des impacts environnementaux. Actuellement AM technologies sont largement étudiés dans l'aérospatiale, les équipements médicaux et l'industrie automobile sur la conception, la qualité de la production et les aspects de la fabrication. Grâce à sa couche héritée par le processus de fabrication couche, il y a une préoccupation concernant l'efficacité des processus de fabrication AM. Toutefois, il existe très peu de recherches sur la productivité d'AM, qui comprend la consommation de temps, la consommation de matière première et l'efficacité de production. Cet article présente une méthode de simulation pour évaluer la productivité des AM. Sur la base de cette méthode, un modèle de productivité de la technologie de Binder Jetting AM est créé. Binder Jetting AM (BJAM) est l'une des technologies de l'AM commercialisés qui peut traiter une variété de matériaux tels que l'acier inoxydable, de céramique, de sable et de polymère. La décomposition du processus est effectuée pour analyser le processus d'impression de BJAM. Durcissement et le processus de frittage ainsi que la procédure de traitement manuel sont également inclus dans le cadre d'un système de production complet de BJAM. La modèle d'analyse du cycle de vie est développée dans le but d'évaluer le processus de production et la relation production-consommation. Des expériences sont menées afin de recueillir des données sur le fonctionnement et la manipulation du temps de la machine et de la consommation de matériau. D'après les données expérimentales, un algorithme d'évaluation a été mis au point pour estimer le temps et la consommation de matériaux en fonction des paramètres géométriques et une partie traitement. Plusieurs paramètres du procédé sont pris en compte, y compris l'épaisseur de la couche, vitesse de propagation, temps de séchage, la saturation de liant, séchage et le durcissement de la puissance et des profils de frittage. En outre, l'efficacité de la production est évaluée sur Indicateur de performance clé adaptée (KPI). Disponibilité machine, machine efficacité, l'efficience des matériaux, Ratio de consommation Matériel, Ratio des déchets et le degré de machines de préparation sont

considérés. Une estimation du temps de production, la consommation de matières ainsi que les KPI à partir du fichier de conception de STL donné et les paramètres du procédé recommandé est donné que la sortie du modèle de la productivité. Enfin, une étude de cas est effectuée pour valider les algorithmes de BJAM et modèle de productivité. Le résultat montre que le modèle de productivité peut fournir une estimation fiable du temps et la consommation de matériaux du système de production de BJAM.

Directeur de Thèse: Prof. Fiona Zhao

Acknowledgements

I would like to take this opportunity to thanks Prof. Fiona Zhao, my supervisor, for her support and guide for my graduate study. I would also like to acknowledge the generous support for this research by the Additive Design and Manufacturing Lab (ADML) of McGill University.

I would also like to thanks Prof. Xinyu Liu for graciously agreeing to serve as reviewer of my thesis.

Also, I would like to thank Yunlong Tang and Han Chen who gives me advises and suggestion for this research. Thanks for the various discussions we had during the development of this thesis.

Table of Contents

List of Figures

Chapter 1: Research Motivation

Additive Manufacturing (AM) refers to a group of manufacturing technologies which evolved from the Rapid Prototyping (RP) technique. The principle of AM, as the name indicated, is fabricating parts by generating contiguous slices layer by layer. 7 types of AM technologies are currently in application [1]. They are differentiate by how the slices being generated. Some of these AM technologies which have already been commercialized:

Binder-Jetting Additive Manufacturing (BJAM): Using liquid binder to glue powders (metal or glass powders) together and form the desired part. Then the part is cured and sintered to increase the mechanical properties.

Stereo lithography (SLA): Using ultraviolet laser to cure actinic photopolymer liquid and form the desired shape.

Laser Sintering (SLS), Direct Metal Laser Sintering (DMLS) and Selective Laser Melting (SLM): Using laser power to sinter or melt powders (metal, polymer or ceramic powder) and form the desired shape.

Electron Beam Melting (EBM): Using high power electron beam to melt metal powder and form the desired shape.

Fused Deposition Modeling (FDM): Extruding or depositing molten material (wood or polymer) to form the design part.

As an ingenious approach in manufacturing domain, this burgeoning AM technology is gradually coming into commercial production in small scale and customized manufacturing. Compared to traditional manufacturing technologies, AM technologies provide more design freedom for innovative product and have less restrictions [2]. It can fabricate physical parts and objects directly from virtual 3D computer data. More recently, it was developed to be able to produce functional products and thus start to demonstrate significant impact on manufacturing and design. The ability to fabricate part directly from a 3D model gives a larger flexibility to the designer. There will be less concern on the manufacturing processes and fabrication constrains but more concentrations on the part structure and mechanical properties. The simplification of production processes and the less material consumption lead to shorter supply chain and more profit space for manufacturers [3].

Moreover, the potential environmental benefit is also one of the strong mainstays of development for the AM technologies for the next 10 year [4]. Nowadays, sustainability has become a hot issue in the industrial world. The energy shortage, greenhouse gas emission and solid wastes have generate great burden to the environment. According to a report of Schipper [5], manufacturing is response for 90% of energy consumption and 84% of energy-related CO2 emission in the industry sector. AM technologies, from general view, are seen as “cleaner” processes compare to the traditional manufacturing technologies. As aforementioned, in AM, parts are fabricated by creating continuous slices on top of each other. As a result, materials are only used to form products, which means AM technologies can consume the exact amount of material while conventional machining produces waste material. With no removing material, AM helps saving a large sum of material compared to subtractive manufacturing. In addition, the only tool of AM is the machine contrary to conventional machining which using a series of machining tools (for instance such as stamping, turning, milling and drilling) [6]. Hence, AM can reduce the life cycle material mass and energy consumption by eliminating scrap and ancillary process. Another advantage of AM process is, resulting to its’ high concentricity, this characteristic affords possibility of reducing supply chain and in turn reducing the transportation energy consumption [7].

From above, AM enables flexible design, overcomes manufacturing constraints and reduces material and energy consumption. However the technology is still far from maturity for pervasive application. One key issue that prevent the AM from large scale production is the lead time [8]. From general view, AM production, due to its manufacturing principles, cannot be able to conduct process line production. Although some of AM technologies contains several post-printing processes, the green part is manufactured, in general speaking, all in one step. This makes AM have shorter supply chain but meanwhile decreases the availability of the machines in each production which in turn increases the production leading time. The work can no longer be divided but only be done in bulk process. This reduces the production flexibility of the AM.

Another concern rises around the AM part quality. The layer by layer process has potential connection issues entre-layer. The powder based process may lead to rough part surface, loss of mechanical properties and oxidization problems [9]. All these potentials come often into practical productions.

Balancing all these advantages and short comings, an AM production evaluation system is needed. Standardization of the evaluation methods are also critical in AM practical production. According to the roadmap that NIST (National Institute of Standard and Technology) published in 2013 [10], the lacking of comprehensive evaluation systems and technical standards are in high priority of industrializing the AM.

1.1. Objective and Significant of Research

The productivity model is part of AM production evaluation system. It aims at evaluate the production ability of BJAM production system. Although AM technologies have been established in 1980s, they are still quite far from massive production. The technology have been progressively improved during the past 20 years. Different technologies appeared and some of them have already been applied to commercial use in small scale. However without production level standards, AM is still stumbling in front of the gate of industrial level of production.

Productivity refers to varieties of fields. It represents the capability of the production systems. It covers the efficiency, the time consumption, the machine reliability, operating complexity, maintainability, the supply chain and etc. Based on different needs, the productivity will emphasize on different perspectives. Key Performance Indicators (KPI) are often used in industrial practical. Different types of KPIs are developed with different needs. Current AM productions have issues with its long lead time and unstable part quality. So the BJAM productivity model is mainly focusing on the time and material consumption of making of a desired part, and its related KPIs. An effective simulation method is developed to model the time and material consumption of BJAM production. The production parameters serves as input of the system together with STL(STereo-Lithography) file.

This research dedicates to develop algorithm to simulate the production process of BJAM and calculate the time and material consumption as well as some of the KPIs related. The given result on time and material consumption are then used in Life cycle assessment to evaluate the sustainability of the BJAM production system.

The method developed by this research will contribute to the landscape of AM technologies in the following aspects:

1. Developing a layer-by-layer based time and material consumption estimation method for AM technologies. The results then provide information on one hand will give a preview of the productivity of the designed part made by AM technologies. On the other hand, the results are used to build the LCI Model for AM technologies. Furthermore, LCI data can support the LCA or cost analyses. Based on these analyzing works, manufacturer can tell if a product is suitable to AM and which kind of AM technology should be used to fabricate the product.
2. By this method, AM engineers or practitioners are able to predict the production time and materials consumptions to fabricate an AM part before the part is really fabricated. Thus, this method can be used as a tool to evaluate the production and material costs for a specific design. Based on this tool, optimization algorithms can be developed to achieve the optimal part geometry or process parameters and improve the performance of the AM production.

1.2. Scope of Research

The productivity analysis can be conducted on different levels depending on the scope of research. Before conducting the research, the scope and the boundaries of the research should be defined first. According to the research of Duflou et al[11], five different levels can be identified: device/process level, line/cell/multi-machine system, facility, multi-factory system and enterprise/global supply chain. Each one of above analysis levels relies on different assumptions, different input and provides different results. This research focus on the multi-machine system of BJAM.

In this research, three processing systems are considered as the whole production line of Binder Jetting printed parts: printer, curing oven and sintering furnace. Each of the system is analyzed on process basis. Individual process is analyzed separately as sequential connection with no intersection. These individual process is defined as unit process. The connection between each of the three processing systems are included as well, including the part transportation procedure, the manual work effort and the machine preparation, auto-cleaning and setting up time. While the process that goes into the whole production system and out from the system are not considered such as inventory transportation, waste management, machine maintenance, raw material production and transportation, post printing part treatment and etc. Figure 1 shows the boundary of the production system of BJAM model. In the three processing systems are printing, curing and sintering. The systems work sequentially in part manufacturing. The connections between each systems are mainly part transportation, setting up and machine preparation. The printing system is BJAM specialized while curing and sintering are general manufacturing procedures that are the same as the conventional manufacturing only with different profile. Hence, the printing system is divided into three sequential subsystem while the curing and sintering system are profile based analysis.

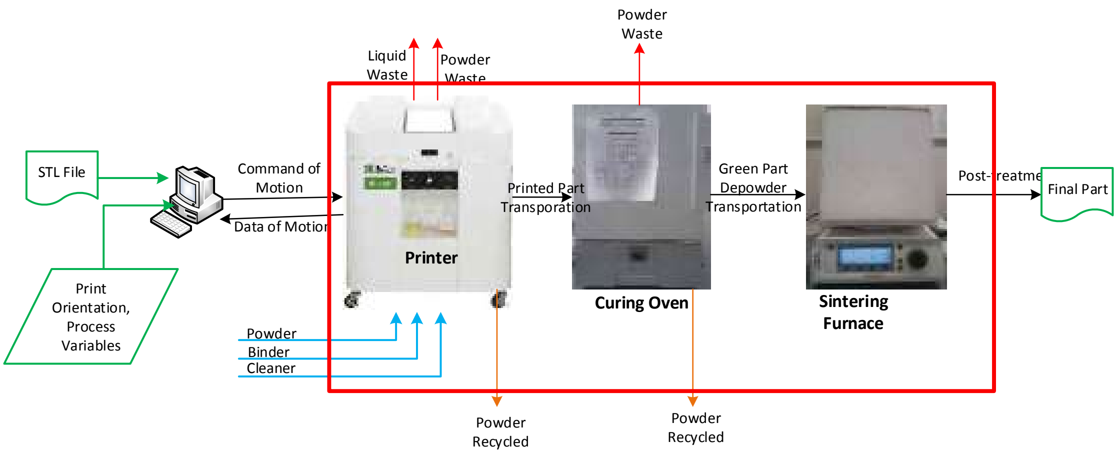

Figure 1: The boundary of BJAM production model

1.3. Outline of Thesis

The rest of the thesis is divided into five chapters. Chapter 2 introduces the framework of the proposed productivity model of AM and the evaluation methods as well as the relevant work. Chapter 3 conducted a research in printed part quality, including the dimensional shrinkage and the part surface roughness. Then, Chapter 4 proposed the time and material consumption algorithm for BJAM production system based on processing parameter recommendation. KPIs are adapted and introduce to the production system too. In Chapter 5, LCA models are introduced the on BJAM production system. The LCA is focus on inventory data and the environmental impact. It is also part of the productivity model of the BJAM system. It is based on the previous result of the time and material consumption. Afterward, Chapter 6 performs a case study that validate the BJAM productivity model and provides several time and material consumption calculation of test cases of BJAM production system. Finally, in Chapter 6, the conclusions of this research are summarized and the scope of future research is presented.

Chapter 2: AM Production System Framework and Research Focus

This research dedicated to develop a simulation model to estimate the production time and the material consumption as well as conducting the LCA studies of BJAM technology as a part of a general AM production evaluation system.

The production evaluation system aims at establishing a mechanism to standardize the evaluation of production capability of the AM technologies. Although it has been more than 20 years since AM technologies existed, it was until recent years that they became accessible in practical production. It is true that AM have significant flexibility in manufacturing, meanwhile, it bears an impression of longer building time and lower production volume. An evaluation mechanism is needed to evaluation the production capability of AM. However, since there are various of AM technologies that are currently in use, there is lack of a unity evaluation system of AM production capabilities.

The following sections will give a brief introduction of the AM production system and state the focus of this research.

2.1. AM Production System Framework

The AM Production System Framework includes all the processes from design to manufacturing. It covers the design phase, the process planning, parameter optimization, the print quality prediction and the production prediction. The quality prediction and the production prediction serves as feedbacks towards the part design and triggers the optimization and modification of the design. The framework forms a close loop back to the design phase.

The inputs to the framework is the design requirement that includes the manufacturing restriction and the part's functional performance. The framework starts from the part design using multi-level design method. The optimization design method leads to a more efficient design. Then the designed parameters are evaluated by the Process Planning Model to decide its AM manufacturing feasibility. If so, the framework suggests the optimized manufacturing parameters and gives out a process plan. If not, a feedback is provided to the designer to instruct modifications. The process plan and manufacturing parameters together with the CAD model will then be passed to the Energy and Material Consumption Model. Estimated consumptions come out as the result. On parallel, the CAD model enters the Production System Model together with the process plan and manufacturing parameters. The Production System Model evaluates the time consumption, the KPIs, the cost of the AM production and other related aspects which will be discussed in the following section. Then the Production System Model gives out a production evaluation of the parts including the possible environmental impacts, the production efficiency, material and time consumption and etc.

The work flow between these four models is defined in IDEF0 diagram in Figure 2. A close loop is formulated to optimize the performance of products and reduce manufacturing cost and time from the design phase to the manufacturing phase. The functions and main principles of each model will be discussed respectively in the following paragraphs.

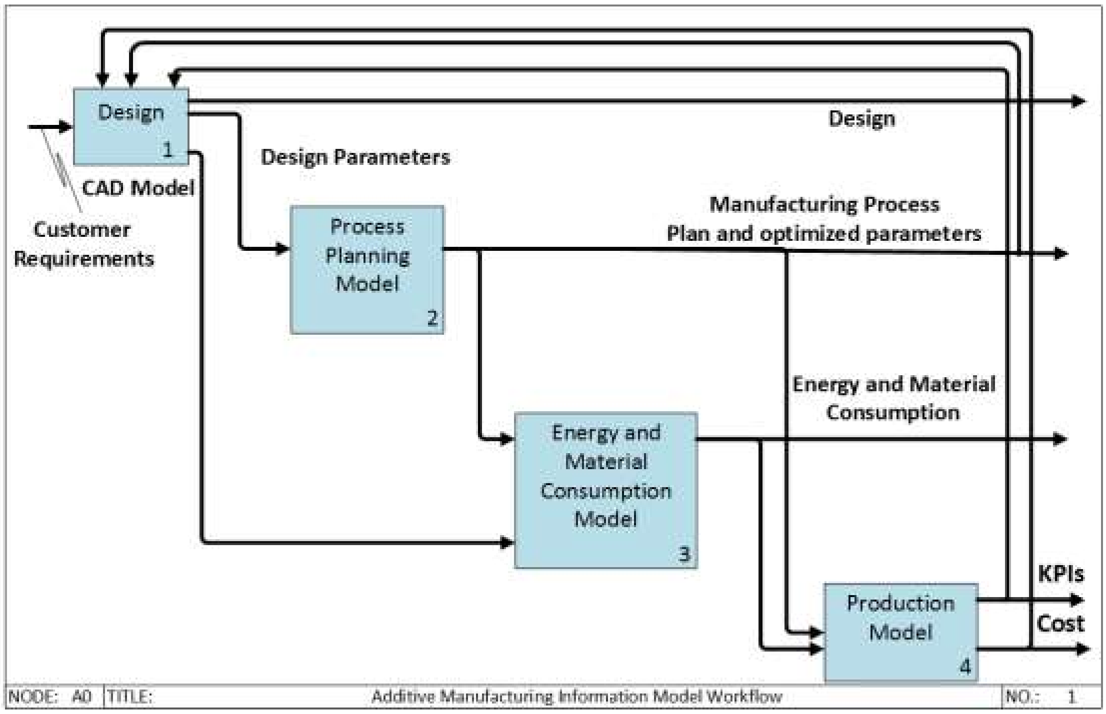

Figure 2:IDEF0 diagram of AM simulation and optimization framework models

2.1.1. Multi-level Design Method

An efficient design method plays a key role to facilitate the wide employment of AM technologies. In the Design Model, the research mainly focuses on design methods to achieve functionality improvement and reduction of assembly in design phase for AM. In the design model, the design methods can be divided into two parts corresponding to different design objectives. The first objective is to improve the performance of the product. In this part, multi-disciplines design optimization method of complex hierarchy structure, or lattice structure is used. The second objective of the design is to reduce assembly. Part consolidation method is used. The two design methods are incorporated in further functional improvement of consolidated parts. In order to integrate multi-level and multi-discipline design methods into single design process, the general design flow is shown in Figure 3.

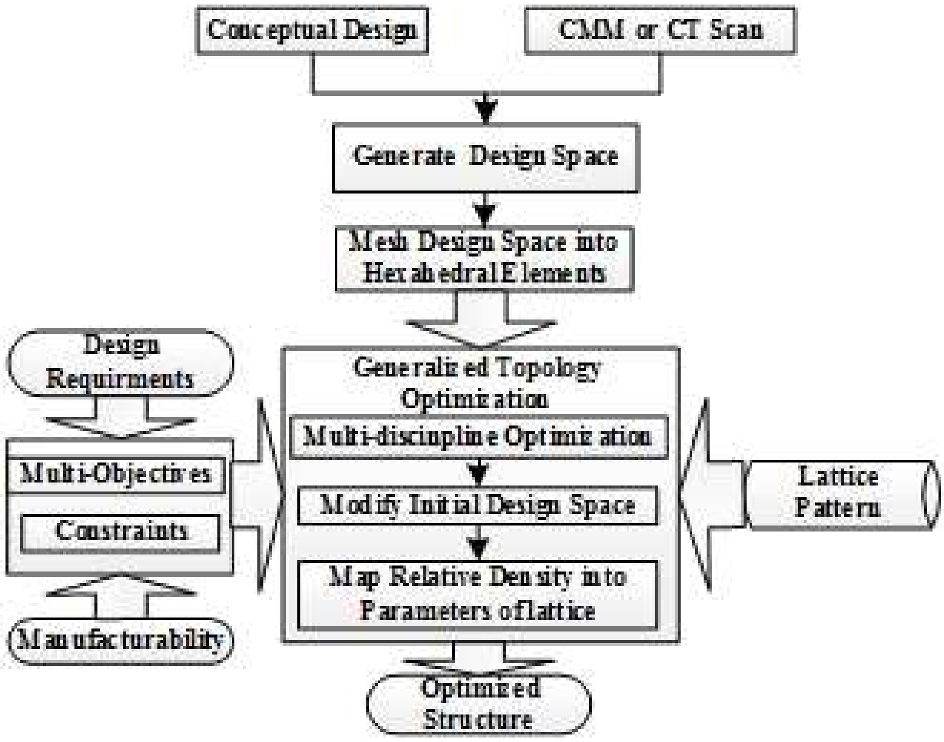

Figure 3: AM Part Design Flow [12]

In this design flow, the initial design space Ω can be generated based on idea from conceptual design or geometry data scanned from existing parts. An automated mesh algorithm is used to divide initial design space into hexahedral elements. These elements can be used for the following generalized topology optimization and lattice structure generation. Meanwhile, the design requirements and manufacturing restriction of certain AM technologies can be converted into multi design objectives and constraints for generalized topology optimization. To solve this generalized topology optimization, Multi-disciplinary Design Optimization (MDO) can be established.

An example of the beam design to support a bearing pedestal is shown in Figure 4. The relative density of each element is regarded as design parameters, and multi-functions in multi-disciplines are regarded as optimization object. Based on homogenization theory, this model can be solved with an optimized relative density distribution as shown Figure 5(a). Figure 5(b) is the result of optimized simply supported beam. The relationship between relative density ρ^* and cross section area s_c of struts in lattice unit cell can be established based on cell's topology which can expressed as:

$$s_c = S_t\ (\rho^*, l) \qquad (1)$$

Where S_t is the mapping function between relative density and cross section area of strut in lattice unit cell; l is the size of unit cell. Based on Equation (1), strut thickness of each lattice cell can be calculated. The elements whose strut's thickness is below manufacturing restriction can be removed, which optimize initial design space in macro level. At the same time, lattice can be generated based on calculated strut thickness and certain topology pattern selected by designers. Thus, the optimized structure in meso-level can be obtained. There are two advantage of this deign method. First, since MDO framework is adopted, design problem for multi-functions in multi-disciplines can be solved. Secondly, an optimization in both meso and macro level can further improvement products' overall performance.

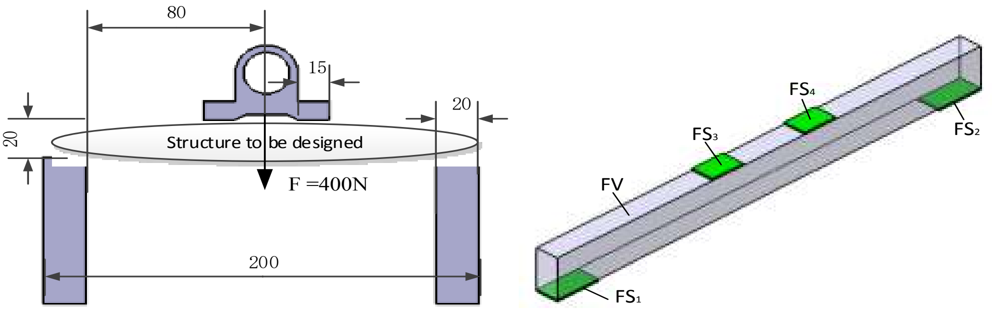

Figure 4: A design example of multi-level design method [13]

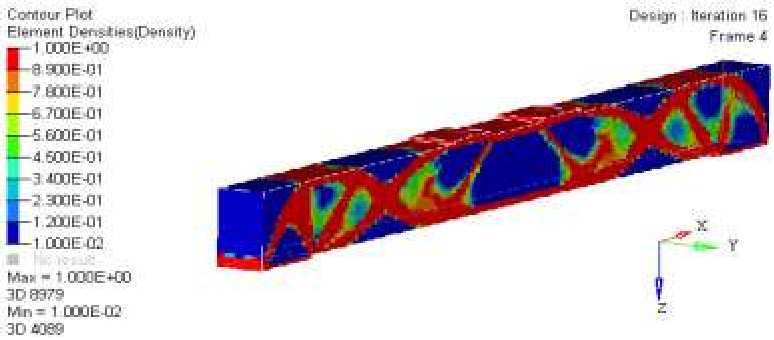

(a). Optimized relative density distribution

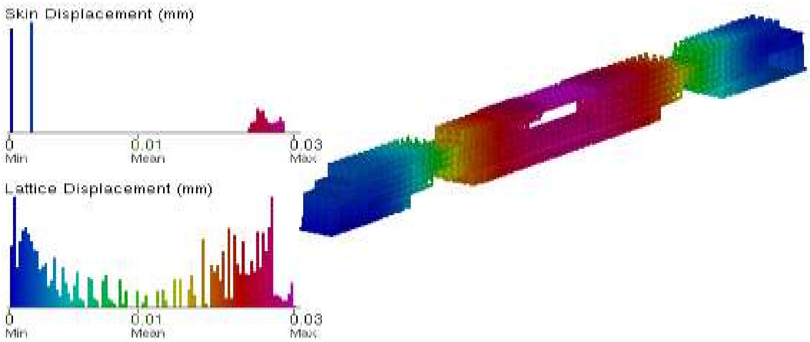

(b). Optimization result of the simply supported beam design

Figure 5: A two-stop optimization of design

2.1.2. Process Planning and Parameter Optimization

The objective of the Process Planning Model is to generate an optimal process plan with optimized manufacturing parameters of an established design. The structure of the Process Planning Model is shown in Figure 5. Two sub models are included. The Process Feasibility and Planning Model, shown as block A21, analyses the design parameters and verifies the feasibility of the initial AM design. An optimal process plan for the given design is generated along with the feasible manufacturing parameters. The second sub model, Parameter Optimization and Recommendation Model, shown as block A22 in Figure 5, further optimizes these manufacturing parameters to achieve better part qualities.

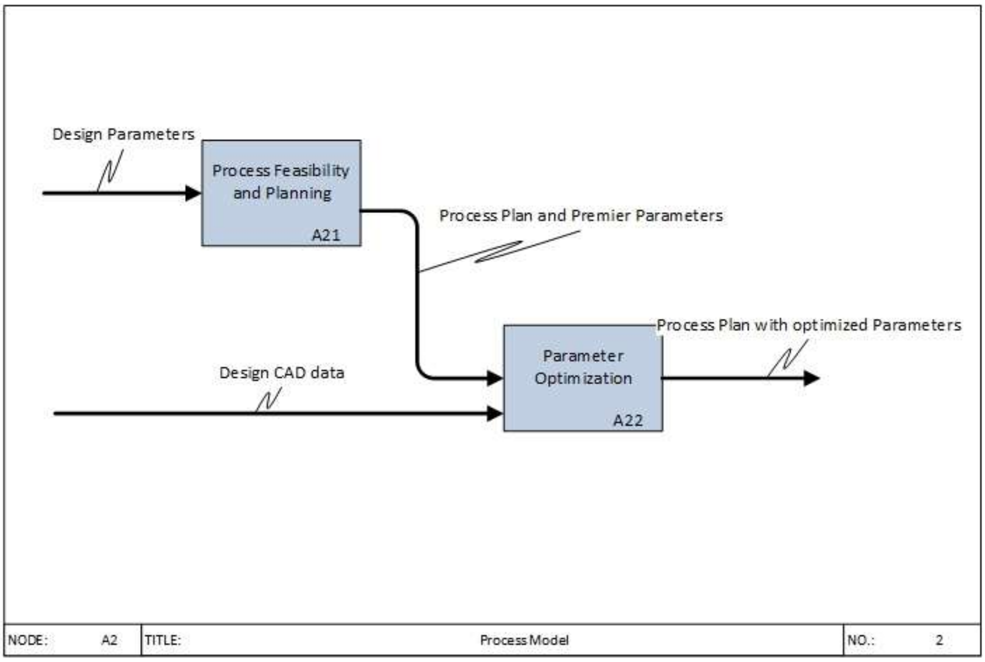

Figure 6: The structure of Process Planning Model

As the main part of the Process Feasibility and Planning sub model, a Computer-Aided Process Planning (CAPP) system, shown in Figure 6 will be developed for the metallic AM process. A typical AM cycle involves CAD modeling, process planning and material processing and the related issues are modeling issues, computational issues, process/materials issues, data transfer issues, integration issues. This research focuses only on AM process planning and it involves determining process planning tasks and the sequence. Process-planning related issues are mostly computational issues. The AM process planning consists of four parts namely build orientation, support generation, slicing and path planning [14]. The CAPP system evaluates a part geometry and determines whether it is feasible to manufacture through metallic additive manufacturing. This multi-objective problem is converted into a single objective problem and user inputs normalized weights (0 to 1) for different objectives depending on the relative importance. The objectives were identified both from the literature and industry survey. The objective functions are yield strength, fatigue, tensile strength, microstructure, surface roughness, build accuracy, build cost, % elongation, impact strength, support structure, energy consumption, build time and micro hardness. The objective functions are developed analytically, numerically and experimentally. For example, Singhal et al(2009) developed an experimental equation as a function of build angle, layer thickness and power. The fatigue function could be modeled as an experimental equation and as a function of laser power, scan speed, layer thickness and build angle. If the geometry is AM feasible, details of the AM process will be determined. If not AM feasible, the system will provide suggestions for the alternative design and process. The output of the CAPP system will include process parameters, tool path to minimize defects, support structures (if applicable), NC codes, cost difference between AM and machining. The CAPP will be developed for the example geometries and any part containing the example geometries can be evaluated.

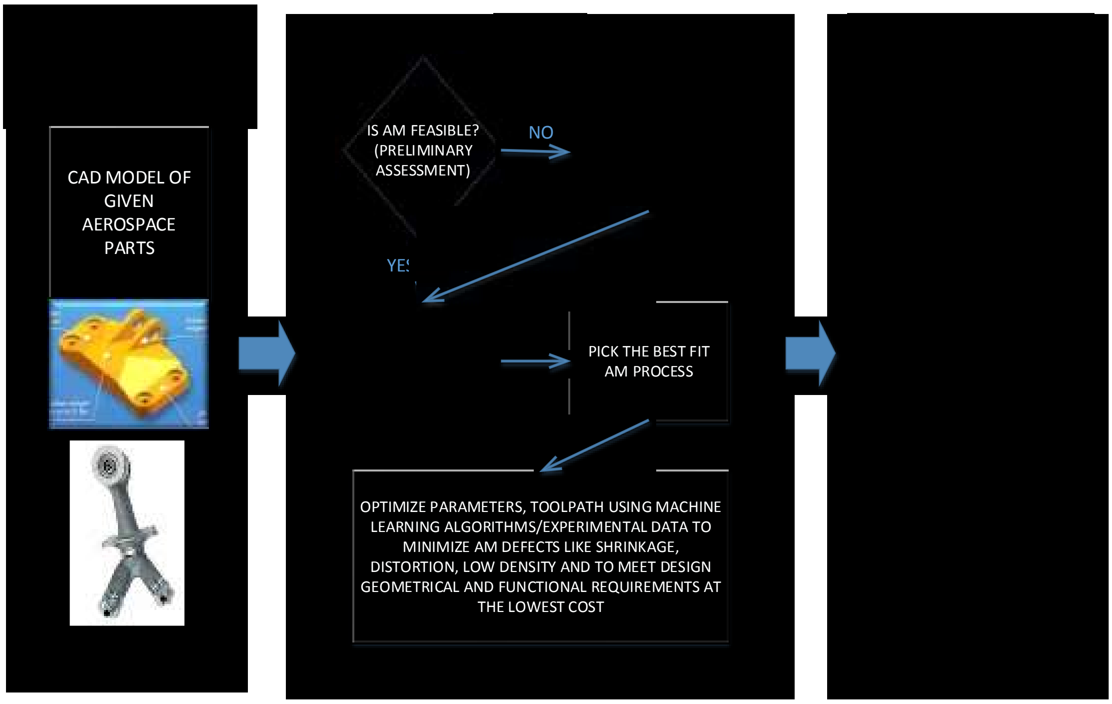

Figure 7: The CAPP system structure

The Parameter Optimization and Recommendation sub model, shown as block A22 in Figure 6, represents the manufacturing process of the AM, and finally describes the deep relationship between the parameters and manufacturing resulting properties. It figures out the important parameters or factors that impact the manufacturing results, and develops a model to properly control the process and predict the key manufacturing results, and finally optimizes the process parameters in order to meet the design requirement. The resulting qualities include mechanical properties, geometric accuracy, and surface finish.

Normally, there are two modelling methods to be used: experimental method and analytical method. By the experimental method, the process model will be obtained from Design of Experiments (DoE). The experiment results will be processed by ANOVA and learning algorithm, such as neural network. This method is straightforward to get a high accuracy and reliable model. However it takes time and cost to conduct experiments and the universality is also low. By the analytical method, the process model will be obtained from mathematical physical equation, such as heat transfer, theory of elasticity. The model will be processed by Finite Element Analysis (FEA) method. This method is complicated to establish a model. Since some assumptions should be made during analyses, the model is not very accuracy. However its universality is high. Considering the model accuracy and research feasibility, the process model in the presented research are first concluded based on experiment method. And these modelling results will be finally integrated into software platform to optimize the process parameters and predict the resulting quality. Later, some basic analytical method will be conducted to verify and improve the entire model universality and propose new optimization algorithm.

As part of the framework, current Parameter Optimization and Recommendation research on BJAM process model is concluded based on Back-Propagation artificial Neural Network (BP-NN) non-linear regression learning algorithm. The modelling process was based on 48-group experiments designed by DoE. Four important parameters (layer thickness, printing saturation, heater power ratio and drying time) were chosen as the input layer factors, and two resulting properties (surface roughness and shrinkage rate) were chosen as the output layer factors. The totally 48 groups experiment results were separated into two sets. One data set is for training the NN. Another data set is testing set, and the mean error of testing data was chosen as the testing performance indicator. The algorithm was implemented in Matlab, the results show as Figure 7.After continuous training by using the data pairs and choosing proper algorithm parameters, this learning result constructs a good mapping relationship between the process parameters and their resulting properties. This model has a 0.8% Mean Testing Error of Surface Roughness and 1.4% Mean Testing Error of Shrinkage Rate. It provides a baseline for manufacturing engineer to predict the process result and choose the process parameters.

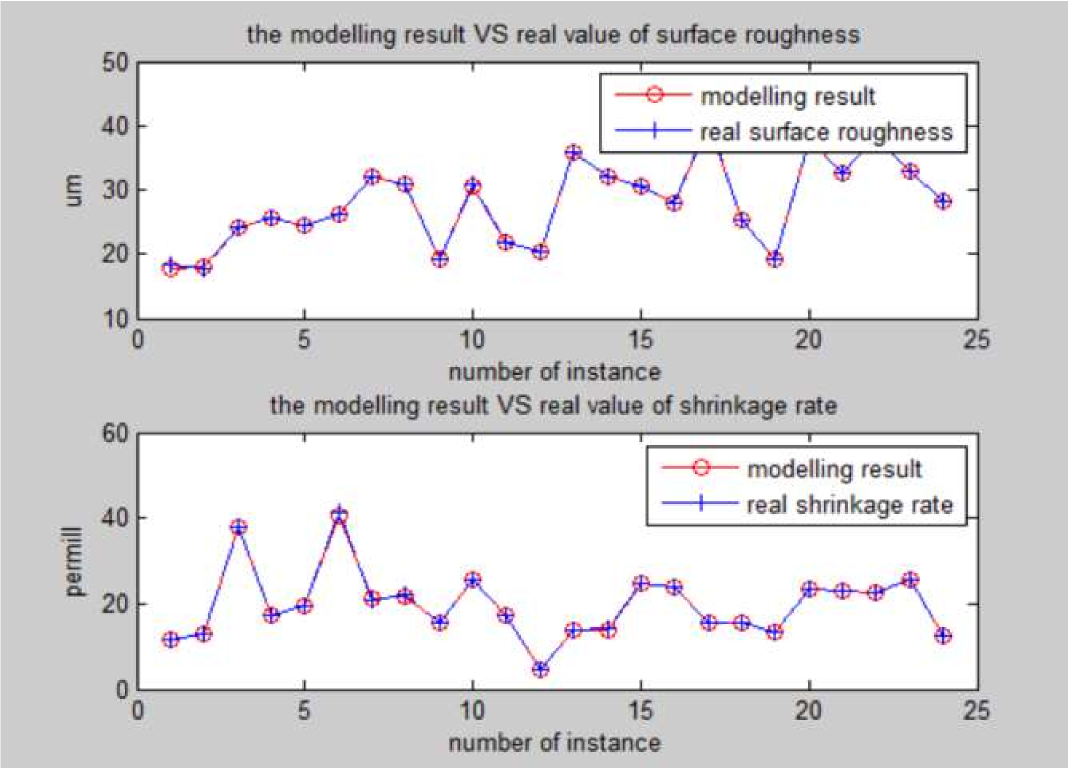

Figure 8: The BP-NN Modelling Result (Activation function: Hyperbolic tangent sigmoid transfer function, the number of hidden layer node: 9)

A robust Process Planning Model is an essential tool for the diffusion of AM. In fact at product development stage, it allows compliance between design specifications and AM capability. And it is useful to determine manufacturing parameters in manufacturing process planning.

2.1.3. Material and Energy Consumption

The third model of our research, Energy and Material Consumption Model, is to provide a method that can predict the energy and material consumption as well as the operation time analysis. As part of the production system model, the Material and Energy Consumption Model is the link between the manufacturing and production and related to manufacturing sustainability perspective.

In this model, part geometry obtained from the optimized design and process parameters obtained from the process model, such as the layer thickness, the part orientation and binder saturation are input as variables for modelling and calculation. Then process time, material and energy consumption of the manufacturing method are calculated and correlated to part geometry and process parameters setting. The material and energy consumption, as well as the operation time is output for further use in evaluation the production system.

An accurate energy consumption model has been established based on the BJAM technology. A simulation algorithm is proposed to model the energy consumption and process build time of Binder Jetting technology based on the part geometry and process parameters [15]. The algorithm slices the part design into layers, and calculates the energy consumption base on each layer's shape, plus the operation time and energy consumption. The total amount of electricity consumed by the manufacturing process is acquired. Through the experiments, the power curves of the machine are recorded. The total energy consumptions of each experiment are calculated from the curves. An example is shown in Figure 8. the power curves measured and the power curve estimated by the model on different orientation of the printed part.

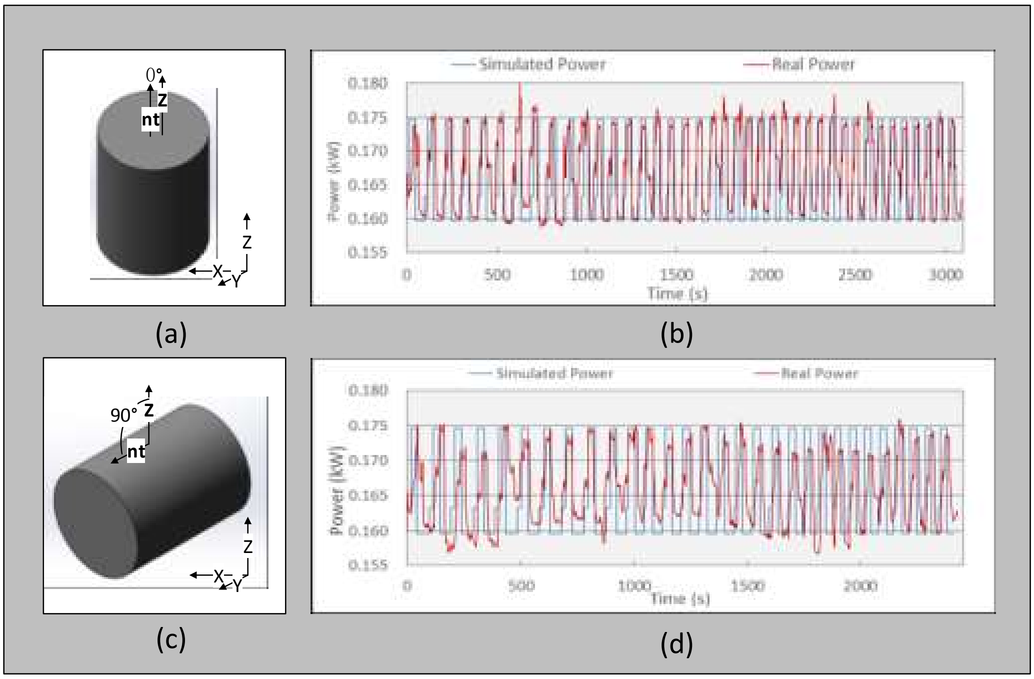

Figure 9: The power curves measured and calculated

(a) Printing orientation of cylinder, γ=0°.

(b) Printing power curve which printed by γ=0°.

(c) Printing orientation of cylinder, γ=90°.

(d) Printing power curve which printed by γ=90°

From Figure 8(b) and (d), it can be seen the comparison between the simulated power curve and the real power curve. The simulated curve in blue and the real measured curve in red match quite well. After calculation, the total energy consumption of the estimated curve has accuracy of above 95%.

2.1.4. Production System Modelling

Production Model is aiming at analyzing the AM process on a commercial production level. A predicable model is pursued to deduct certain Key Performance Indicator (KPIs) based on the design and the set of process parameters generated by the previous model discussed section above. The model integrates the process information, material cost and energy consumption into a data framework which can calculate the KPIs of each stages of the production work flow. It also gives out an optimized production strategy on the machine schedule and arrangement. It can help the management team to evaluate and optimize the production procedure. The KPIs could also be used in evaluating the profitability of the AM on a business level. The manual work time, the cost of energy and material will be analyzed and optimized accordingly to improve the business performance of the AM. Figure 9 shows the production model structure of AM.

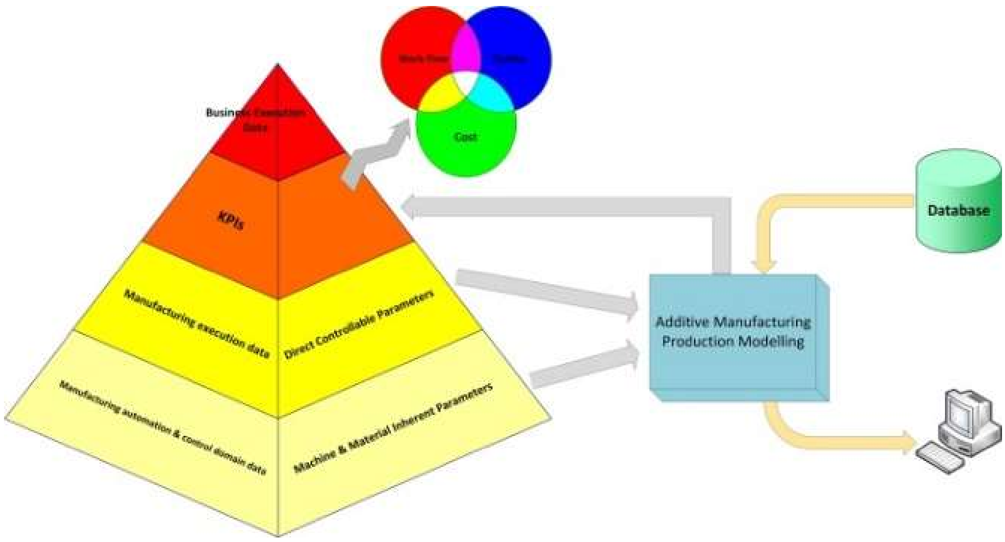

Figure 10: The hierarchy of the manufacturing business model

The KPIs are closely related to the manufacturing parameters we discussed in the Parameter Optimization and Recommendation Model. The Production System Model is designated to estimate the production KPIs and produce a production optimization strategy based on the collected data. The Production System Model could be used as an interface between the production and business administration in the upper level

Manufacturing Execution System (MES) or the even upper ERP system at a company level.

The AM simulation and optimization framework aims at providing a platform of designing, simulating, evaluating and optimizing the whole production-cycle of AM production. Through multi-level design method, process planning and parameter optimization, energy and material consumption estimation and production modelling, the whole AM procedure is presented qualitatively and quantitatively through the four models. All the models form a close loop of self-adjust and optimization from design to final production. The information estimated by the Process Planning Model, Energy and Material Consumption Model and Production Model will be used as a feedback on the design side. The part design in return will be optimized according to the estimated information provided by the other models.

2.2. AM Production System Evaluation Mechanism and Research Focus

AM is an ingenious approach in manufacturing domain. This burgeoning technology is proper for small scale and customized manufacturing. However the technology is still far from maturity for pervasive application.

The AM Production System Evaluation Mechanism proposes a system model of the AM production system and establishes an evaluation mechanism for different AM technologies in practical production. Beyond the AM framework modelling, several more aspects are taken into consideration. Some of the framework models are divided into more details sub models. The Production System Model is presented by the Energy Consumption Model, Material Consumption Model, Process Model, Quality Model, LCA Model, LCC Model, Time Consumption Model, Operation Model (efficiency, complexity and human effort involvement), Supply Chain Model and Reliability Model (robustness, risky, maturity and standards). The evaluation mechanism will retain the results from the practical production system or the simulation modelling. Then a score indexing system will be established based on the results. The score indexing system is origin from the standard KPI system but specialized for AM based production. The outline of the whole production system is shown in Figure 11.

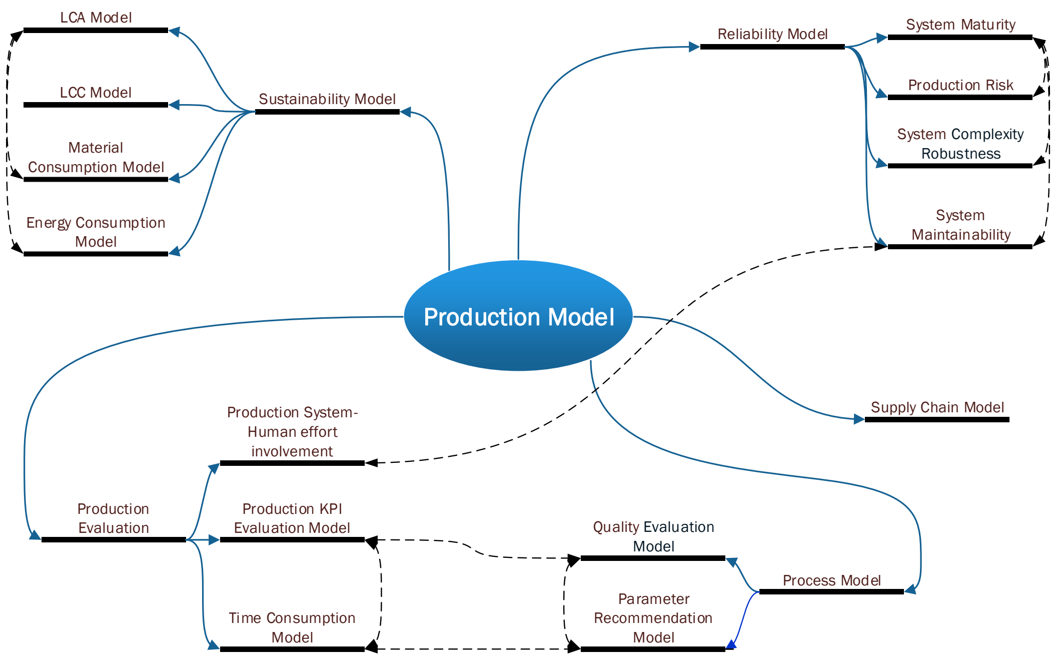

Figure 11:The Production Model and Evaluation System Structure

The evaluation mechanism looks mainly into five big categories of AM in practical production, the Sustainability, the Reliability, the Production, the Process, and the Supply Chain. Each of the categories covers several aspects as shown in Figure 11. Different models need to be developed corresponds to different aspects in order to perform simulation and evaluation. The models between each category are correlated to each other, sharing data or using the same algorithm. For example, the System Maintainability Model will contribute to the Human Effort Involvement Model in the Production categories. The Production Time Consumption Model and the Production KPI Evaluation Model may share part of the algorithm. The evaluation will based on the result of these models of each categories. The results will be interpreted and a score of each module will be given from the result.

At the first step of building up the evaluation system, each model will be developed and the result will be assessed organically before generalizing a unity scoring system. In the previous research on the AM Optimization and Simulation Framework, the Energy Consumption Model and Parameter Optimization and Recommendation Model based on BJAM have already been developed on Matlab platform. This research will continue looking into the sustainability category of AM production developing the Material Consumption Model, conducting the life cycle assessment and building up LCA Model. At the same time, the production analysis of BJAM is conducted. An algorithm of the operation time consumption is developed. Combining the results of the Material Consumption Model and the Time Consumption Model, the Production KPI Evaluation Model is build.

The LCA Model is built from the raw material manufacturing phase towards the AM production phase. It is a cradle-to-gate process. The manufacturing of AM machine, including printer, the curing oven and the furnace are not included. This research also include the human work effort into the LCA Model. The LCA analysis of BJAM production is linked to the Material Consumption Model and the Energy Consumption Model. The inputs of the LCA Model is actually the simulation results of amount of material and the energy needed provided by these two models. The LCA Model, based on the given raw material and energy, will generate the environmental impact results (LCIA).

The Process Optimization and Recommendation Model and Quality Model have been partially developed in the previous work. The recommended process parameters, as the framework shows, are the inputs of the Production Model. Here the parameters are taken to calculate the material needed and the operation time of the BJAM production.

The Reliability Model, Supply Chain Model and Operation Model are beyond the discussion of this dissertation.

All the simulation models in the production evaluation system are program based model. A general platform will be developed on PC. It includes a Graphical User Interface (GUI) and a COM API modules to call and acquire results from other models. The current general program structure is shown in Figure 12 below.

As mentioned in the framework, the inputs of the close loop AM system is mainly the STL design file as well as the manufacturing requirement, such as the surface fineness and precision. The GUI is an integration of all the simulation models. It serves as passing the STL file and manufacturing requirement to each models through COM.

The square boxes in the figure represent the model while the diamonds shape represent the data flow. The top tier model is the Process Optimization and Parameter Recommendation Model. It reads the STL file and the required manufacturing settings. Through machine learning algorithm, the model gives out an optimized set of process parameters. These optimized parameters are then passes to the second tier together with the STL file where the material consumption, the energy consumption and the operation time are estimated. The operation time can be used to generate the production schedule of availability. The algorithms of the three models are developed in Matlab. A common GUI can be shared by the three models of tier 2. In tier 3, there are the KPI Evaluation Model, LCA and LCC Models, the Supply Chain Model, the Operation Model and the Reliability Model. The LCA and LCC Model are developed in Umberto NXT, a LCA platform with Ecoinvent 3.0 database. It is initialized by the material and energy data estimated by the previous models. A special API is needed to invoke the Umberto software and pass the data in. The KPI evaluation algorithm is developed in Matlab too and share the common interface with the Time Consumption Model and the Material Consumption Model. The data diamonds in red will be taken into consideration for the AM production system evaluation.

This dissertation is focused on the research work done on the Material Consumption Model, the Time Consumption Model, the LCA Model and the KPI Estimation Model.

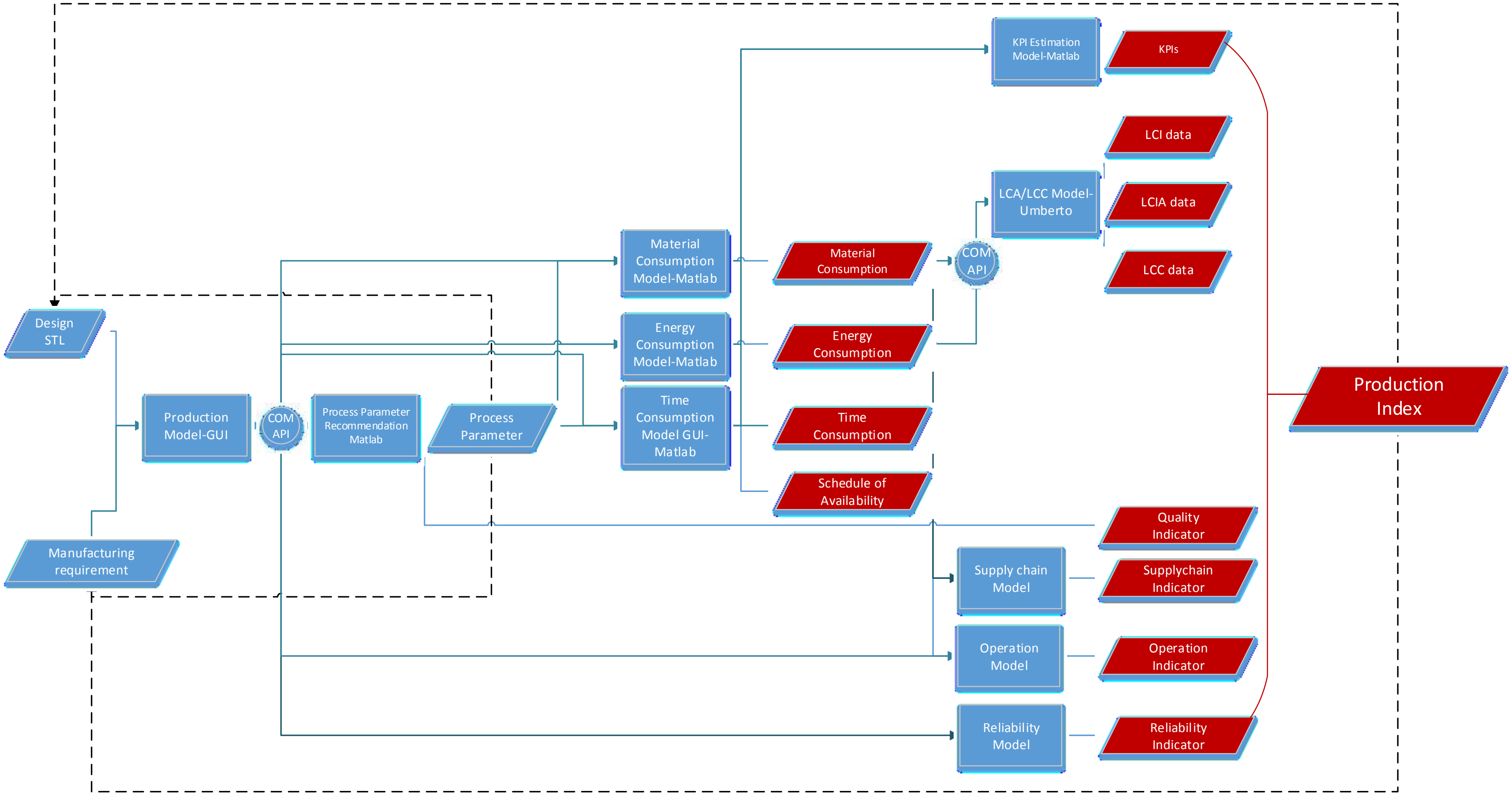

Figure 12: The structure of the production evaluation modelling system

Chapter 3: Manufacturing Process Parameter Optimization Model and Experiments Design

In the Production Evaluation System, the process parameter settings are related to many following models. As shown in Figure 12, the process parameters is derived from the STL file and the manufacturing requirement. An optimization model is built up to recommend the process parameters according to the STL file and the manufacturing requirement.

Previous researches on the BJAM process parameter optimization have established a parameter recommendation algorithm [9] based on the given manufacturing requirements. Back Propagation Neural Networks (BPNN) is used in determine the best set of process parameters combination. This algorithm is inherited in the current research.

3.1. Process Parameters Identification and Selection

BJAM technology is capable on different materials such as stainless steel powder, sand, ceramics powder and etc. Different types of binder are applied according to the type of the powder. To achieve the best printing quality, the process parameters needs to be adjusted according to different materials and different part functions. There are many different manufacturing process parameters that may have direct or indirect effects on the end-products' properties. The relationships between the process parameters and quality properties are complicate. The research focus on the relations between the manufacturing process parameters of BJAM and the end-products properties. A quantitative analysis of key independent process parameters and part's quality are conducted. The input-output model is built in order to control and improve product performance. The parameter optimization algorithm focuses on four key process parameters in the principal printing process of BJAM, the layer thickness of the each powder layer, the binder saturation, the heating powder ratio when drying the binder, and the drying time that each printed layer will go through. On the output side, the algorithm focus on part dimensional accuracy and surface roughness. Definitions and interpretation of the four key control parameters are list as following.

Layer thickness is the parameter that determined the basic step of the layer based AM. The designed part will firstly be sliced into layers and spread layer by layer on the print bed. In the BJAM system, it is the distance that the print bed lowers after printing on layer. In AM technologies, layer thickness always represents the resolution of the machine. It constrains the smallest structure that the AM machine can make. Normally, the thinner the layer is, the better the end-products performance.

Binder Saturation is the percentage of air space that is occupied by a binder volume in the print bed during printing. It is defined as

$$s = \frac{V_{binder}}{V_{air}} \tag{2}$$

Saturation represents how much binder will be deposit during the printing process. It has a great impact on the mechanical properties of the printed part. It also constrains the part manufacturability. Insufficient binder will lead to printing failure. Excessive binder will adhere extra powder joining the parts leading a bad surface finish or structural failure.

Heating Power Ratio represents the energy level of the electrical infrared heater that drying the binder saturated powder. The heating power ratio is defined as

$$\mathrm{R_{hp}} = \frac{P_c}{P_m} \tag{3}$$

where $\mathrm{P_c}$ is the current heater power, and $\mathrm{P_m}$ is the maximum heater power. It defines the heating speed on the printed powder. It is closely related to the drying level of the liquid binder. When the binder is too moist, the next layer of powder may adhere excessive powder. If the binder is too dry, the next layer of powder may not be well adhered to the current layer.

Drying Time defines the time that the print bed under the electrical infrared heater. On the part quality aspect, it affects the process stability. Too long or too short drying time may lead to lower part properties. It constrains the total operation time as well.

3.2. Design of Experiments

The BJAM process parameter model is built based on meta model. Taguchi Design of Experiment (DoE) method that employs Orthogonal Arrays (OA) is used to significantly reduce the experiments runs. L_{16} OA is chosen in the algorithm because it provides more combinations of the parameters that leads to a more reliable results. The 16 sets of experiments with different parameters combination are conducted as shown in Table 1.

Table 1: The parameters setting of the experiments group

No.	Layer Thickness(μm)	Binder Saturation (%)	Heating Power Ratio (%)	Drying Time (s)
1	50	60	55	15
2	50	75	70	30
3	50	90	85	45
4	50	105	100	60
5	100	60	70	45
6	100	75	55	60
7	100	90	100	15
8	100	105	85	30
9	150	60	85	60
10	150	75	100	45
11	150	90	55	30
12	150	105	70	15
13	200	60	100	30
14	200	75	85	15
15	200	90	70	60
16	200	105	55	45

The experiments samples are made from 420 Stainless Steel powder with average particle size of 30μm (distribution: 22μm – 53 μm) that is gas atomized and produced by ExOne^{TM}. The sample part is testing cylinder sample with 38mm length and 13mm diameter designed according to ASTM E9-89a (2000) standard [48]. In the 16 sets of experiments, 48 samples are made with 3 samples in each experiment. Then measurements are conducted on the dimensions along the Y-axis and Z-axis as well as the surface roughness.

Besides the four variable process parameters, the other manufacturing profile is listed in Table 2.

Table 2: Experiment Specification

Printer	ExOne X1-Lab
Powder	PM-R1-S4-30, 30µm 420 Stainless Steel
Binder	PM-B-SR1-04, Polymer based ink
Cleaner	PM-C-R1-02
Curing Profile	5 Hours of 175 °C
Sintering Profile	ExOne^{TM} S4-One-Step no infiltration
Build Speed	1 minute/ layer
Print Resolution	X/Y 0.0635 mm, Z set by layer thickness
Surface Finish Measurement Tester	Mitutoyo, SURFTEST SJ-410
Dimension Measurement Tester	Digimatic Standard Caliper

At the same time, the experiments are also served in building up the Time Consumption Model and Material Consumption Model. Each set of experiment is recorded for its operational time including manual work time and material used.

3.3. Process of Empirical Model

Artificial Neural Networks is adopted to building up the empirical model from the data acquired from the experiments. Since the relationships between these four manufacturing process parameters and the quality properties are unclear and may be of huge complexity, the analytical model is impossible to generate due to its reliance of large amount of data. In this case, the Neural Networks is more proper in building up the model. Because it is metamodeling method that has a massively parallel-distributed process made up of simple processing units (neurons)[16]. Simulating interconnected neurons working in parallel, NN is a simplified mathematical model to imitate neural behaviour[17]. It is also open used when the relationship between the variables is unknown or in the situation where the process is not completely understood [18] as the case of BJAM process. Besides, Neural Network methods have already been used in modelling many other types of AM process such as the Fused Deposition

Modelling(FDM)[19], Selective Laser Sintering(SLS)[20] and Stereo lithography(SLA)[21].

The architecture of the neural network used in building up the process parameter models is a typical three-layer Back-Propagation Network. The three layers are the input layer, the middle hidden layer and the output layer. The input layer is receiving the training sample data, that is the data obtained directly from the experiments. The middle hidden layer is the connection between the input layer and output layer and is in charge of processing and training the data. The output layer returns the training results. Different weight is assigned to the connection between two neurons in consecutive layers. The activation function is used to produce the output by receiving the weighted sum from the hidden layer [18]. And the Sigmoid function as shown in Equation (4) is used to model the non-linear relationship.

$$S(t) = \frac{1}{1+e^{-t}} \tag{4}$$

The weights of the connections between two neurons are tuned during the training process until the error reduces to an acceptable level. In Back-propagation algorithm, the model and weights are modified according to the redistribution of the error associated with the output.

The experiments results in modelling the manufacturing process parameters are the input of the BPNN training as shown in table 3.

Table 3: The Experiments results and the inputs of the BPNN

No.	**Surface Roughness(μm)**	**Shrinkage Rate Y-axis (%)**	**Shrinkage Rate Z-axis (%)**
1	17.57	1.41%	1.75%
2	12.87	0.43%	0.42%
3	17.92	1.19%	1.43%
4	16.64	1.24%	1.76%
5	17.89	0.70%	0.50%
6	21.29	1.75%	1.95%
7	15.97	0.63%	0.71%

8	18.22	0.99%	0.91%
9	27.87	1.73%	2.50%
10	22.24	0.86%	1.23%
11	18.83	0.34%	0.32%
12	28.07	0.90%	1.12%
13	28.75	1.14%	1.06%
14	26.35	2.97%	2.15%
15	24.39	1.22%	1.42%
16	26.66	1.35%	1.18%

The training work is performed using Matlab Neural Networks tool. The 16 inputs are divided into two groups, the training group, the validation group and the test group with 12 sets and 4 sets of data separately. The error evaluation function is Mean Square Error (MSE). Figure 13 shows the Neural Network regression plots on surface roughness, Y-axis shrinkage and Z-axis shrinkage. The plots show the actual network output associated with the target value. According to Matlab documentation [22], the networks output-target relationship closely intersect the bottom-left and top-right corners in the plot. So from Figure 13, the research has obtained a well-trained model.

In order to test the predictability of the developed process model, the validation experiments are conducted. From the validation data shown in Table 4, the mean errors between the real value and predict value for three quality properties are 1.98%, 5.83% and 16.58%. This result shows the accuracy of the empirical model.

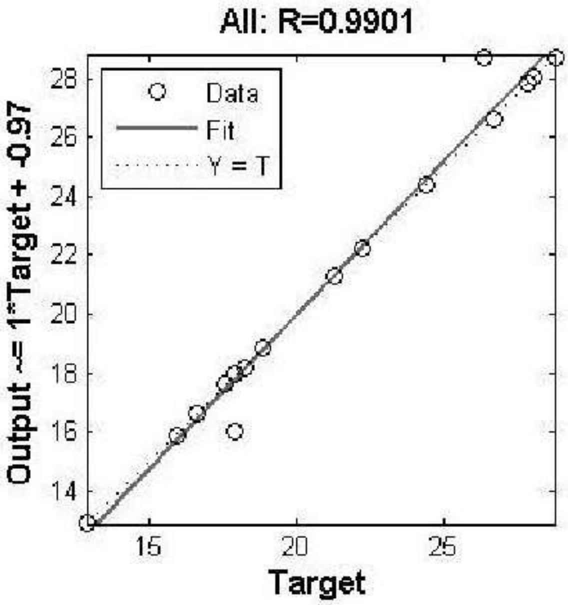

(a) Regression Plot for Surface Roughness Training

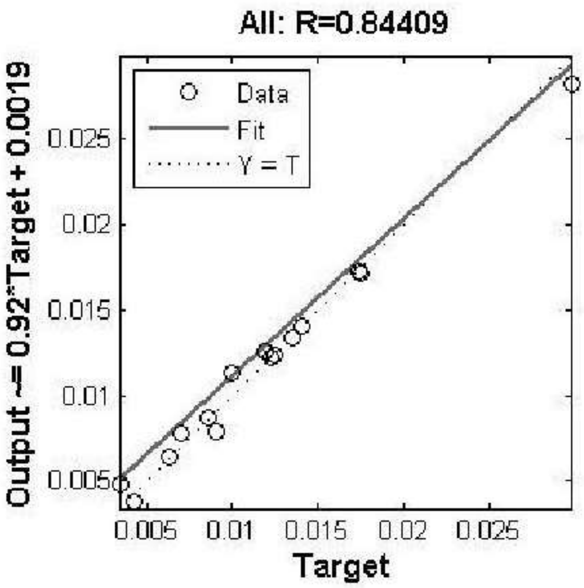

(b) Regression Plot for Y-Axis Shrinkage

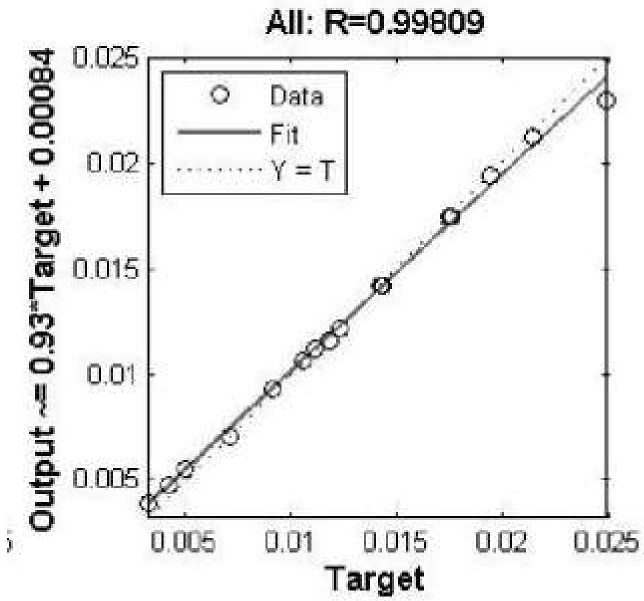

(c) Regression Plot for Z-Axis Shrinkage

Figure 13: Regression Plot for Training Result

Table 4: The Validation of the experiments

No.	Surface Roughness (μm)			Y-axis Shrinkage Rate (%)			Z-axis Shrinkage Rate (%)		
	Real	Pred.	Err %	Real	Pred.	Err %	Real	Pred.	Err %
1	12.80	12.82	0.2	0.50	0.52	4.0	0.50	0.54	8.0
2	24.57	22.99	-6.4	0.28	0.30	7.1	0.79	0.56	29.1
3	22.15	23.41	5.6	0.87	0.79	-0.92	0.24	0.27	12.5
4	15.05	13.77	8.5	0.51	0.61	19.6	0.36	0.31	16.7
Mean Error	1.98%			5.38%			16.58%		

3.4. Parameter Optimization and Recommendation Model

In practical case, due to the machine limitation, the process parameters are not able to be set arbitrarily. There are only discrete values within the range to be chosen from as shown in Table 5. The system has set fixed interval for these parameters within their feasible range. There are 16,000 different process parameters combinations.

Table 5: The setting levels of Process Parameters

Process Parameter	Range	Interval	Total Number of levels
Layer Thickness (μm)	50-200	10	16
Binder Saturation (%)	60-105	5	10
Heating Power Ratio (%)	55-100	5	10
Drying Time (s)	15-60	5	10

The Parameter Optimization and Recommendation Model is built on a customer-demand structure. Since the process parameters cannot achieve a single optimization result regards to the end-product properties due to the machine capability, the process parameters are on a balancing situation. So a compromise will have to be decided by the customer or the designer to have the part produced in practice. The end-product properties each can be set on a percentage basis where 100% means that the user want to yield to get the best performance of the machine in this property. 0% means that the user do not care about this property at all of the end-product.

The optimization problem can be expressed as:

Objective

$$max\ \boldsymbol{P}(l, p, h, d; \boldsymbol{x})$$

Subject to

$$l_{min} \leq l \leq l_{max}$$
$$p_{min} \leq p \leq p_{max}$$
$$h_{min} \leq h \leq h_{max}$$
$$d_{min} \leq d \leq d_{max}$$
$$\boldsymbol{g}(P_{suface}, P_y, P_x)=0$$

Where

$$\boldsymbol{P} = \{P_{surface}, P_y, P_x\}^T$$
$$\boldsymbol{g} \in \boldsymbol{BPNN} \tag{5}$$

In Equation (5), *l* represents the layer thickness, *p* represents the binder saturation, *h* represents the heating power ratio, *d* represents the drying time. $\boldsymbol{g}$ is the constraints that descript the relations between the three end-product properties: $P_{surface}$ the *surface roughness*, P_x the *X-axis shrinkage* and P_y the *Y-axis shrinkage* and the process parameters. The relation is obtained and modelled by BPNN algorithm.

In the user-demand Process Parameter Optimization and Recommendation Model, the end-product properties is adjusted by the user on a percentage scale based on the practical needs. For example, if the surface roughness is of high demand according to the functional requirement then on the UI, the user should set the Surface Roughness bar to 80%-100%. The same goes for the Y-Axis and Z-Axis shrinkage. The UI is shown in Figure 14. However, if all the three quality requirements go to 100% no recommendation will be available. There has to be compromise on the quality. The Model will load the STL file of the design and the user's demand percentage on the three quality properties. Then the Model will give out the recommend manufacturing process parameters and the predicted results of the three end-product properties.

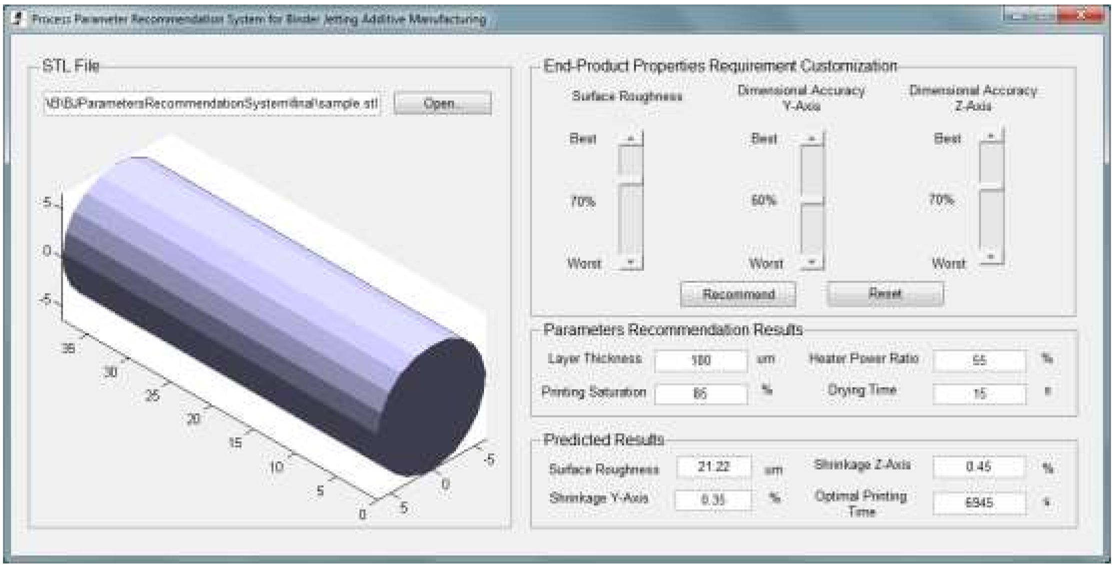

Figure 14: The UI of Process Parameters Recommendation Model

The Process Parameter Optimization and Recommendation Model has provided a direct relationship of the BJAM process parameters and the desired the quality. It also provides a set of manufacturing parameters for the practical printing and gives out the estimated analytical result of the end-product properties.

3.5. Conclusion

In order to improve the process ability of BJAM process and help the manufacturing engineer to choose the proper process parameters, a MATLAB GUI based process parameters optimization and recommendation system is developed. It is built based on BPNN empirical modeling algorithm and trained from 16 groups' experiments designed by Taguchi Method. A process parameters estimation model is also developed and integrated into the recommendation system to predict the end-product performance based on the part geometry and process parameters. This system can efficiently recommend a set of parameters to meet the users' customized quality requirements and take the minimal printing time. Finally, it will increase the working efficiency and speed the wide acceptance of BJAM process by industries.

Chapter 4: Production Time Material Consumption & KPI Model

In the previous Chapter, the Manufacturing Process Parameters Model has developed the algorithm in parameters optimization. The Model will recommend the feasible production parameters on respects to the desired the parameters. Based on the given parameters, the second tier of the production system model: the Time Consumption Model, the Material Consumption Model and the Energy Consumption Model can be built.

In this Chapter, the algorithm based on the process parameters in calculating the production time consumption and the material consumption will be discussed. The third tier KPI Estimation Model is based on the result of the time and material consumption as descripted in Figure 12. The KPI Estimation Model will also be discussed in this Chapter. A Matlab GUI is also developed with the integration of the previous Process Parameters Recommendation System.

The flowchart in Figure 15 shows the process and interaction between different models that will be discussed in this Chapter. Starting from the design STL file, a default process parameters are set according to ExOne™ Recommendation. The Process Parameters Recommendation System can be used by the user to acquire an optimized set of process parameters that satisfies the needs. Then the parameters list will be updated according to the recommended parameters. The process parameters can also be adjusted and customized according to the recommendation. Then the parameters as well as the STL file will be taken by the time consumption algorithm and the material consumption algorithm. An estimation of time and material consumption will be given. These data will then be taken by the KPI Estimation Model, through calculation, basic KPIs will be given. As marked red in the flowchart, the time and material consumption estimation data and the estimated KPIs will open to be used by the other models of the previous discussed Production Evaluation System in Chapter 2.

The following sections will go through the flow chart and explain the mechanism of the algorithm in the STL file reading, the time and material consumption estimation and the KPI estimation.

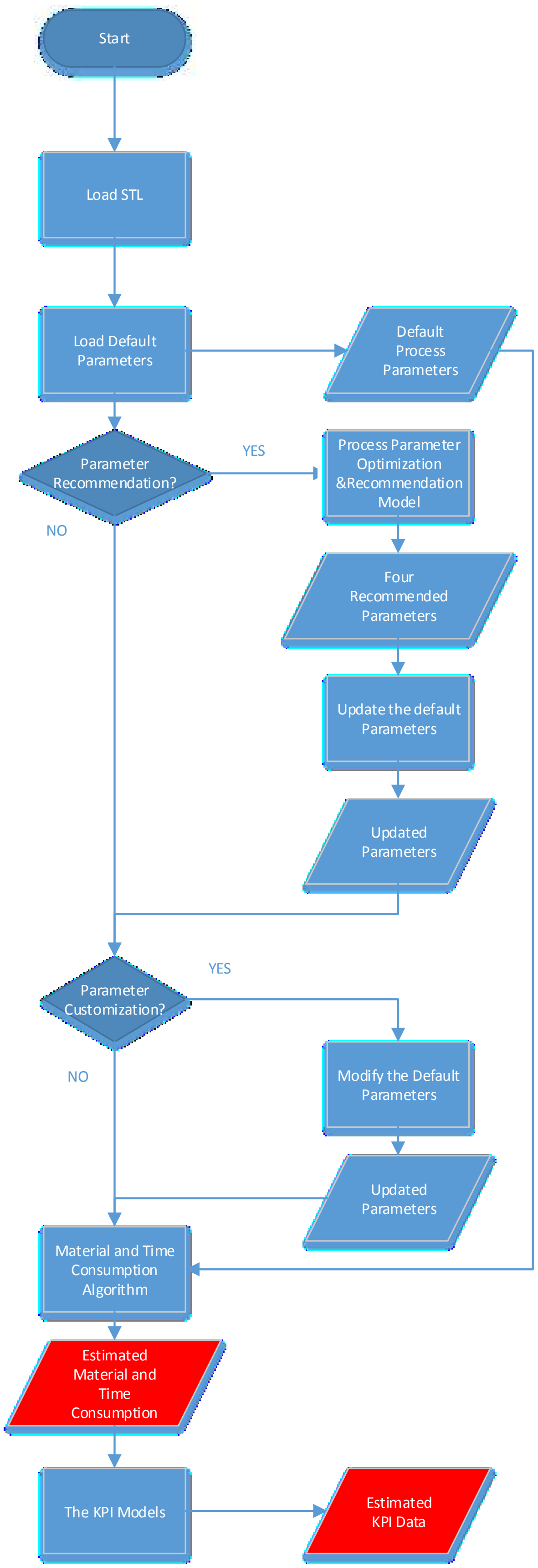

Figure 15: Flowchart of the Production Evaluation System (From STL file to KPI estimation)

4.1. STL file reading and Part Slicing

In order to conduct the estimation, the design STL file will be loaded. As a simulation to the practical printing process, the STL file is sliced into layers. The time consumption and material consumption estimation algorithm works on a layer-by-layer basis. So reading STL file and conducting accurate slicing is critical to the algorithm. A triangles slicing algorithm is introduced in this research[23]. The flowchart in Figure 16 shows the principle of the slicing algorithm developed by Xin[23]. The contour of each layer is output and will be used in the time and material consumption estimation.

Firstly, the geometry information of the part is derived from the STL file by a STL reader. Then the print layer thickness as well as the part printing orientation are defined by the user according to the need. Afterwards, a slicing loop is performed. The layers are sliced in the perpendicular direction towards the print orientation. When the slicing is finished, the contours is output to support the time and material consumption estimation. A brief introduction of the STL reader and slicing loop are demonstrated in the following sections.

4.1.1. STL file reader

The functions of the STL file reader are to read the triangles from a STL file and generate two lists to save these data: the facet list and vertex list. Both the ACSII STL file and Binary STL file have the information sets of triangles data[24]. In these sets, a normal vector of a triangle is always represent by three vertexes of the triangle. According to this rule, when the STL file is read, each triangle will be added into the facet list following by three vertexes are added into the vertex list which corresponds to the triangle. The structure of the two lists are shown in

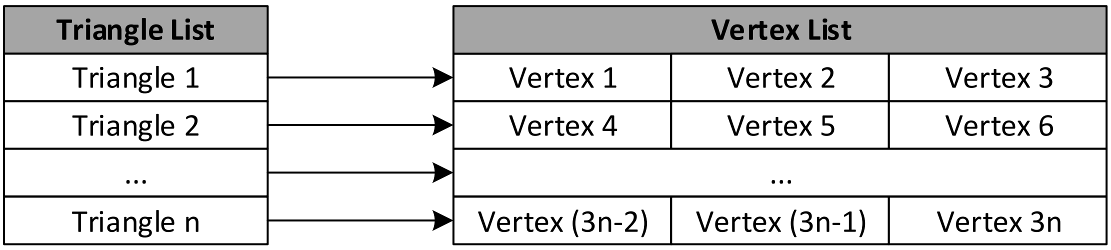

Figure 17

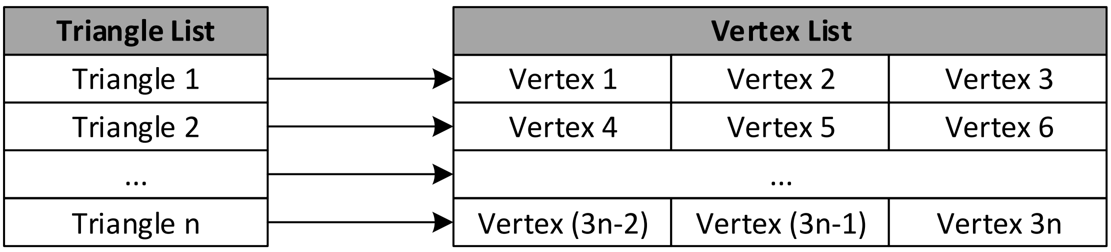

Figure **17**. If the part contains n triangles in the STL file. Then the triangle list is an $\mathrm{n} \times 1$ array while the vertex list is an $\mathrm{n} \times 3$ array. The triangle list is used as an index list to locate the elements in the vertex list.

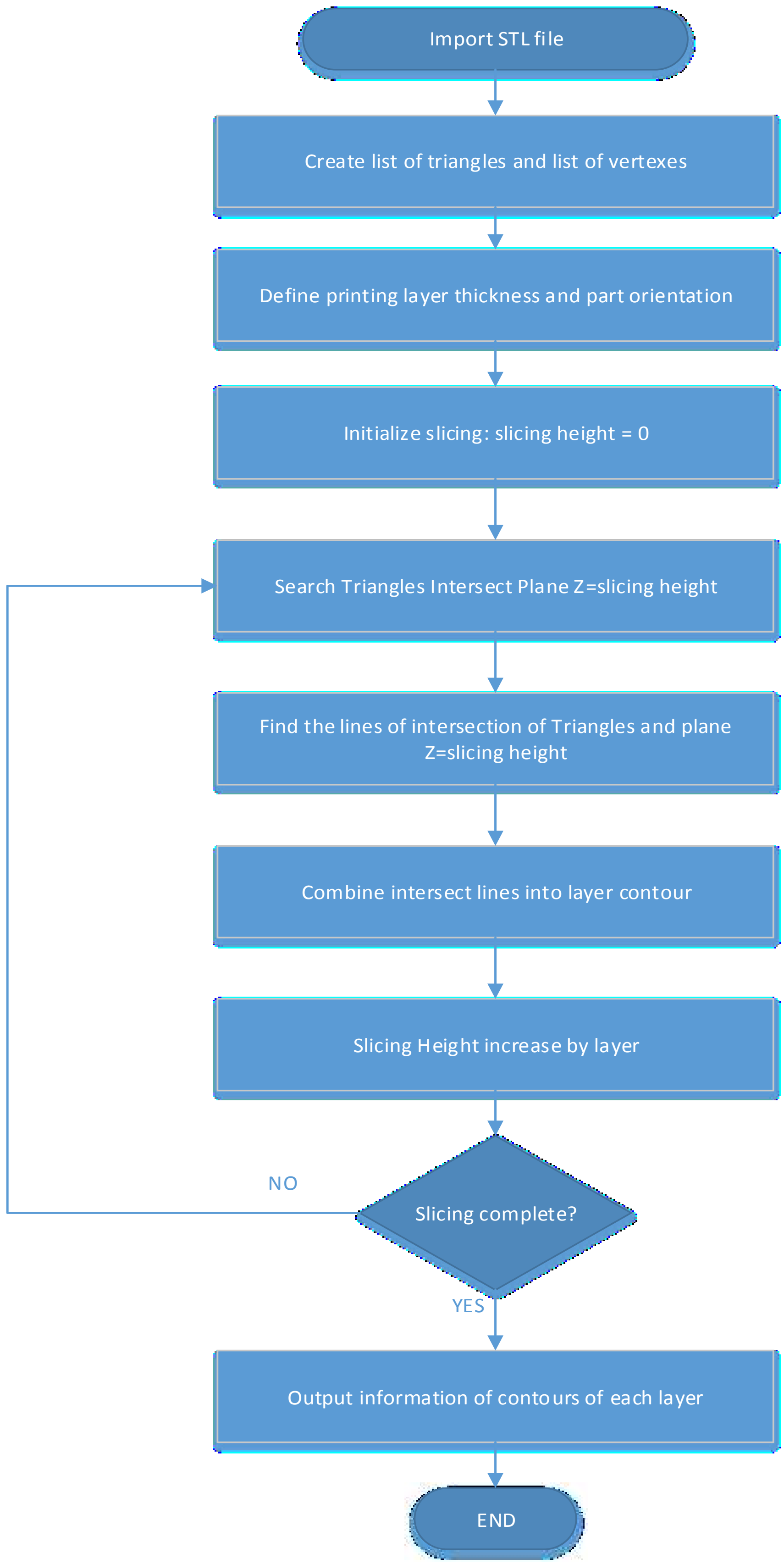

Figure 16: The STL slicing algorithm flowchart

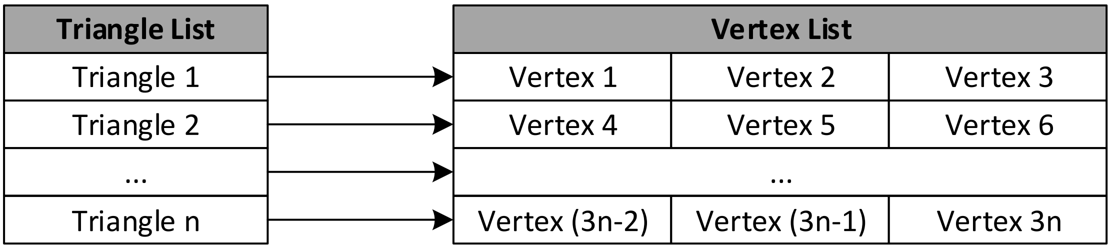

Figure 17: The structure of the STL file Triangle List and Vertex List [23]

4.1.2. Identify Intersecting Triangles

Once the STL is read into the program, slicing the part into layers and finding intersections of the layers is coming next. Since the slicing is conducted along the Z axis perpendicular to the layers, the first step is to determine the triangles intersecting the plane $Z = Z_{Slice}$ where Z_{Slice} is the height of the current slice. A top and bottom vertex list in introduced to perform the intersecting check. Each triangles in the sliced layer is recorded by its top vertex $(\mathrm{X_i}, \mathrm{Y_i}, \mathrm{Z_i})_{\mathrm{top}}$ and bottom vertex $(\mathrm{X_i}, \mathrm{Y_i}, \mathrm{Z_i})_{\mathrm{bottom}}$ together with the index of the triangles, form a $3 \times \mathrm{n}$ array.

Eight possible position relations existed between triangles and the slicing plane as shown in Figure 18. From the figure we can tell, to claim the intersection, as shown in triangle [B C D E F G] two conditions have to be satisfied.

$$Z_{top} \geq Z_{slice}$$

$$Z_{bottom} \leq Z_{slice}$$

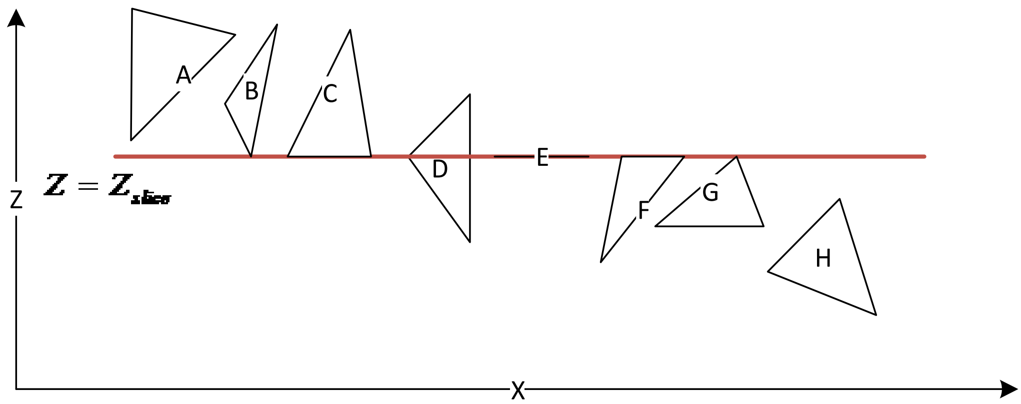

Figure 18: Triangles' relative position with the slice surface[23]

On the programming level, the intersecting triangles are sorted out by the two operations below:

1. Add any triangles with $Z_{bottom.i} \leq Z_{slice}$ from the top and bottom list into the intersecting triangle list.
2. Remove any triangles with $Z_{top.i} < Z_{slice}$ from the intersecting triangle list.

For the example shown in the Figure 18, the first step adds triangle [B C D E F G H] into intersecting list. And the second step removes [H].

4.1.3. Calculate Intersection on Slicing Plane

The intersection between a triangle and a plane is a segment. This segment can be located by the two end points. If a vertex is on the plane, then it is one of the end points. The conditions are discussed as following:

1. One vertex is on the slicing plane and the rest of the triangle is above or below the plane (as triangle B or G in Figure 18). Under this condition, the whole intersection is a point and it is not computed.
2. One vertex on is the slicing plane and the slicing plane is intersecting one side of the triangle (as triangle D in Figure 18). In this case, the vertex on the plane is one of the end points of the intersection segment.
3. Two vertexes of triangle are on the slicing plane (as triangle C and F in Figure 18). In this case, a side of the triangle is on the plane and it is directly treated as the intersection.
4. All of the three vertexes of triangle are on the slicing plane (as triangle E in Figure 18). Then the three sides of the triangle are all treated as intersection.

Other than the four situations, for any segment of the triangle with vertex on the both side of the slicing plane, the intersection point is computed linearly from the vertexes of the triangles as:

$$X_i = \frac{(Z_{slice} - Z_1) \cdot (X_1 - X_2)}{(Z_1 - Z_2)} + X_1. \tag{6}$$

Similarly:

$$Y_i = \frac{(Z_{slice} - Z_1) \cdot (Y_1 - Y_2)}{(Z_1 - Z_2)} + Y_1. \tag{7}$$

Till the end point of the intersecting segment being computed, the segment of intersection is located. This process is performed iteratively for all of the intersecting triangles. As a result, the segments of the whole layer are derived and they are combined together to form the contour of the layer.

4.2. Binder Jetting Operation Modelling

As mentioned in the previous chapters, the BJAM Production System Model consists of different sub models. In Chapter 3, the Process Parameters Model is a Meta model built based on the experimental data. While the Time Consumption Model and the Material Consumption Model mainly rely on the physical operation process of the BJAM. Since the operation processes of BJAM are sequential, the analysis is operation based. Each operation is analyzed and estimated separately. The sum of each operation will give the final result of the whole system.

In Chapter 1, we defined our scope of study. The BJAM production system has three sub system: the printing machine, the curing oven and the sintering furnace. The curing and sintering process are simple and taken as a whole in the analysis while the printing process is a complex iteration of different sub processes. The connection processes in between each process is also considered. In the following section, each sub process of the printing, as well as the curing and sintering process and the connection processes will be presented and discussed.

Figure 19 shows the workflow of sub processes. The whole process is divided by the three main process: printing, curing and sintering. The connection process in between is set as the transportation and set up process that includes in the following process. The process in orange is the process that have human work involved. Such as the Printhead Testing, and Initial Layer Spreading, the worker needs to maneuver the printer and check manually the testing result and the spreading quality. The transportation between each machine, the machine set-up and the post processing are also considered as manual work.

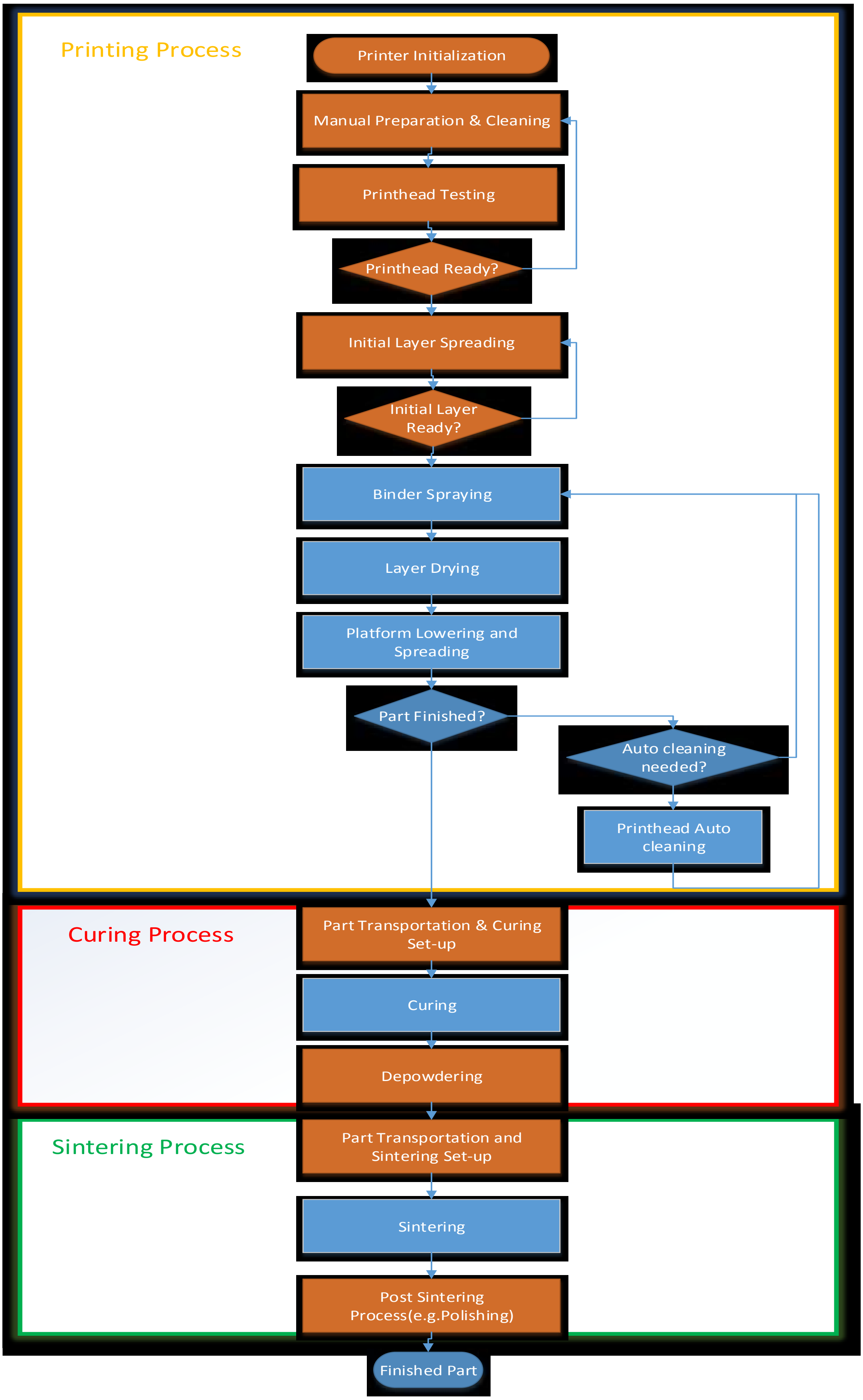

Figure 19: The workflow of BJAM process

4.2.1. Printer Initialization, Preparation, Cleaning and Testing

Before starting the printing tasks, the printer needs to be initialized, and set-up according to the parameters. Besides, the binder, cleaner containers and the powder supply box have to be filled up and the waste containers should be emptied. The printing platform should be cleaned to ensure a smooth printing process.

In order to ensure the well-functioning of the printhead and printing quality, the printhead needs to be cleaned and tested several times before printing. The cleaning cycle is performed automatically by the machine but is set by the worker. It serves at dredging the blocked nozzles. After cleaning, a test pattern is printed on the cardboard to identify the blocked print nozzles. The worker identifies the blocked nozzles by visual check. The printer itself can compromised a limited number of blocked nozzles after identification. Several iterations of cleaning and testing are performed until the worker thinks the printhead is ready to work, i.e. no blocked nozzles or the blocked nozzles can be compromised by the printer itself. The identification and printing compromising is shown in Figure 20.

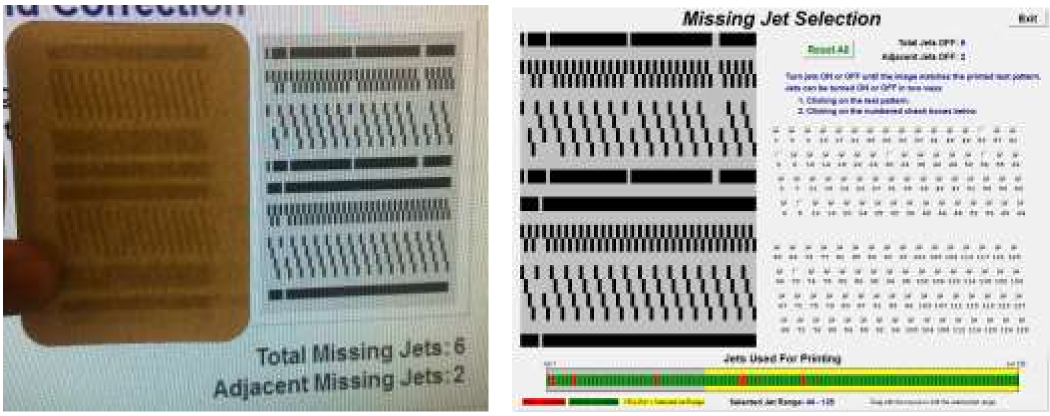

Figure 20: Blocked Nozzles Identification and Printing compromise

This part of work is mainly down manually. The time varies on different situation. In modelling these processes, we use the experiment data that we obtained from the 26 sets of experiments (see Appendix I). The time consumption of these processes are counted as a whole in the experiments. The data of the experiments shown in Appendix I has shown a consistency in these process. The Printer Initialization time is around 2-3 minutes with average of 2.45 minutes and variation of 0.11. The Printing Preparation Time which includes the setting-up time, the printhead cleaning and testing time, is around 26.38 minutes of average with the minimum of 20 minutes and maximum of 37 minutes. So in the time consumption algorithm, this part of time consumption is treated as a fixed value, the average of the experiment data.

Considering the material consumption, the binder and cleaner are consumed in the printhead cleaning process. A smaller amount of binder is used in printing the test pattern. In the manual cleaning phase, several different cleaning operation may be performed according to the printhead's performance. So it is hard to estimate the exact consumption of binder and cleaner. And the waste disposal. However, based on ExOne's recommendation as well as our practical experiments, in most of the case, two times of default cleaning cycle and two times of prime and fire, two test pattern printing are enough for regular use. From this, we can have a roughly estimation of the binder and cleaner used in this process as well as the waste generation.

From the experiments data, a default cleaning cycle will take about 30ml of cleaner and 5ml of binder. Since the binder is not at all spray onto the powder, the total waste generated is 35ml per cleaning cycle. Another two times of prime and fire also take about 5ml binder. The test pattern printing takes 3~5ml of binder too. So in total, the printer initialization, preparation and testing takes around 60ml of cleaner, 26~30ml of binder and generates about 70ml of waste.

4.2.2. Binder Spraying Process

The binder spraying process is the core sub process of the printing process. In this process, the printhead moves several times across the build box as shown in Figure 21. The motion of this process consists of 3 parts: printhead moves from the cap position to the print bed, printhead passes and binder spray over the print bed and the printhead return to the cap position.

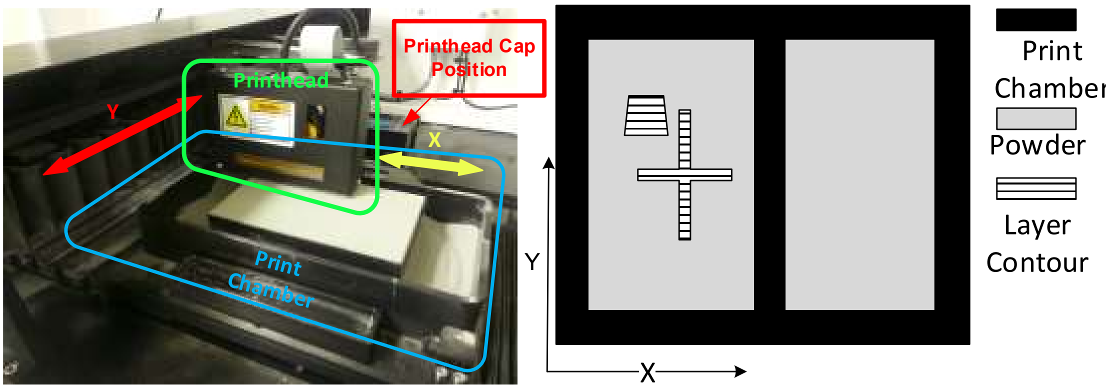

Figure 21: The Printhead binder spraying process

As shown in Figure 21, the printhead moves along the Y axis and deposit binder droplets on the powder bed according to the intersection of the part at each layer. The printhead contains a set of nozzle array. So it can be considered that all the binder droplets are sprayed at the same time in one print pass. The nozzles are so approach to the print bed surface that the binder dropping time is neglected. The motion of the printhead is controlled by a belt system and this system is driven by a step motor. Since the step motor can start and stop immediately, the acceleration and deceleration of printhead are negligible. The motion of the printhead has two settings, the printing pass speed v_{pass} and the printhead moving and returning speed $v_{printhead}$. The number of printing passes per layer N_{pass} can be customized by the user. The distance between the cap position and the print bed D_{c-p} and the width of the print bed $W_{printbed}$ are normally fixed. It depends on the Model of the BJAM printer. The multiple amount of passes ensure the binder to be sprayed evenly on the desired intersection. To be mentioned, only one cycle binder spraying process is perform in printing each layer, that is one movement from the cap position to the print bed, one back and several print passes. The time consumption of one binder spray cycle is expressed as Equation (8).

$$t_{spray} = 2 \times \left(\frac{D_{c-p}}{v_{printhead}}\right) + \frac{N_{pass} \times W_{printbed}}{v_{pass}} \tag{8}$$

The binder spray process is also where the binder is actually being used. 90% of the binder consumption of the whole printing system is come from this step. However, the binder consumption cannot be specified in this process. It depends on the binder saturation and the actual needs of the part (volume). So the binder consumption is calculated based on the part volume and will be explained in the later sections.

4.2.3. Layer Drying Process

After each layer is printed, the sprayed binder on the powder surface needs to be dried to solidify. This process serves at preventing the binder from diffusing through the particle space of the powder and forming undesired shape. In this step, excessive solvent is also removed from the binder to make the binder stickier thus enable the adherent of the powder particles of the next layer.

The heater is IR driven and is located at the end of the X-Axis along which the print chamber is moving. The print bed moves under beneath the IR heater and heat for a certain amount of time before spreading the new layer. The heater position is shown in

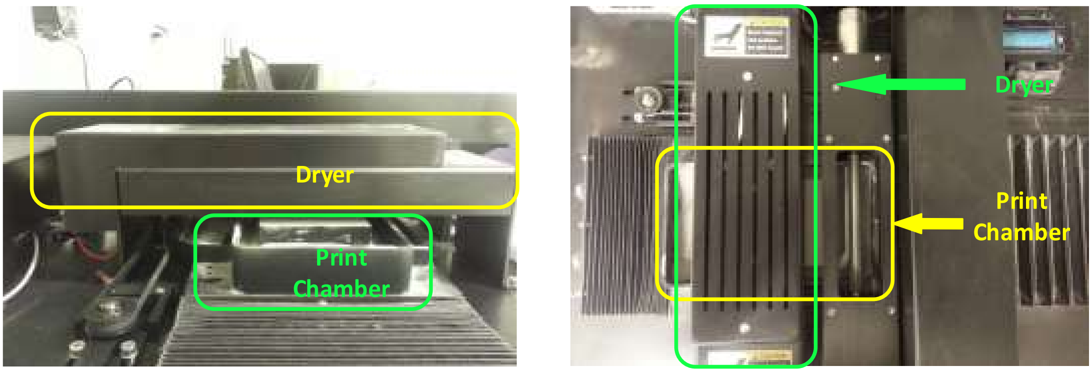

Figure 22.

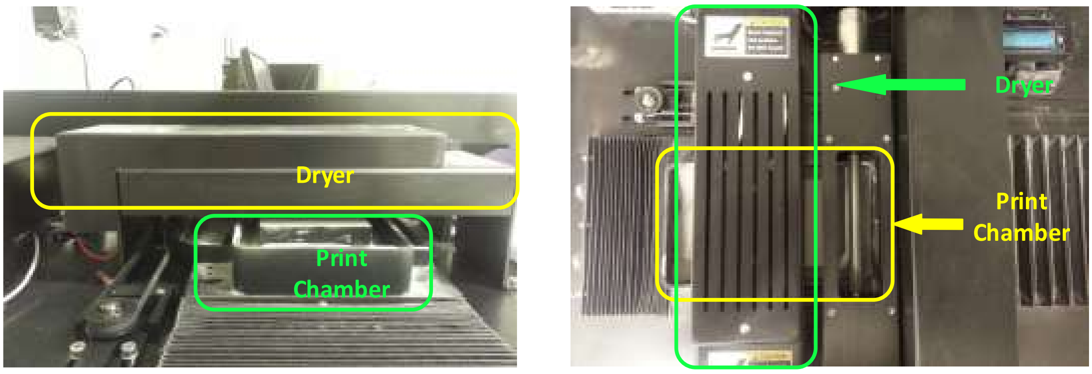

Figure 22: The Layer Drying system of BJAM printer

During the layer drying process, the print bed is firstly moved from the printing position to the heating position. The distance D_{p-d} is a fixed parameter that depends on the Model of the printer. In this process cycle, three actions is performed. The print chamber move from printing position to the drying position with a speed $v_{printchamber}$. The IR heater starts to dry the layer when the print bed stays beneath. The print chamber returns to printing position after spreading. The spreading is another operational process that will be discussed in the following section. The print chamber's motion along X-Axis is driven by step motor that has relative large torque. So the acceleration and deceleration time can be neglected. The print chamber moving is considered as uniform linear motion. The print chamber covers a distance of D_{p-d} in moving towards the IR heater position and covers another $D_{p-d} - L_c$ returning to the printing position in a constant speed of $v_{printchamber}$. L_c is the print bed length that the spreading cover. The drying time is a user defined manufacturing parameters that is critical to the product quality. The drying time is considered in our Process Parameter Model.

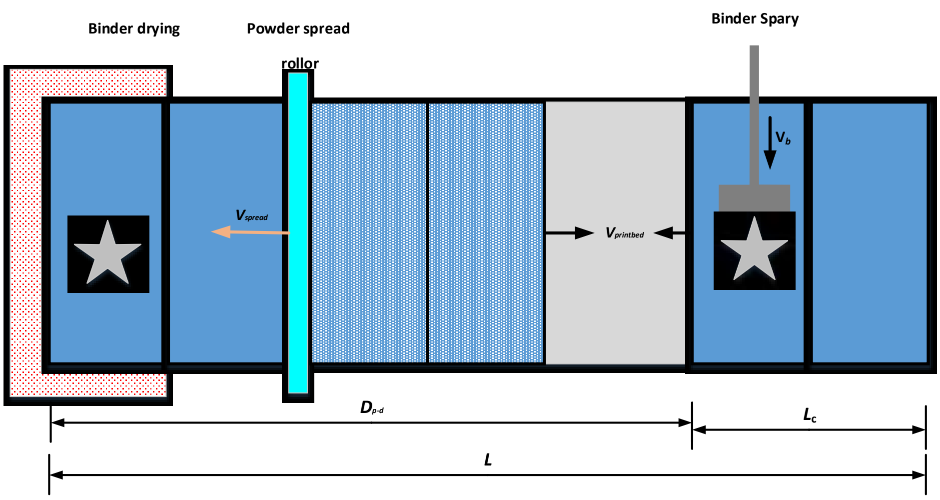

Figure 23: The Drying Process

In this process, the time consumption can be calculated in two parts, the motion time and the drying time. The motion, as assumed above, can be view as uniform linear motion. So for each layer dried, the time is calculated as shown in Equation (9). This time is equal for each layer. So the total time of the print chamber motion is the number of layers times the time of each layer. The express is shown in Equation (10)

$$t_{movlayer} = (2D_{p-d} - L_c)/v_{printchamber} \tag{9}$$

$$t_{mov} = N_{layer} \cdot t_{movlayer} = N_{layer} \cdot (2D_{p-d} - L_c)/v_{printchamber} \tag{10}$$

The user defined drying time is a fixed value for each layer dried. However, the drying time may vary layer by layer expressed as t_i for layer i. So the time consumed in the heating process is calculated as an integration of each layer. N_{layer} is the layer count of the part.

$$t_{heating} = \sum_{i=1}^{N_{layer}} t_i \tag{11}$$

To summarize, the total time consumed in this process is the sum of t_{mov} and t_{drying} :

$$t_{drying} = t_{mov} + t_{heating} = N_{layer} \cdot (2D_{p-d} - L_c)/v_{printchamber} + \sum_{i=1}^{N_{layer}} t_i \tag{11}$$

In this process no material is actually consumed.

4.2.4. Powder Spreading Process

As mentioned in the previous section of the Layer Drying process, the Spreading Process is situated in between the heating and print chamber returning. The Powder Spreading Process serves as adding a new layer to the current dried layer. The spreading process can be described as in

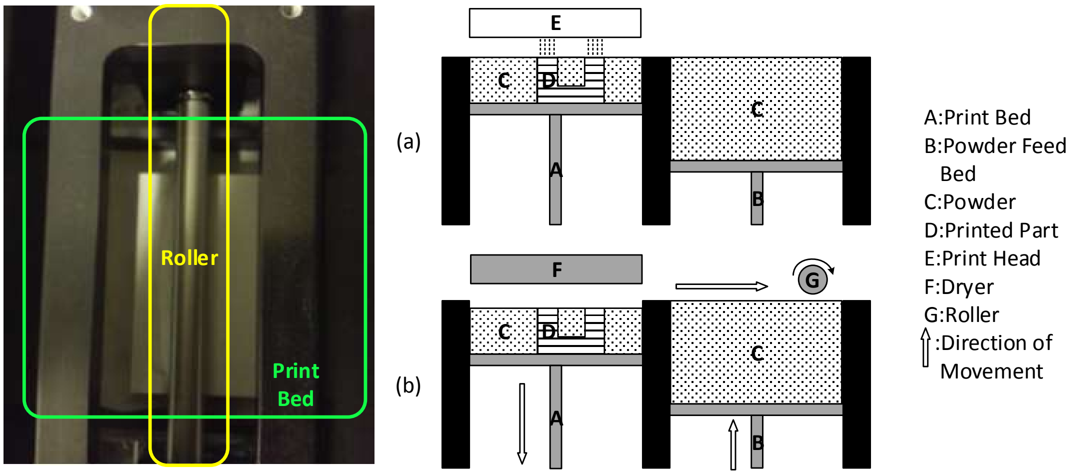

Figure 24. In the left, (a) shows the powder drying process. Afterwards, in (b) the print bed lower one layer height while the powder feed bed goes up to a certain amount times of one layer depending on the *Feed Ratio* R_{feed} parameter set by the user.

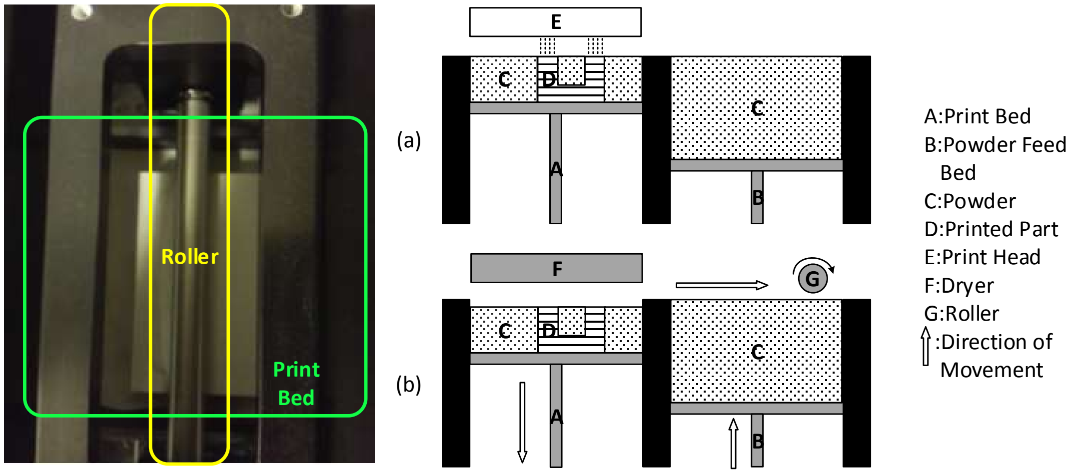

Figure 24: Powder Spreading Process

The *Feed Ratio* is normally set from 1.7 to 2.5 according to the surface size of printing intersection and layer thickness to ensure the full coverage of the print bed with a new layer of powder. Lower *Feed Ratio* when the printing intersection is large will lead to insufficient powder for the next layer and may cause the printing failure. Higher *Feed Ratio* may cause the insufficient powder to supply the printing due to the limitation of the powder feed bed, since excessive amount of powder will be spread off during the spreading process.

A roller is used to spread the powder from the powder feed bed towards the print bed with the print bed traversing slowly under. The *spreading speed* v_{spread} is also a user define process parameter. Although the previous described Process Parameters Optimization and Recommendation Model doesn't take into account of this parameter, it is critical in assuring the layer quality. The spread speed is related to the *Feed Ratio* and the printing intersection area. The spreading needs to assure the flatness of the new layer of powder. Too fast may cause the insufficient solidarity of the powder in the new layer. Too slow will lead to an extra amount of unnecessary time. In practical of ExOne BJAM printer, to increase the printing speed, the spreading only starts when the roller has moved away from the powder feed bed and entering the print bed. When the roller is on the powder feed bed, the print bed moves at regular speed $v_{printchamber}$ as the motion in the Layer Drying Process. When the roller comes onto the print bed, the print chamber starts to move with a much slower user defined spread speed v_{spread}. The same as the layer drying time, the spreading speed can also be adjusted from layer to layer according to the user's demands. With the fix length of the print chamber L_c, and the equality of the print bed and powder feed bed, the time consumption in spreading a layer i is $t_{i-spread}$ is shown in Equation (12) with the spreading speed $v_{i-spread}$. The total time consumed during the Powder Spreading Process t_{spread} is expressed in Equation (13).

$$t_{i-spread} = \frac{L_c}{2v_{printchamber}} + \frac{L_c}{2v_{i-spread}} \tag{12}$$

$$t_{spread} = \sum_{i=1}^{N_{layer}} t_{i-spread} = \frac{N_{layer} \cdot L_c}{2v_{printchamber}} + \sum_{i=1}^{N_{layer}} \frac{L_c}{2v_{i-spread}} \tag{13}$$

In this process, the powder is consumed. From the previous description, the powder used in this process is calculated from the size of powder feed bed $S_{feedbed}$, the layer thickness h_{layer} and the *Feed Ratio* R_{feed}. It can be expressed as:

$$M_{all-powder} = N_{layer} \cdot S_{feedbed} \cdot h_{layer} \cdot R_{feed} \tag{14}$$

However the actual powder that covers the print bed is less since the *Feed Ratio* is larger than 1. The extra amount of the powder is spread off from the print bed goes into the chamber. They will be recycled after printing. Additionally on the layer of the print bed only the powder that covers the intersection of the layer will go into the final part. The extra amount of powder will serve as the supporting material that will not be sprayed with binder and will be recycled too. So in considering the powder consumption, only the powder goes into the final part will be taken. It is calculated layer by layer too based on the area size of the intersection in layer i $S_{i-intersection}$. The powder consumption is counted as:

$$M_{part-powder} = \sum_{i=1}^{N_{layer}} S_{i-intersection} \cdot h_{layer} \tag{15}$$

The other amount of used powder will be recycled. But not all of them. A powder recycle rate $R_{recycle}$ is derived from the experiment data. So the powder waste can be expressed as:

$$
\begin{aligned}
M_{waste-powder} &= (M_{all-powder} - M_{part-powder}) \times (1 - R_{recycle}) \\
&= (N_{layer} \cdot S_{feedbed} \cdot h_{layer} \cdot R_{feed} \\
&- \sum_{i=1}^{N_{layer}} S_{i-intersection} \cdot h_{layer}\ ) \times (1 - R_{recycle})
\end{aligned} \tag{16}
$$

From equation it can be seen that the powder consumption is actually a function of the size of intersection, in other words, it is related to the part volume V_{part} and the powder pack rate R_{pack}. It is not directly relevant to the printing operation.

4.2.5. Automatic Cleaning Process

During the printing process, the printhead will be constantly cleaned after printing a certain number of layers or after a certain amount of time. The frequency is set up by the user according to needs as well as the cleaning cycle. On the ExOne M-Lab BJAM printer, by default, the cleaning frequency is once every 12 layers printed and the cleaning cycle includes 2 times of wiper cleaning, 2 times of cap cleaning, 2 times of printhead wiping, 2 times of prime and 2 times of nozzle fire

In our modelling work, the default value is taken since in seldom location, the cleaning cycle and frequency are changed by the users. The auto cleaning consumes around 300 seconds of time every time and the total time consumption of auto cleaning during the print is shown in Equation (17).

$$
t_{autocleaning} = \left\lfloor \frac{N_{layer}}{f_{autocleaning}} \right\rfloor \times t_{cleaningcycle} \tag{17}
$$

The $f_{autocleaning}$ represents the auto cleaning frequency during the print. $t_{cleaningcycle}$ is the time consumed of each automatic cleaning. A floor integer is acquired as the times of auto cleaning performed during the printing.

In this process, the binder and cleaner are consumed and the waste is generated. As mentioned in the Printer Initialization, Preparation, Cleaning and Testing Process, the default cleaning cycle consumes around 30ml of cleaner, 5ml of binder. 35ml of waste is generate as well. So we can conclude that the binder consumption, the cleaner consumption and the waster generation is expressed as:

$$M_{b_{autocleaning}} = \left\lfloor \frac{N_{layer}}{f_{autocleaning}} \right\rfloor \times M_{b_{cleaningcycle}} \tag{18}$$

$$M_{c_{autocleaning}} = \left\lfloor \frac{N_{layer}}{f_{autocleaning}} \right\rfloor \times M_{c_{cleaningcycle}} \tag{19}$$

$$M_{w_{autocleaning}} = \left\lfloor \frac{N_{layer}}{f_{autocleaning}} \right\rfloor \times M_{w_{cleaningcycle}} \tag{20}$$

4.2.6. Curing Preparation and Setup

After finishing the printing operation, the printed green part is to be sent into the curing oven and to remove the binder residual. A special designed container is used to transport the green part together with its surrounding powder to the curing oven as shown in **Error! Reference source not found.**. This operation needs to be done manually and carefully. The container as well as its base will go into the curing oven together with the green part and its surrounding powder.

The curing oven setup is simple and easy. The operation pad is shown in **Error! Reference source not found.**. On the time consumption aspect, the experiments data (see Appendix I) shows an average of 8 minutes with a minimum of 4 minutes and maximum of 12 minutes. While on the material consumption side, the container is not 100% concealed. So during the transportation, a small amount of powder may fall. This happen too in the depower process. A rough estimation of 14% in both process is assigned to the waste powder.

Figure 25: Curing container

4.2.7. Curing Process Profile

The curing process is quite simple. It serves at remove the binder from the printed part. Because binder residual will affect largely the mechanical properties of the part. The idea is to heat the part in an oven at a certain temperature and for a certain amount of time to make sure the binder in between the powder particle evaporate as much as possible.

The curing profile is related to the binder saturation and the binder physical properties. According to ExOne's recommendation, the curing process for S4 Stainless Steel and R1 binder is 5 hours at 175°C. For the current research, further investigation is needed to look into the physical properties of the binder and the relationship of the binder evaporation and the curing temperature. At current stage, 175°C for 5 hours is considered only. While the curing process also includes in temperature rising and cooling down. From the curing oven manual, the temperature rising rate R_{rising} and the cooling down rate $R_{cooling}$ can be acquired. Theoretically, the time needed in temperature rising and cooling down can be expressed as:

$$t_{rising} = \frac{T_{target} - T_{room}}{R_{rising}} \tag{21}$$

$$t_{cooling} = \frac{T_{target} - T_{room}}{R_{cooling}} \tag{22}$$

In the regular operation of the ExOne M-Lab BJAM machine, the room temperature is kept at 25°C (297K). The temperature rising and cooling down rate are $R_{rising} = 0.13K/s$ and $R_{cooling} = 0.0179K/s$ separately[25]. Also the time recorded during the experiments (see Appendix I), is in accord with the experiment data. It takes about 20 minutes for the temperature to rise from 25°C to 175°C and about 2 hours 20 minutes to cooling down.

4.2.8. Depowdering Process

After the curing process, when the curing oven temperature falls back to the room temperature, the cured part is taken out from the container and separated from the supporting powder. This action is call depowdering. The process pictures are shown in **Error! Reference source not found.**.

Figure 26: Depowdering Process

The depowdering is a human intensive work. It requires familiarity of the part sshape and patients. Air blow and soft brushes are used to ensure that no extra powder is adhered to the green part. Especially if there is hollow structure in the part. In the printing process, the hollow structure is filled by the supporting powder. It is critical to clean the extra powder. For example, in printing grid lattice structure as shown in Figure 27, the lattice unit cells are often very small and sometimes the unneeded powder will not be easy to get out. To maintain the structure and the desired mechanical properties, high pressure air blow is needed. Meanwhile, in this phase since most of the binder are evaporated, the part is very fragile. So delicate work is required too.

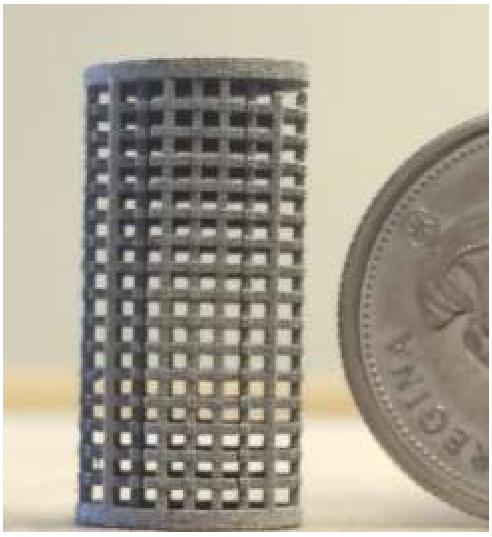

Figure 27: Well-depowdered Lattice Cylinder

Depowdering process is the most human work consumed process, depending on the complexity of the part and the worker's skill, the time may vary. From experiment data (see Appendix I), the depowdering time is recorded. The depowdering process are all conducted by the same person. The recorded data show an average of 20 minutes work with the minimum time of 18 minutes and maximum of 23 minutes.

In this process, the extra powder will be recycled. However, during the air blow, some of the powder may be blew out of the base of the container. This part of powder cannot be recycled. From the experiments, an estimation of 14% powder waste rate is obtained combining the curing and pre-curing process.

4.2.9. Sintering Preparation and Setup

The sintering preparation refers to set the cured green part into the crucible with supporting quartz. If infiltration is required, then the infiltration material should be weighted and set up in the container and positioned alongside with the part.

The sintering can either start directly after the depowdering process or on any depowdered part from the inventory. Sometimes, due to the long duration and the protection gas limitation or shortage, serval different parts are stored after depowdering and to be sintered together in the same batch.

Figure 28: Sintering crucible with different parts

The setup time also includes the sintering furnace profile setup. The ExOne furnace has already imbedded several often used profiles. Unless setting up a new customized profile, this part doesn't take much time. The most time consuming work in the sintering set up is the infiltration material weighing and positioning. The stream guidance of infiltration material container has to be touched to the part surface but if the contact area is too large, the stream guidance will be connected to the part after sintering. This work requires human effort too. The time may vary due to the familiarity of the worker.

In the current experiment, no infiltration is needed, the data recorded for this process is around 2 minutes.

According to the calculation tool of ExOne, if infiltration is needed, the required amount of the bronze is 1.18 times the weight of the green part.

4.2.10. Sintering Process Profile

Sintering serves at drying out the any left-over binder in the cured part and generate solid connections of among the powder particles of the part. Infiltration also happens during the sintering process. The temperature of the sintering will reach 1100°C that will melt the steel powder. Since the powder pack rate is about 60%, shrinkage will happen during the sintering. Also neutral protection gas is needed to prevent the part from oxidization.

Different sintering profile applies to different needs. Different sintering profile has different temperature curve. Customized temperature curve can be programmed on the furnace UI. In sintering profile, several different operations are conducted, including vacuuming, injecting protection gas, turning off protection gas, temperature rise, cooling down and tone alert. Several default profiles have been imbedded in the oven[26]. S4-One step is often used for ExOne S4 stainless steel. The sintering temperature curve is shown in Figure 29.

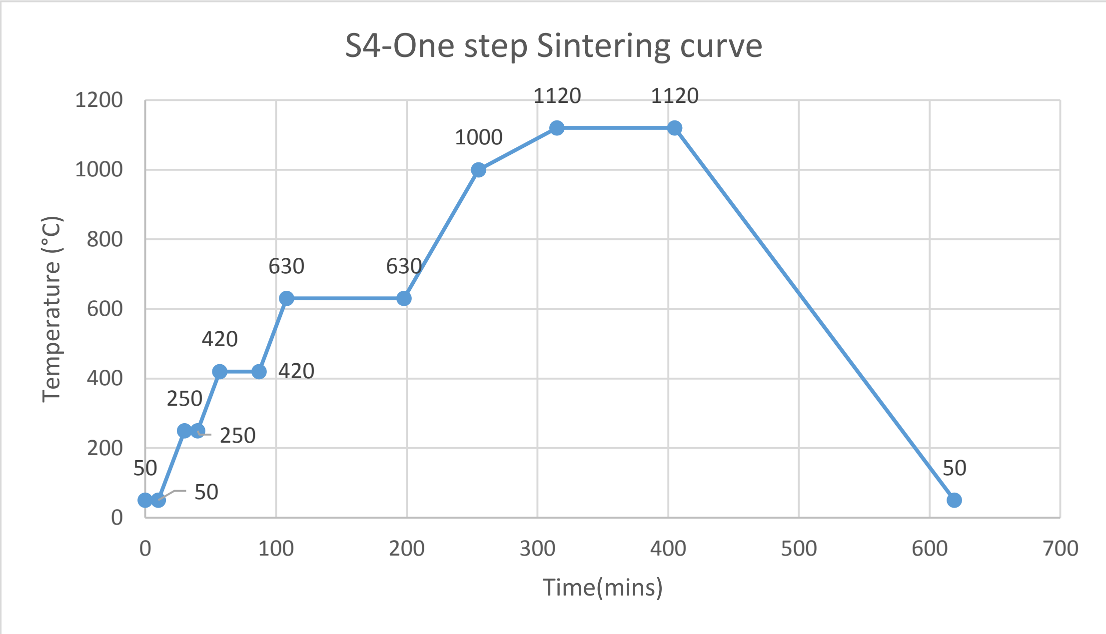

Figure 29: S4-One step Sintering Profile

In this process, the time consumed is exactly obtained from the sintering profile. For example, in the S4-One step profile, 619 minutes is used. The default sintering profiles has the precise time consumption.

Considering the material consumption, if infiltration involved, then as mentioned in the previous chapter, 1.18 times of the printed part mass bronze is needed. The protection gas is not considered in the current research since no standard flow rate has established nor been used in the sintering.

4.3. Time Consumption Model and Algorithm

The algorithm serves to predict the time consumption of BJAM production from the design and manufacturing process parameters. On the input side, two modulus are developed, to load and slice the STL file and to read the manufacturing process parameter data from either the user defined parameter or the recommended parameters given by the Process Parameter Recommendation System descripted in Chapter 3. On the output side, the algorithm will give the time consumption of each sub processes, the manual working time and the total production time.

Following the process of section 4.2, the Time Consumption Model can be concluded as the follow flowchart.

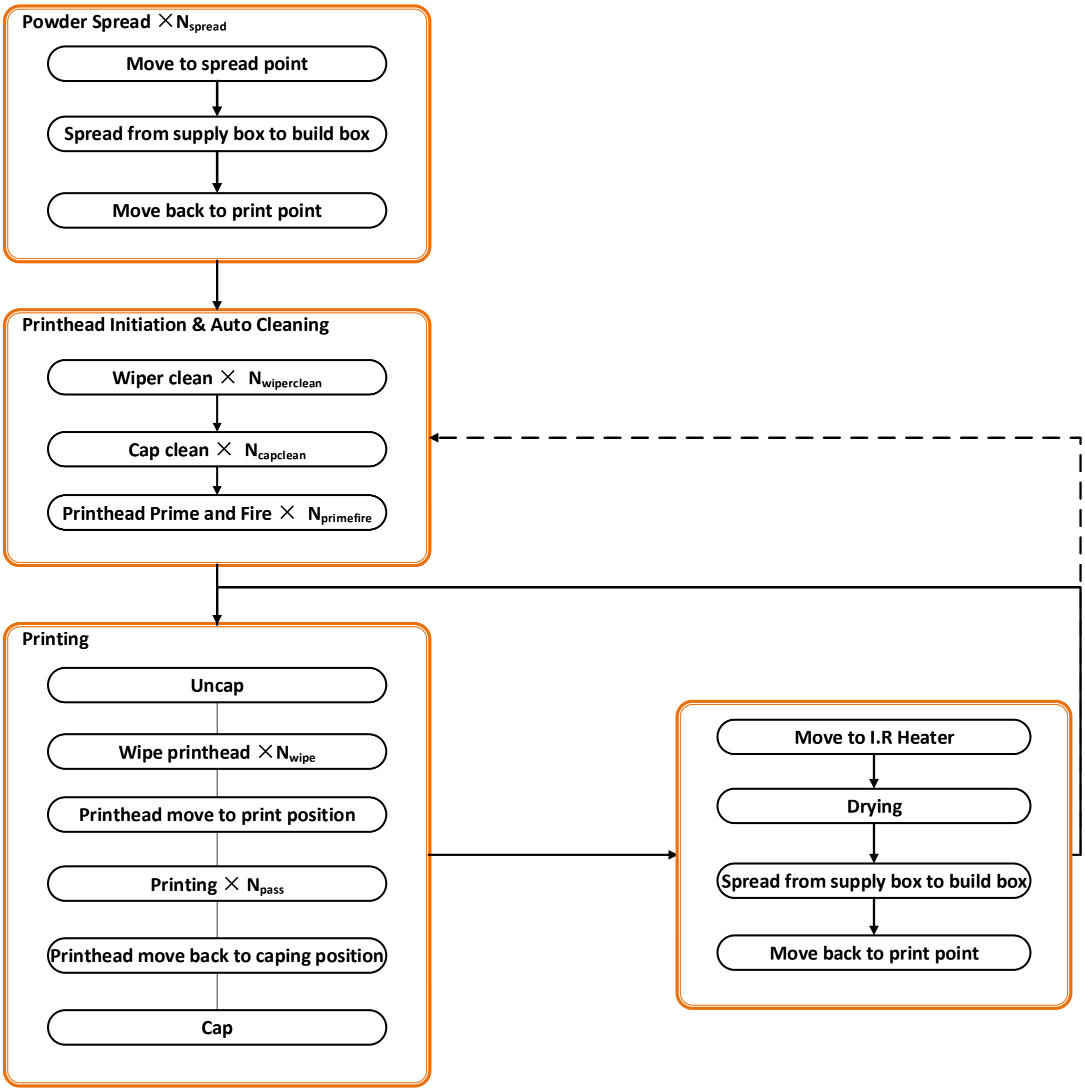

Figure 30: Time Consumption Algorithm flowchart

In detail, the algorithm read the printing orientation and part dimension on Z-axis from the STL file, combining the parameters obtained including the layer thickness, the drying time, spread speed, the curing profile and the sintering profile to calculate the time consumption. The algorithm is presented in Figure 31.

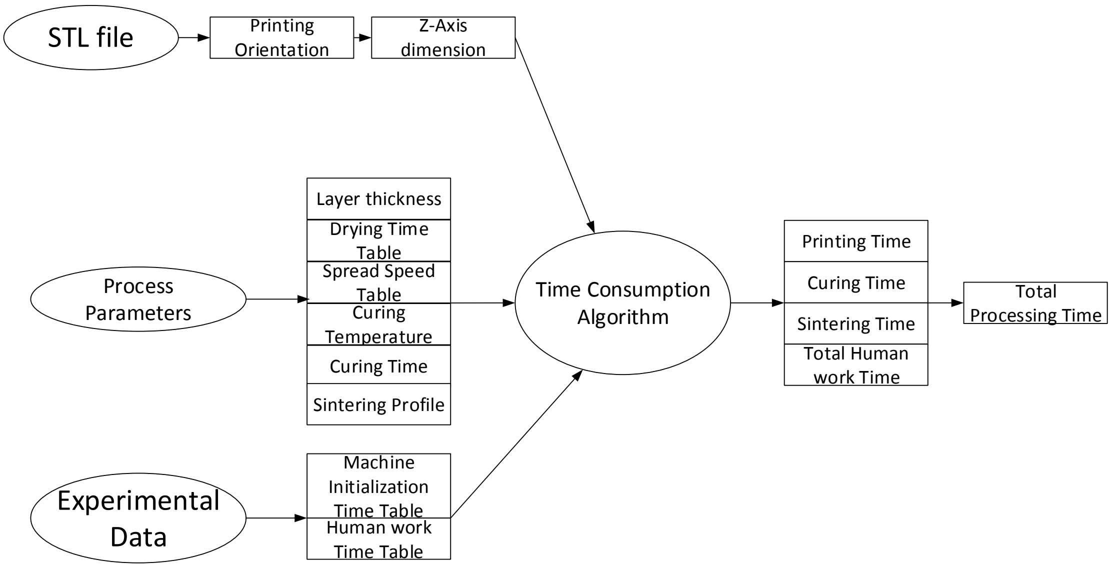

Figure 31: The structure of the Time Consumption Algorithm

From previous discussion in section 4.2, the time consumption is simply the sum of each operation. For one part printed, the time can be expressed as:

$$t = t_{printing} + t_{curing} + t_{sintering} \tag{23}$$

Where printing time includes the printer preparation, setup time $t_{printinit}$, the N_{layer} times of iteration of binder spraying, layer drying and powder spreading time, plus $\frac{N_{layer}}{f_{autocleaning}}$ of auto cleaning time. To be mentioned, the layer drying and powder spreading time may not be the same for different layers. These time cannot be calculated directly by multiply the number of layers. The binder spray time of each layer t_{spray} is identical and independent to the size of printing area because the printhead has multiple nozzles that works simultaneously. The total drying time and powder spreading time can be obtained from the drying time table and the spreading speed table as shown in Equation (11) and Equation (13). Then we have,

$$t_{printing} = t_{printinit} + N_{layer} \cdot t_{spray} + t_{drying} + t_{spread} \tag{24}$$

The $t_{printinit}$ is the average value from the experiment data. The N_{layer} is obtained from the part dimension on Z-axis and the layer thickness as:

$$N_{layer} = \frac{h_{part}}{h_{layer}} \tag{25}$$

The Time Consumption Model is integrated in the Matlab GUI together with the Process Parameters Recommendation System.

4.4. Material Consumption Model and Algorithm

Similar to the Time Consumption Model, the Material Consumption Model extracts data from the input STL model and the process parameters. As mentioned in the previous section, the material consumption is mainly based on the part design, especially the powder and binder consumption. Only waste binder and powder are related to the operations. While the cleaner consumption is operation based. It is consumed in the printer initial cleaning and the auto cleaning during the process. The material consumptions related processes is shown in Figure 32.

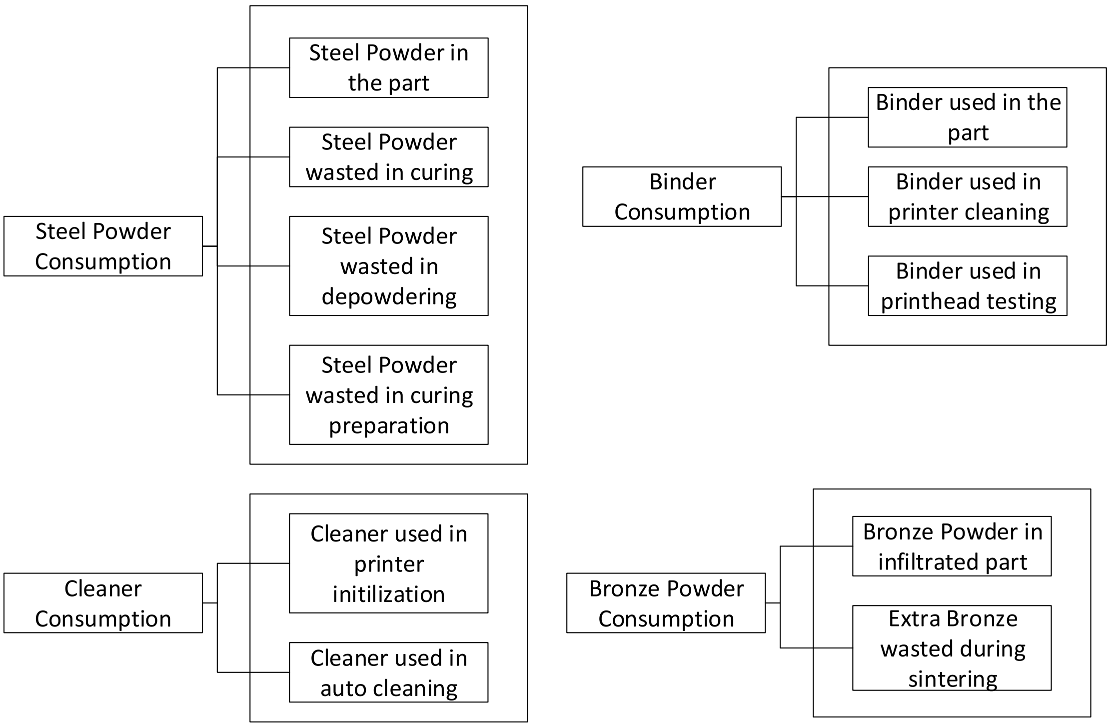

Figure 32: Material Consumptions in possible processes

So in the algorithm, the most important function is to get the part's geometric properties of each layer to calculate the binder and powder needed for each layer. The area size of the layer intersection and the layer thickness are two related factors. Also, in order to calculate the binder and powder needed for each layer of the part, the binder saturation and the powder pack rate are two volume related factors that need to know. Sintering profile is to identify if there is bronze-involving infiltration. The waste of powders in each step is largely based on the experiment data since no analytical model existed. The algorithm structure is shown in Figure 33.

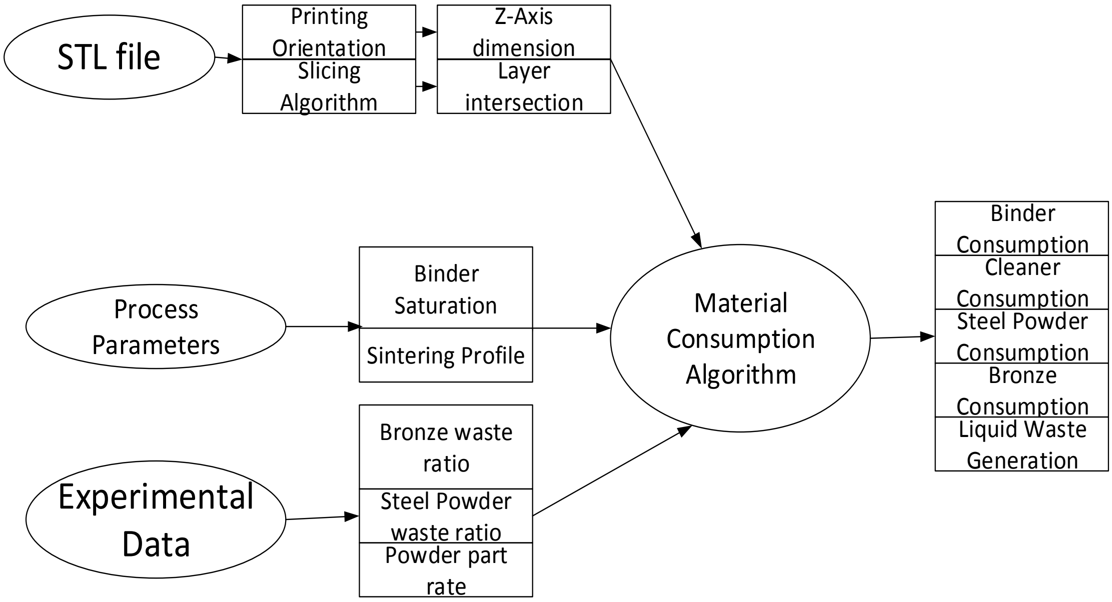

Figure 33: Structure of Material Consumption Algorithm

The steel powder consumption is calculated layer by layer from its volume. Since the powder are not fully dense, only 60% of pack rate is achieved. So it can be expressed as:

$$M_{powder} = \sum_{i=1}^{N_{layer}} S_i \cdot h_{layer} \cdot R_{pack} \cdot \rho_{powder} + M_{powderwaste} \tag{26}$$

S_i represents the area size of the layer i. R_{pack} represents the steel powder pack rate. ρ_{powder} is the powder density. The wasted steel powder is the average value obtained from experiments. About 14% in total has been wasted.

The binder consumption is also calculated layer by layer by the part's volume and the binder saturation which defines the density of the binder. Similar from the steel powder, it can be expressed as:

$$M_{binder} = \sum_{i=1}^{N_{layer}} S_i \cdot h_{layer} \cdot R_{pack} \cdot S_{binder} \cdot \rho_{binder} + M_{b_{cleaningcycle}} \cdot \left\lfloor \frac{N_{layer}}{f_{autocleaning}} \right\rfloor + M_{binderinit} \tag{27}$$

The binder used for printhead testing, printer initialization and the printer initial cleaning are about 26~30ml according to section 4.2.1. The binder used per auto cleaning is about 5ml refer to the experimental data.

The cleaner consumption is calculated from the cleaning process both in the printer set up and the auto cleaning cycle.

$$M_{cleaner} = \left\lfloor \frac{N_{layer}}{f_{autocleaning}} \right\rfloor \times M_{c_{cleaningcycle}} + M_{cleanerinit} \tag{28}$$

In each auto cleaning cycle, 35ml cleaner is used, the printer initialization phase cost 70ml of cleaner as mentioned in section 4.2.1.

The waste is mainly generated from the binder and cleaner used in the cleaning process. They can be expressed as:

$$M_{waste} = M_{cleaner} + M_{b_{cleaningcycle}} \cdot \left\lfloor \frac{N_{layer}}{f_{autocleaning}} \right\rfloor + M_{binderinit} \tag{29}$$

The bronze powder consumption if the infiltration is involved is mainly related to the part's weight. According to the recommendation of ExOne Inc, 1.18g bronze is needed for each gram of the part printed in steel powder. So if bronze is used in infiltration, the consumption is:

$$M_{bronze} = 1.18 \cdot M_{powder} \tag{30}$$

The Material Consumption Model is integrated in the Matlab GUI together with the Process Parameters Recommendation System and Time Consumption Model.

4.5. KPI Model and Algorithm

KPIs are critical in evaluating a production system. Different categories of KPIs may be used in the evaluation according to different needs. Based on the Time Consumption Model and the Material Consumption Model developed in this research, time and resource related KPIs are able to be calculated.

On the machine schedule aspect, *Availability, Preparation Degree and Machine Efficiency* are calculated from machine operation schedule as shown in Figure 34.

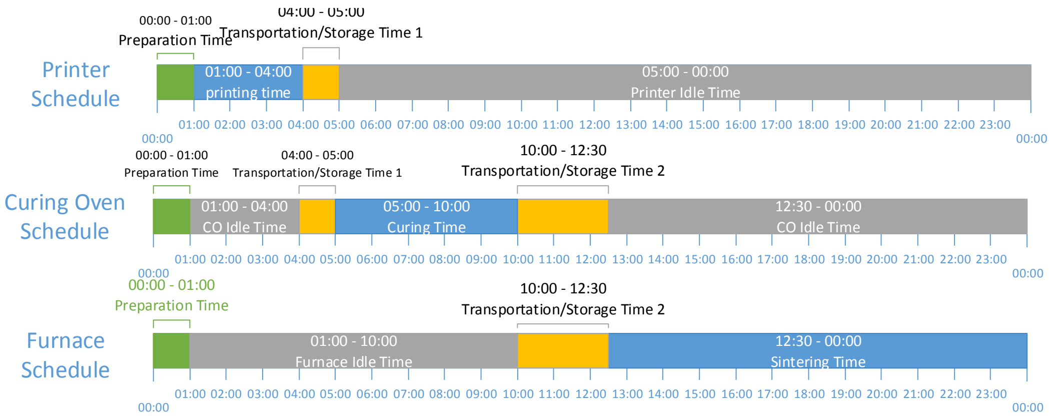

Figure 34: Machines Schedule of BJAM production system

Availability presents the degree of capability that the machine is able to work on other tasks during the production process. Higher *Availability* means more efficiency of the whole production system. It can be calculated as:

$$\begin{aligned} Machine\ Availability &= 1 - (busy\ time / total\ processing\ time) \\ &= idle\ time / total\ processing\ time \end{aligned} \tag{31}$$

As shown in Figure 34, the *busy time* is the time that the machine are not available for other tasks, including the working, preparing, breaking down and maintaining status. The *total processing time* is the time of the whole production time.

The *Preparation Degree* represents the level of preparation needed before conducting the value added work. Lower *Preparation Degree* means less time is needed when the machine switch tasks after finishing one. The shorter the preparation time, the higher efficiency the production system will have. *Preparation Degree* is calculated as:

$$\begin{aligned} &Machine\ Preparation\ Degree \\ &\qquad = preparation\ time(setup\ time)/busy\ time \end{aligned} \tag{32}$$

Efficiency represents the portion of the value added process in the whole production time. Higher *Efficiency* means during the production, the machine waste less time in the non-value added process.

$$Machine\ efficiency = operation\ time(value\ added)\ /\ busy\ time \tag{33}$$

The *operation time* is the time that the machine is working on the products.

On the material consumption and waste generation aspects, *Material Efficiency* and *Material Consumption Ratio* can be obtained from the Material Consumption Model.

Material Efficiency represents the portion of material used in the value added function in the total material consumption. Higher *Material Efficiency* means lower rate of waste in the production which will lead to a great saving in the budget.

$$Macterial\ Efficiency = amount\ of\ value\ added\ /amount\ used \qquad (34)$$

In the BJAM Model, only binder and powder are used in the value added process. The cleaner will not have an efficiency evaluation since no wasted cleaner exists. And as mentioned in the previous section, the steel powder wasted during the whole curing process is obtained from the experimental data as a fixed value of *14%*. So the *Material Efficiency* of steel powder is *1/ (1+14%) = 87.72%.*

Material Consumption Ratio is how much material is used in producing one unit of the products. Since the AM has a flexible production type, unlike the conventional production line where one product is produced in massive amount, the unit product of AM is defined as gram of parts. So the *Material Consumption Ratio* of AM is defined as the material used per gram of parts. In this case the steel powder *Consumption Ratio* is actual the same as the *Material Efficiency.* While the binder and cleaner are then measure in *ml/g. Waste Ratio* is also calculated in the same logic. The *Material Consumption Ratio* is always used in evaluating the cost of a certain product in practical production.

$$Macterial\ Consumption\ Ratio = amount\ used\ /\ unit\ product \qquad (34)$$

The KPI Model is also integrated into the Matlab GUI together with the previous models.

4.6. Model Integration

A Matlab GUI has been developed to integrate all the models together to act as production prediction tool as shown in Figure 35.

The GUI includes 5 parts shows in the red frame in Figure 35: the STL file load, the Process Parameter Recommendation System, the User defined Process Parameter

Part, the Time and Material Consumption Prediction and the KPI estimation. The user needs to load the STL file in the first place. Then if the Recommendation Parameters are needed, the three desired quality bars should be adjusted accordingly before generate the recommended parameters and predicted the quality properties. The user can also use self-defined parameters input in the GUI to calculate the time and material consumption as well as the KPI predictions.

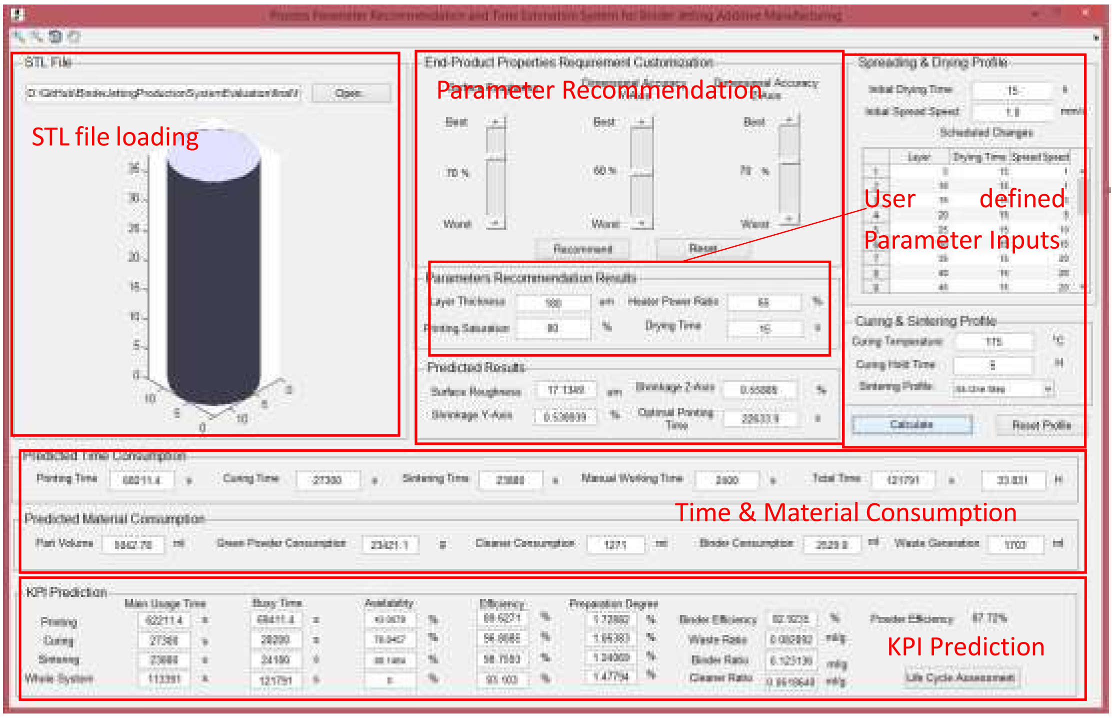

Figure 35: Matlab GUI Integration

In order to validate all the models, a case study is performed. An optimized engine bracket is produced by BJAM production system. The predictions of time and material consumption is conducted using the Matlab GUI tool and compared to the practical data. The result will be shown in Chapter 6.

Chapter 5: LCA and LCIA Analysis of BJAM

"Life Cycle Assessment (LCA) is a structured, comprehensive and internationally standardized method. It quantifies all relevant emissions and resources consumed and the related environmental and health impacts and resource depletion issues that are associated with any goods, services or products. " [27]. LCA considers all of energy consumption, resources consumption and environmental and health impact associated with the product. The full life-cycle of a product are included from the extraction of resources, through production, usage and up to the End-of-Life (EOL) treatments. According to Ashby[28], the whole life cycle of a product can be divided into five phases: the raw materials extraction, the manufacturing, the transportation, the use phase and the EOL. LCA aims at evaluating the resource consumption and the environmental impacts of a products. It can be divided into two section, Life Cycle Inventory (LCI) assessment and Life Cycle Impact Assessment (LCIA). The former focus on the material and resource consumption, while the later focus on the environmental impacts. The comprehension of LCA can avoid resolving one problem while creating others. LCA method is widely used in the production design and development in the manufacturing industry. LCA is considered as a reliable and powerful tool to help make decisions, complementing other methods and provide data for sustainability analysis.

The relevance of a LCA study relies strongly on the quality of the database used concerning the materials and processes studied. For instance, turning and milling are very well documented whereas for more "exotic" processes such as AM, "LCA database is often unavailable, not representative of real situations or based on unrealistic assumptions"[11]. Moreover, "most of the available data on manufacturing processes are incomplete: the focus is often limited to theoretical energy consumption, and data on potential process emissions are rarely found"[29]. The commercial database such as EcoInvent, GaBi are continuously improving, more and more data will be included.

5.1. Methodology and Principles of LCA

LCA is a phased and systematic approach [27]. According to Ashby [28], it consists of four components. The relationships are shown in Figure 36.

1. Goal definition and scoping: Define and describe the product, process and activity. Establish the context in which the assessment is to be made as well as identify boundaries and environmental impacts to be reviewed for the assessment.
2. Inventory analysis: Identify and quantify energy, resources and material usage and environmental release.
3. Impact assessment: Assess the potential human and ecological effects of energy, resources and material usage and environmental release identified in the inventory analysis.
4. Interpretation: Evaluate the results of inventory analysis and impact assessment to select the preferred product, process or service with a clear understanding of uncertainty and the assumption used to generate the result.

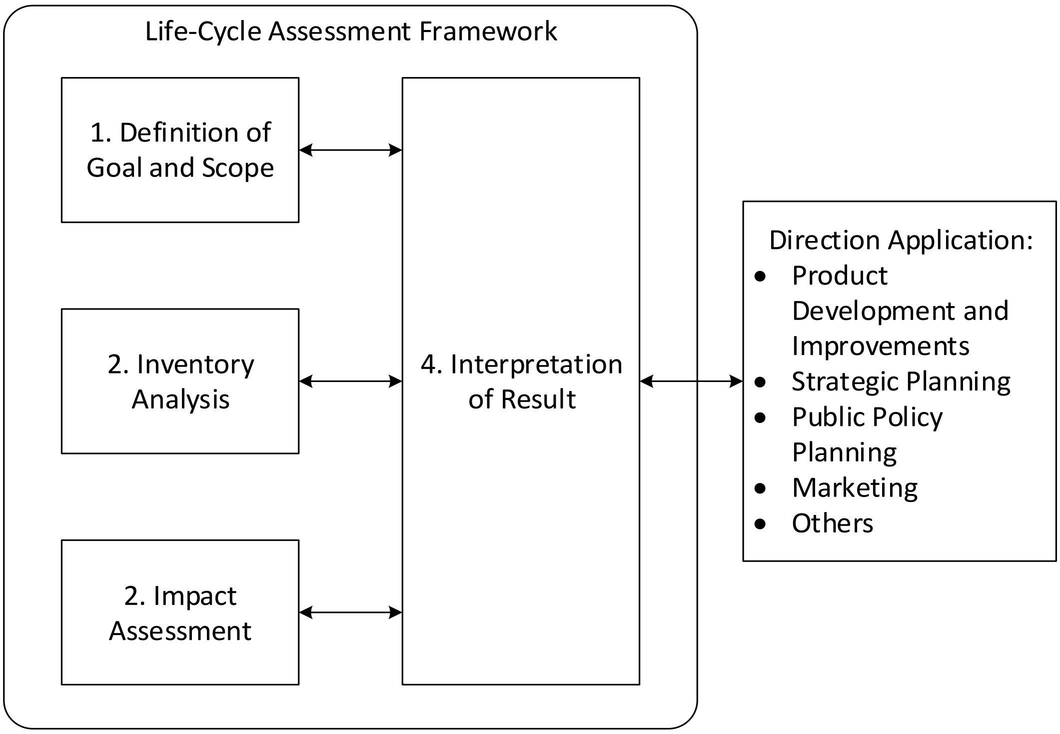

Figure 36: LCA Framework[30]

5.1.1. Life Cycle Inventory Assessment

The first step of Inventory analysis is to define a basic process with inputs and outputs flows as shown in Figure 36.

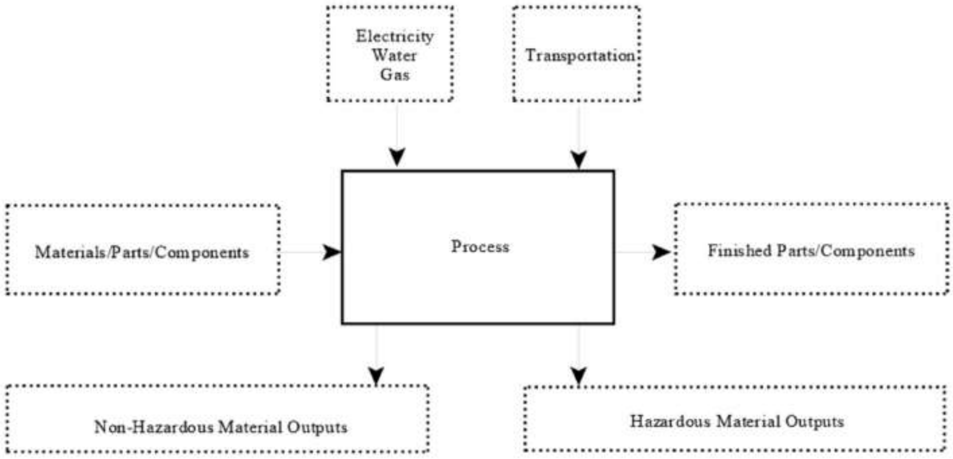

Figure 37: Generic Process of LCA[31]

Process flow diagram method is the most straight forward way to calculate LCI data. As the name suggests, this compilation is based on a process flow diagram. It appears in early LCA researches and guidelines such as works of [31], [32] and [33]. A brief sample of this method is given in research of [34]. As shown in Figure 38, a process flow diagram shows how the commodity flows connect the processes together of a toaster product system.

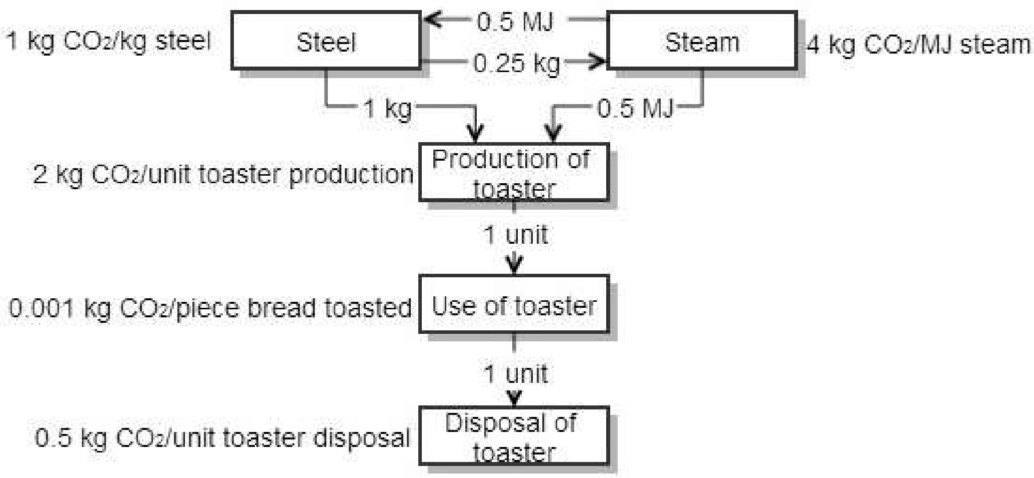

Figure 38: LCI example of Toaster

In Figure 38, squares represent the processes and arrows represent resource flows. For each process, there is a ratio of between the inputs and outputs. In this example, only CO_2 is considered as output, other assumptions are made as following:

A toaster is produced from 1 kg of steel using 0.5 MJ of steam power while generate 2 kg of CO_2. Producing 1 kg of steel requires 0.5 MJ of steam and generates 1 kg of CO_2. Producing 1 MJ of steam needs 0.5kg of steel and generates 4 kg of CO_2. The life-time of a toaster is 1000 times of toasting. Toasting 1 piece of bread generate 0.001 kg of CO_2 and disposal of toaster generate 0.5 kg of CO_2.

This above provides the fundamental data for LCI calculation. After collecting data, the amount of energy, material consumed and emission generated are calculated for the functional unit, here, the toaster. To produce 1000 pieces of bread, the CO_2 emission can be calculated:

$$\begin{aligned}&\left(\frac{1\ kg\ CO_2}{kg\ steel}\cdot 1\ kg\ steel\right)+\left(\frac{4\ kg\ CO_2}{MJ\ steam}\cdot 0.5\ MJ\ steam\right)\\&\quad+\left(\frac{2\ kg\ CO_2}{unit\ toaster\ prod.}\cdot 1\ unit\ toaster\ prod.\right)\\&\quad+\left(\frac{0.001\ kg\ CO_2}{piece\ bread\ toasted}\cdot 1000\ pieces\ bread\ toasted\right)\\&\quad+\left(\frac{0.5\ kg\ CO_2}{unit\ toaster\ disp.}\cdot 1\ unit\ toaster\ disp.\right)\\&\quad=6.5\ kg\ CO_2\end{aligned} \tag{35}$$

However, for the toaster system in the example, as shown in Figure 38, there is a loop existing between steel and steam which means the steel production process indirectly uses its own output, the steel through steam production. It's also the same situation for the steam. To calculate the emission generated by this kind of loop, [33] proposed a iterative method to find out the answer. For the toaster example, it solved as following:

$$\begin{aligned}&\left(\frac{4\ kg\ CO_2}{MJ\ steam}\cdot 0.5\ kg\ steel\right)+\left(\frac{1\ kg\ CO_2}{kg\ steel}\cdot 0.25\ kg\ steel\right)+\left(\frac{4\ kg\ CO_2}{MJ\ steam}\cdot\right.\\&\left.0.125\ kg\ steel\right)+\left(\frac{1\ kg\ CO_2}{kg\ steel}\cdot 0.0625\ kg\ steel\right)+\left(\frac{4\ kg\ CO_2}{MJ\ steam}\cdot\right.\\&\left.0.03125\ kg\ steel\right)+\cdots\\&+\left(\frac{1\ kg\ CO_2}{kg\ steel}\cdot 0.25\ kg\ steel\right)+\left(\frac{4\ kg\ CO_2}{MJ\ steam}\cdot 0.125\ kg\ steel\right)+\\&\left(\frac{1\ kg\ CO_2}{kg\ steel}\cdot 0.0625\ kg\ steel\right)+\left(\frac{4\ kg\ CO_2}{MJ\ steam}\cdot 0.03125\ kg\ steel\right)+\cdots\end{aligned} \tag{36}$$

Through calculation, the total CO2 emission for the toaster system is $6.5+4=10$ kg CO2.

5.1.2. Life Cycle Impact Assessment

The LCIA concerns the impacts towards the environments and society. The LCIA consists of 7 parts:

- Impact Categories: to which aspect the impact affect such as global warming, human health,etc.
- Classification: relating the inventory results to the impact categories;
- Characterization: convert results into scientific characterization factors such as the Global Warming Potential (GWP);
- Normalization: convert the data into comparable indicators such as CO_2 equivalent;
- Grouping: put impact categories into sets such as different level of affection, local or global;
- Valuation: assigning weight to the different impact categories to make a hierarchy between them. Relies on the goal definition;
- Evaluate and document the LCA results: verifying the accuracy of the results and documenting the results, methodology, systems, boundaries and assumptions.

Following the 7 parts, a lot of different LCIA indicators are developed in order to unify the eviromental impacts and make different products comparable, such as EcoIndicator99, ReCiPe. Different indicators may have different ways of categorization and normalization. Some indicators also include the short term impacts and long term impacts. For the same LCA model, different LCIA indicators can be used according to the user's needs. Most of the commercial LCA tools are capible to different LCIA indicators.

5.1.3. Interpretation

The two objectives of LCA interpretation have been defined by ISO as:

1) analyze, reach conclusions explain limitations and provide recommendations;

2) Provide a readily understandable, complete and consistent presentation of the results of an LCA study.

Several analytical methods are used in analysis the LCA. The contribution analysis, the uncertainty analysis, the sensitivity analysis, etc. The interpretaion aims at explaining the results to the stakeholders or designers of the products to amerliorate the production process either to have less material consumption or have smaller enviromental impacts.

5.2. BJAM LCA Modelling

This section describes the method used to create a LCA model of BJAM process. It can be extrapolated to make the model of any process. It is composed of five main steps, summed up in the following flow chart representing the method.

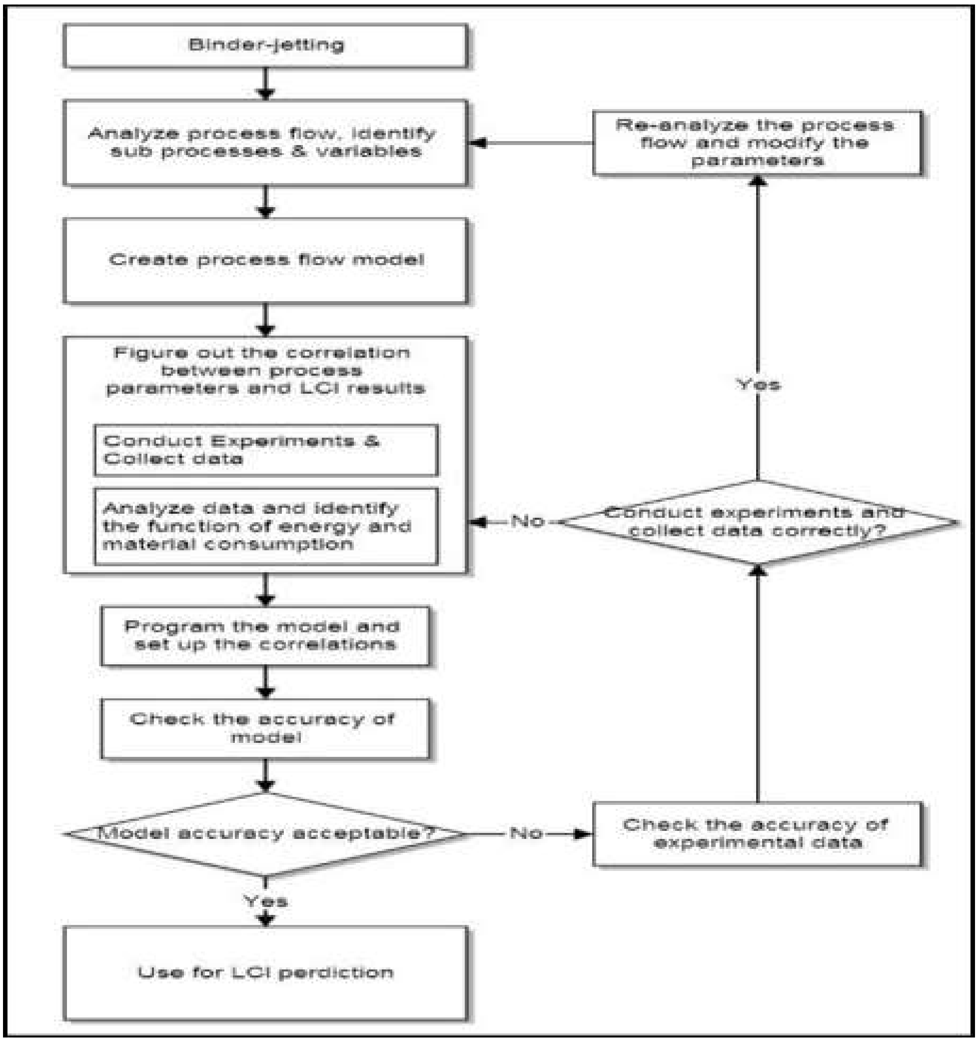

Figure 39: BJAM LCA Modelling workflow

5.2.1. System Border Definition

System border study is necessary before starting modelling. The question of what is the result wanted is essential and must be answered before any modeling work. In the BJAM modelling, the modelling focus on the “Cradle-to-Gate” process, that is from the raw material extraction to the final product, the printed, cured and sintered part. On the other aspect, the LCA focus only on the production of the part itself and related material and energy consumption. The facilities such as the making of the machine, the accessory equipements and the material transportation are not included. To be mentioned, the human work effort is also considered as a material flow in the LCA. The boundary of the system is shown in

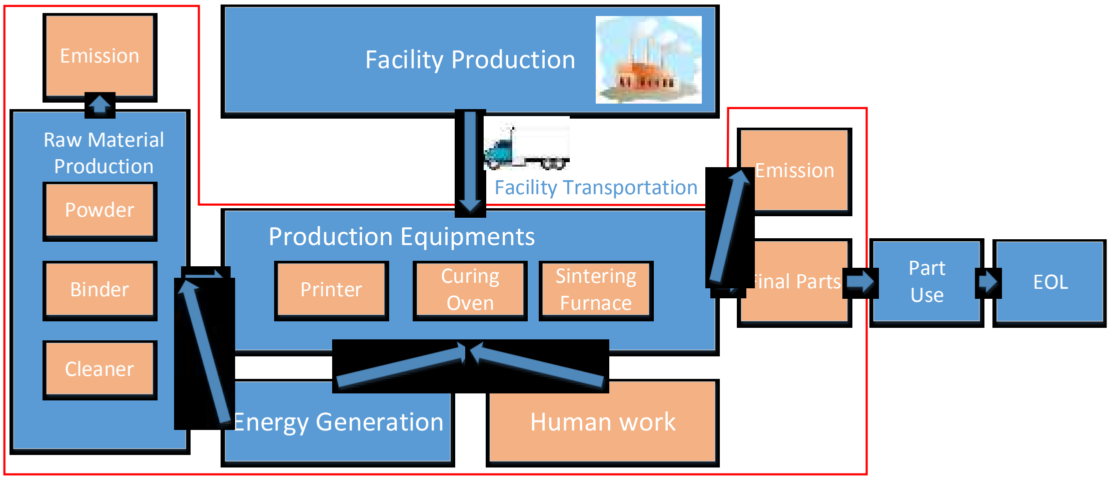

. The red line indicates the boudary of LCA model.

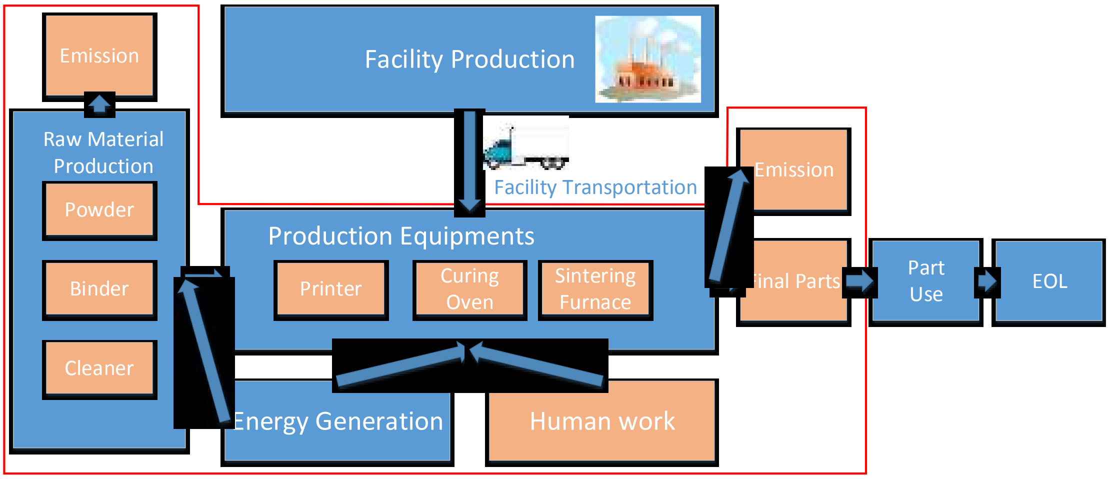

Figure 40: LCA Boundary of BJAM

5.2.2. Identification of Sub-process

The first step of modelling is to identify all the sub-processes involved in the the process studied. This identification must be the most exhaustive possible in order to have a complete view of the steps between raw material and finished product. Then for each sub-process a complete identification of the inputs and outputs must be done including energy, materials, waster etc. At this stage no element can be neglected.

The BJAM LCA Modelling made accordingly with the M-Lab™ machine from ExOne Inc. As decripted in Chapter 4, three main subprocess involved in the production phase: the printing, curing and sintering. Besides, the upper streans of the production, the making of the materials and the generaltion of electicity are also considered. These processes can be found in the database of EcoInvent™ Version 3.0. The database has covered all the life cycle of making of these materials, i.e. the binder, the cleaner, stainless steel and bronze powder, from the ore extraction to the final products including the energy consumption and emissions. So only the production processes are looked into.

In the printing phase, each of the action is counted. The printer platform is shown in Figure 41.

Figure 41: Printer Platform

The numbered elements of the machine are:

- (1): Powder Feed bed
- (2) : Print bed

- (3) : Print chamber
- (4): Print head
- (5) : Spread Roller
- (6): Infrared heater

Here are the steps of the process:

A. The first step is to fill (1) with green powder, the amount of powder used is larger than the volume of the platform because of the spilling.

B. Then the platforms (1) & (2) are leveled to prepare the deposition of the first layer

C. The chariot goes then under the heater (6) to heat the powder.

D. After the powder is heated, (1) is lifted and (2) is lowered.

E. Then the roller (5) is put in rotation and the print chamber(3) goes under it, spreading a layer from (1) on (2).

F. When the spreading is done, the printhead (4) drops binder on the powder layer, creating the shape of a slice of the part.

G. The process starts again from step C. until the whole part is printed

H. The printed part and the surrounding powder in the part-build area are put in the oven to be cured.

I. The part is taken from the oven and put in the furnace to be sintered and infiltrated. The remaining powder is recycled.

According to the steps described above, we can identify 13 sub-processes, summed up in Table 6: **The sub process table with inputs and outputs**:

Table 6: The sub process table with inputs and outputs

Sub-process	Inputs	Unit	Outputs	Unit
Fill Powder Feed system	Green powder (1)	kg	Green powder (3)	kg
	Reused powder (2)	kg	Reusable powder (4)	kg
Level the platforms	Elec. (1)	kWh	Green powder (3)	kg
	Green powder (2)	kg	Reusable green	kg

			powder (4)	
Go to heat spot	Elec. (1)	kWh	Green powder (3)	kg
	Green powder (2)	kg		
I.R. heater	Elec. (1)	kWh	Green powder (3)	kg
	Green powder (2)	kg		
Spreading speed	Elec (1)	kWh	Green powder (3)	kg
	Green powder (2)	kg		
Roller	Green powder (1)	kg	Reusable powder (2)	kg
			Green powder (3)	
Go to print point	Elec. (1)	kwh	Green powder (3)	kg
	Green powder (2)	kg		
Printer head movement	Elec. (1)	kWh	Green powder (3)	kg
	Green powder (2)	kg		
Binder drop	Green powder (1)	kg	Printed powder (3)	kg
	Binder (2)	kg	Waste of binder liquid (4)	kg
Curing	Elec. (1)	kWh	Heat Loss (3)	kWh
	Printed powder (2)	kg	Cured Powder (4)	kg
Depowdering	Cured powder (1)	kg	Cured powder part (2)	kg
			Reusable powder (3)	kg
			Waste powder (4)	kg
Neutral gas protection	Elec. (1)	kWh	Neutral gas (4)	m3
	Neutral gas (2)	m3	Cured powder (5)	kg
	Cured powder (3)	kg		
Sintering and infiltration	Elec. (1)	kWh	Part (4)	kg
	Cured powder (2)	kg	Waste of Bronze (5)	kg
	Bronze powder (3)	kg	Heat loss (6)	kg

5.2.3. Flow Map

The next step of the modeling is to create the flow map of the system. The IDEF0 is used and for more visibility, the print chamber displacement has been integrated to other sub-processes and the Neutral gas protection sup-process to the Sintering. Figure 42 shows the level1 IDEF0 chart of the whole process. The flow map helps to clearify the connections of the subprocesses and their inputs and outputs.

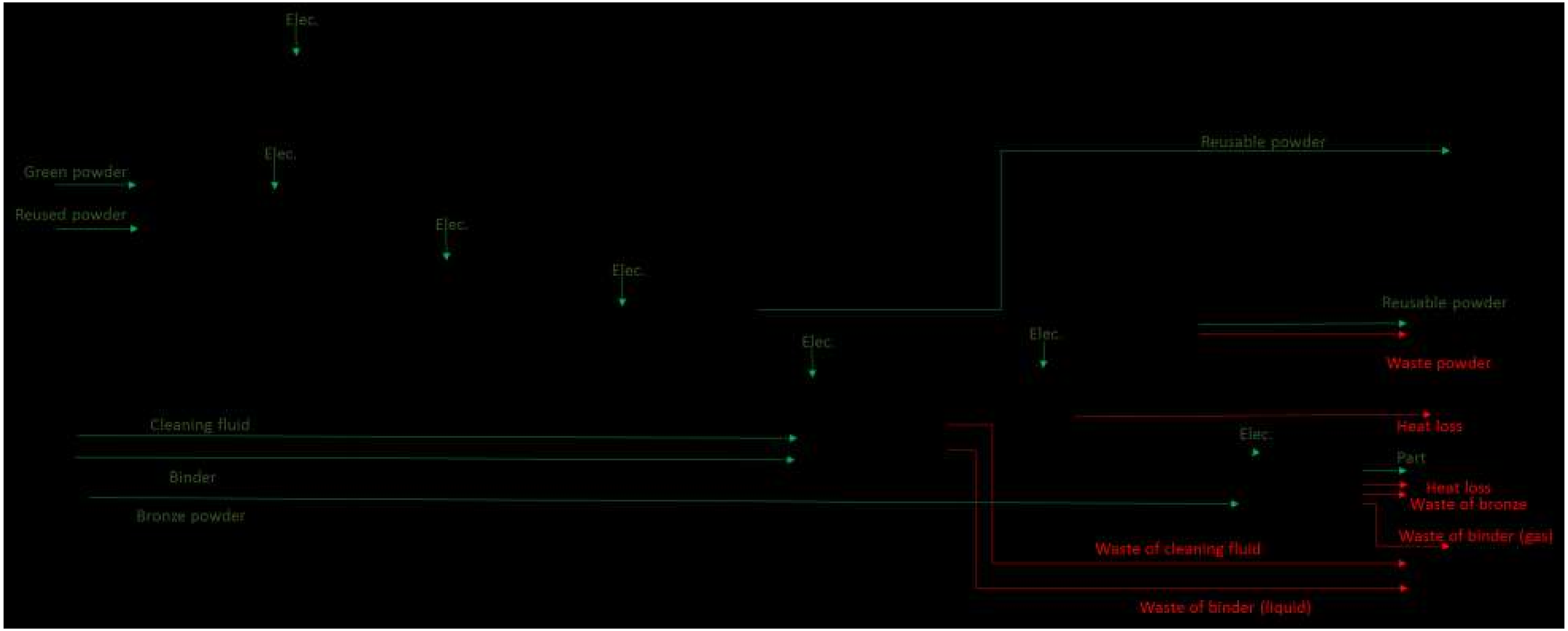

Figure 42: IDEF0 of the BJAM LCA process[15]

5.2.4. Define the correlations

Now that the sub-processes have been identified and linked one to another, the correlations have to be defined with mathematical formulas. These formulas will link inputs to outputs via the use of parameters. In previous work of Simon Metyer[15], the relationship has been established of each sub prcess mentioned in section 5.2.2.

In this research, the LCA Model is built based on the correlation between each sub process and inputs and outputs. Several interprocess activities have beend added in order to model the process in practical way. The raw material productions, human work involved are included too.

The interprocess activities include machin setup and part transportation and storage between each sub process. In these activities, human work effort are mainly involved. Potential material wastes are include too as mentioned in Chapter 4.

5.2.5. Modelling on Umberto NXT LCA platform

Commercial softwares are often used in modelling of the LCA. The softwares are able to import data from database, visulaized the flow map and conduct calculation for LCI and LCIA based. Commercial LCA softwares are often capable to work with different LCA databases and LCIA indicators.

UMBERTO NXT LCA has been chosen amongst other software such as GaBi or SimaPro because it allows to model processes with formulas and parameters which is a very powerful function to make studies compared to other software which makes only numerical modeling. An illustration of the graphic interface and of the definition of relations in a process is shown in **Error! Reference source not found.**.

The modelling work is based on the mathematical correlations of the processes. Parametric tables have been developped. Four different types of parameters are set: machine dependent parameters, material dependent parameters, part dependent parameters and part dependent parameters shown in Table 7.

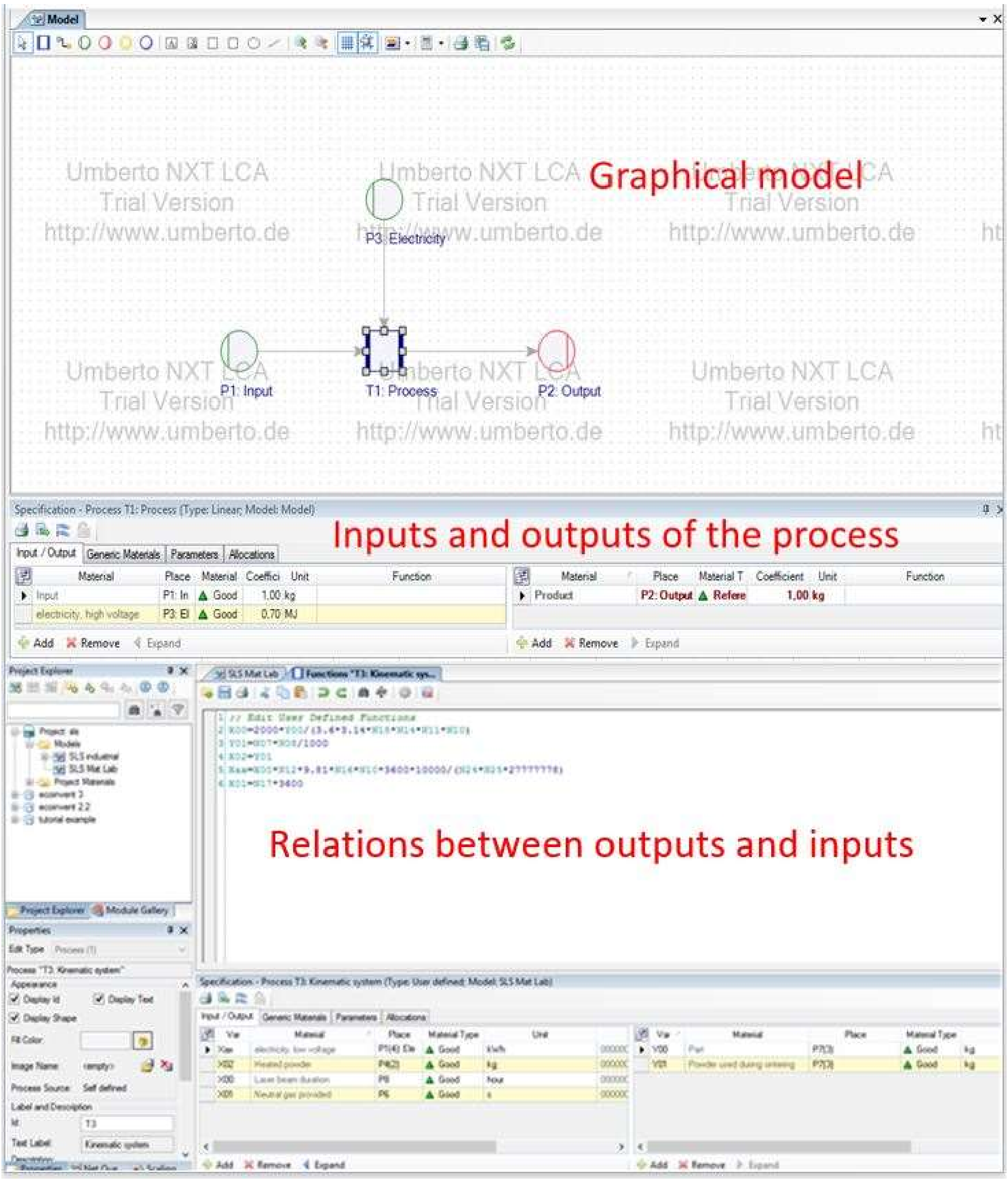

Figure 43: Umberto NXT LCA Interface

Table 7: BJAM LCA Parametric table

Machine dependent parameters		
Parameter	**Symbol**	**Unit**
Volume of supply platform	V_{supply}	mm^3
Screw diameter	D_{Screw}	mm
Mass of platforms	$M_{platform}$	kg

Platforms' section	$S_{platform}$	mm2
Screw's pitch	p	mm
Efficiency of transmission for supply and part build platforms	$\eta_{transmsupply/partbuild}$	%
Efficiency of motors for supply and part build platforms	$\eta_{motsupply/partbuild}$	%
Friction coefficient in screw-nut systems	$f_{screw-nut}$	Unit
Mass of chariot	$M_{chariot}$	kg
Friction coefficient in chariot's guiding	$\mu_{slideways}$	Unit
Distance print spot-heat spot	$L_{print-heat}$	mm
Efficiency of pulley-belt for roller	$\eta_{pulley-belt}$	%
Efficiency of motor for chariot	$\eta_{motroller}$	%
Maximum power of infrared heater	$P_{heatermax}$	W
Furnace volume	$V_{furnace}$	mm3
External pressure	p_{ext}	Pa
Pump's mechanical efficiency	η_{pump}	%
Distance spreading	L_{spread}	mm
Distance end of spread spot-print spot	$L_{spread-print}$	mm
Print-head stroke	$L_{phstroke}$	mm
Mass of print head	$M_{print-head}$	kg
Friction coefficient in print-head guiding	$\mu_{print-head}$	Unit
Efficiency of rack and pinion for print-head	$\eta_{\mathrm{r\&p}}$	%
Power of uncapping	P_{uncap}	W
Specific heat capacity of the apparatus for curing	$Cp_{apparatus}$	J/kg/K
Specific heat capacity of the recipient for sintering	$Cp_{recipient}$	J/kg/K
Specific heat capacity of the support powder	$Cp_{supportpowder}$	J/kg/K
Specific heat capacity of the infiltrant	$Cp_{infiltrant}$	J/kg/K

Surface of oven	S_{oven}	mm2
Convection coefficient inside the oven	$h_{intoven}$	W/m2/K
Convection coefficient outside the oven	$h_{extoven}$	W/m2/K
Convection coefficient inside the furnace	$h_{intfurnace}$	W/m2/K
Convection coefficient outside the furnace	$h_{extfurnace}$	W/m2/K
Thermal resistance of oven wall	R_{oven}	m2.K/W
Thermal resistance of furnace wall	$R_{furnace}$	m2.K/W
External temperature	T_{ext}	K
Mass of recipient for sintering	$M_{recipient}$	Kg
Operator dependent parameters		
Parameter	**Symbol**	**Unit**
Percentage of filling supply platform	$\%_{filling}$	%
Mass of reused powder	M_{reused}	kg
Layer thickness	δ	mm
Feed ratio	R_{feed}	Unit
Percentage of heater’s maximum power	$\%_{heater}$	%
Vacuum pressure desired	p_{fin}	Pa
Argon flow-rate	D_{vAr}	mm3/s
Mean time between two consecutive layers	t_{layer}	s
Number of overlaps	$N_{overlaps}$	Unit
Saturation ratio	R_{sat}	
Mass of binder waste per layer	$M_{binder/layer}$	kg
Mass of cleaning fluid waste per layer	$M_{clean/layer}$	kg
Mean time to print a layer	$t_{printlayer}$	s
Mean temperature during curing	$T_{meancuring}$	K
Total duration for curing	$t_{totalcuring}$	s
Duration of maintain phase for curing	$t_{maintaincuring}$	s

Mean temperature during sintering	$T_{meansintering}$	K
Total duration for sintering	$t_{totalsintering}$	s
Duration of maintain phase for sintering	$t_{maintainsintering}$	s
Infiltrant ratio	$R_{infiltrant}$	Unit
Material dependent parameters		
Parameter	**Symbol**	**Unit**
Density of powder	ρ_{powder}	g/mm3
Packing ratio	$\%_{pack}$	%
Proportion of reusable powder	$\%_{reusable}$	%
Density of binder	ρ_{binder}	g/mm3
Specific heat capacity of the powder	Cp_{powder}	J/kg/K
Part dependent parameters		
Parameter	**Symbol**	**Unit**
Height of part	h_{part}	mm
Volume of part	V_{part}	mm3

The Model consists three phases, the raw material production phase, the product production phase and the disposal phase. The raw material production is generated using the data of EcoInvent LCA DatabaseVersion 3.0.

The binder is made from 80% of Ethylene Glycol Monoethyl Ether, 10% of Diethylene Glycol and 10% of water according to ExOne Material Safety Data Sheet[35]. The cleaner is made from 90% of Ethylene Glycol Monbutyl Ether and 10% of water. The S4 stainless steel powder consist 12-14% of Chromium, 1% of Silicon, 1% of Manganese and 84-86% of Iron and is made from Chromium Steel 18/8. The bronze powder and the steel powder are made from atomization process.

The material production phase is shown in Figure 44. All the processes in this phases are inherent from EcoInvent database.

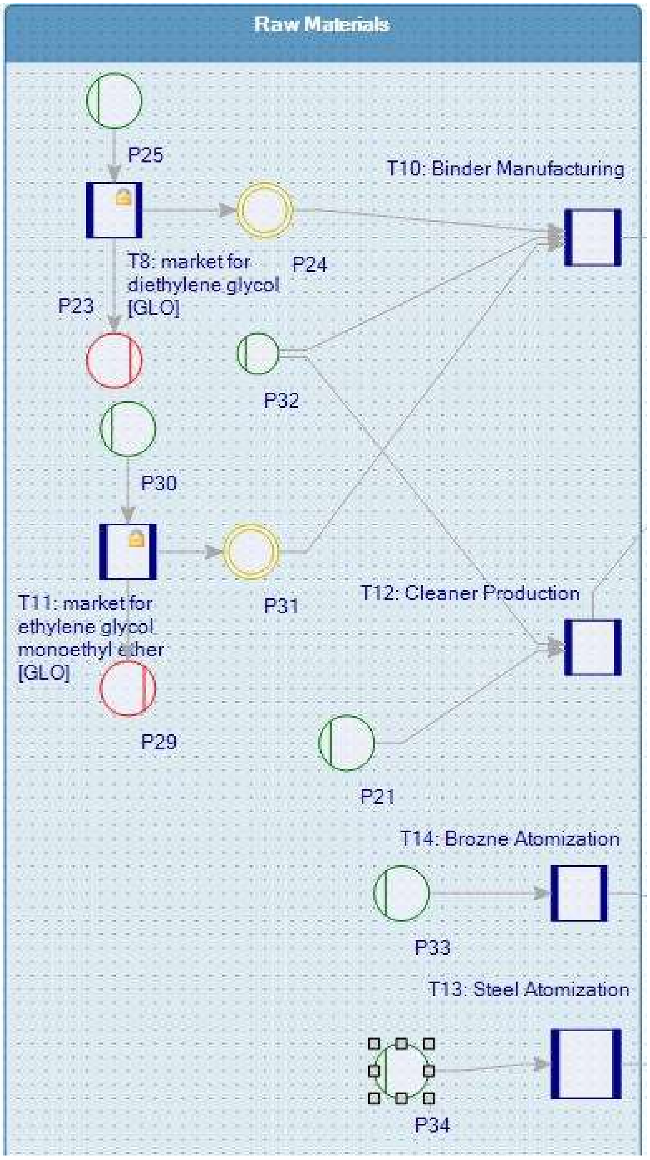

Figure 44: Raw material production of BJAM LCA Model

In the manufacture phase, two subnets are involved. Since the printing process and the sintering process comprise several sub processes. Both of them are decomposed into smaller processes with subnets. In manufacture phase, are the process are user defined. Mathematical expressions are used to express the relationships between the inputs and outputs. For example, the relationship between the inputs cured powder, the printed green part and the human work effort and the outputs reusable green powder, cured green part, of depowdering can be expressed as:

```
;; Edit User Defined Functions
X01=0.2
X00=Y00+Y01
Y00=C03*N10*N03/1000000-Y01
X02=Y01
```

Figure 45: User defined relation of BJAM process

In the expression, variables with 'X' represents the inputs, variables with 'Y' represents the outputs, the 'C' and 'N' represent the global parameters and net parameters.

The main net model of the production phase is shown in Figure 46. From the figure, we can see the printing and sintering process have subnets (see Appendix II). The thicker arrow output from the sintering process is the reference flow of the BJAM LCA Model. Reference flow represents usually the purpose of the LCA. In this model, the reference flow is the weight of the final part.

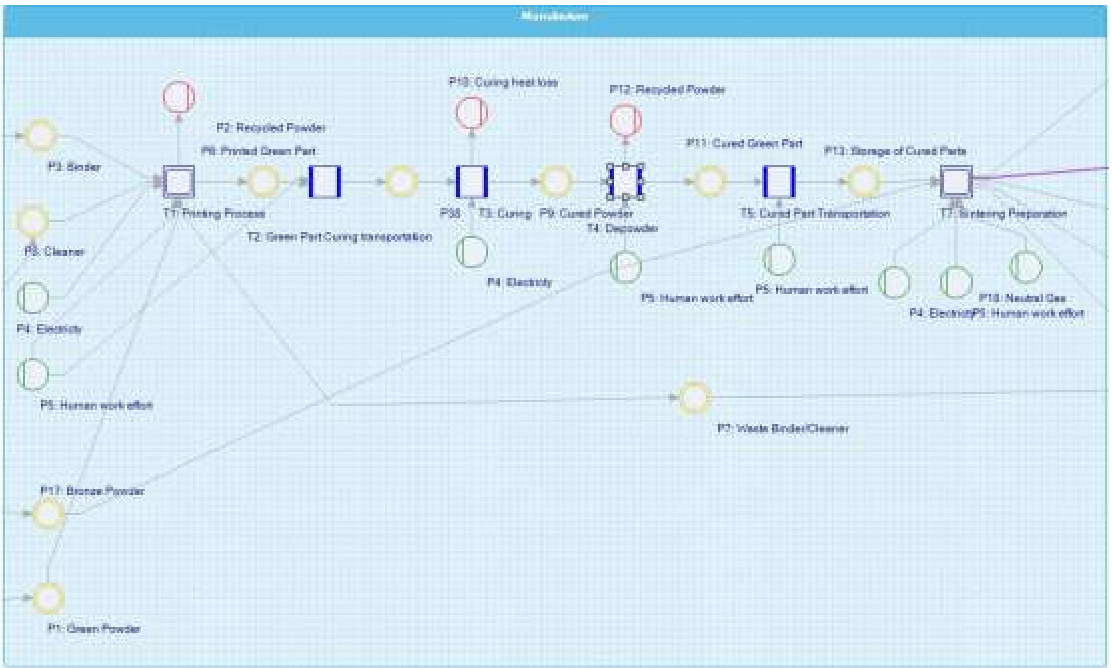

Figure 46: Production Phase of BJAM LCA Model

Since no waste treatment is considered in the LCA, the waste disposal phase is mainly evaluating the amount of the waste, including the waste of the printing which is generated by a mixture of binder and cleaner, the waste steel and bronze powder, the heat loss and the emitted neutral gas. The final part is also located in the disposal phase as the output of the production phase. The disposal schema is show in Figure 47.

Figure 47: Disposal phase of the BJAM LCA Model

To perform the LCA calculation, user needs to provide the two part dependent parameters on the main net, the height of the parts and the volume of the part as shown in Table 7. The user also needs to input the weight of the part as the reference flow.

Chapter 6: Case Study: Optimized Engine Bracket Model

In order to validate the Production System Model, a case study is conducted. An engine bracket design is introduced in this chapter following the framework described in Chapter 2.

Firstly, the topology optimization is conducted in the design phase to obtain a minimum material consumption. Then the model is scaling down to the dimension that can fit ExOne M-Lab printer. The Process Parameters Recommendation is firstly performed using the Parameter Recommendation System described in Chapter 3. With proper manufacturing parameters, the Time Consumption, Material Consumption and Production KPIs are estimated by the methods proposed in Chapter 4.

After the simulation conducted by the models, the part is printed by ExOne M-Lab BJAM production system, from printing to sintering. Due to the lower stability of infiltration, no infiltration is involved in the sintering process. All the time and material consumption data are recorded during the production process. Comparison will be made between the practical data and the simulation result from the models.

6.1. Simulation by Productivity Model

As described in Chapter 2 the AM Production System Framework, AM enables flexible design. With little manufacture limitation, optimization of design will have fewer constraints. Topology optimization methods are developed in optimizing the part design to obtain fewer consumptions while maintain the required functionalities.

In this case, topology optimization on an engine bracket design has been performed. The optimized design is shown in Figure 48. The design has achieved a lighter bracket with fewer materials while maintaining the same functionality.

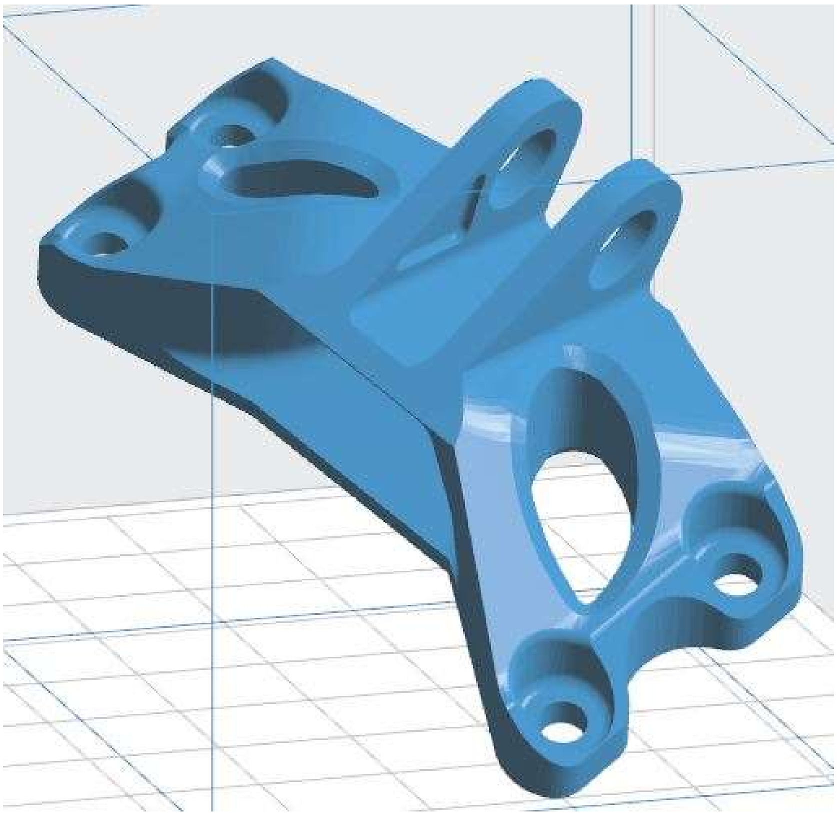

Figure 48: Optimized Engine Bracket Design

The part is designed to be $170 \times 107 \times 62.5$ mm and scaling down to 28.24% of $48 \times 30.2 \times 17.65$ mm to fit in the printing chamber of ExOne M-Lab printer. The scaled-down STL file is then loaded in the Matlab GUI tool. Due to the print chamber space limits, the part can only be printed bottom to top as shown in Figure 48. So in the Matlab Productivity Model, the part's printing orientation is set in the same direction. According to the STL reading file, the CAD model should have the Z-Axis set to the printing orientation.

Since the engine bracket is an assembly part, the part dimension is critical, so in the Parameter Recommendation Model, the shrinkage on Y-Axis and Z-Axis are set to 100% which means little shrinkage may occurs. In order to acquire possible solution, the surface roughness is set to 80%. The recommended parameters are given as in Table 8. The other parameters are set to the default as recommended by ExOne as shown in Figure 50. Since no infiltration will be performed, the sintering profile is selected as S4-One step.

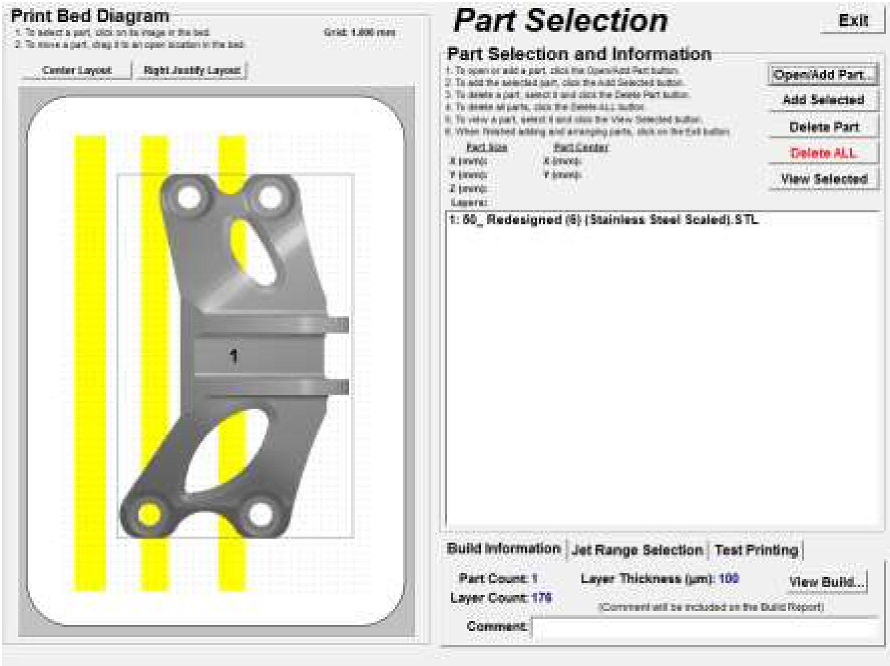

Figure 49: Part printing orientation

Table 8: Recommended Process Parameters and Predicted Quality Properties

Recommended Parameters		Predicted Quality	
Layer thickness (µm)	100	Surface Roughness (µm)	14.2869
Binder Saturation (%)	70	Shrinkage Y-Axis (%)	0.48
Heater Power Ratio (%)	75	Shrinkage Z-Axis (%)	0.3789
Drying Time (s)	30		

The calculation results of time and material consumption are given by the Matlab GUI as shown in Table 9.

Table 9: The estimated time and material consumption by the BJAM Productivity Model

Time Consumption Estimation		Material Consumption Estimation	
Printing Time (s)	7457.04	Powder Consumption (g)	39.5606
Curing Time (s)	27300	Cleaner Consumption (ml)	844
Sintering Time (s)	23880	Binder Consumption (ml)	746
Manual Working Time (s)	2400	Waste Generation (ml)	1021
Total Time (s)/(h)	61037.04/16.95		

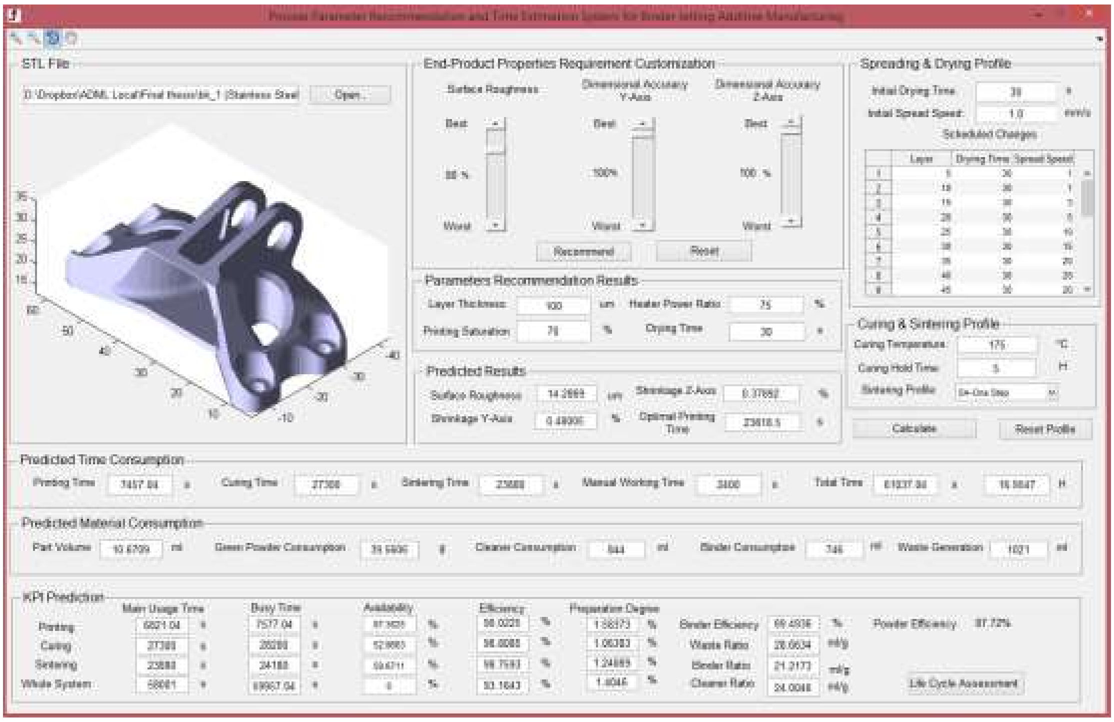

Figure 50: The Matlab UI result of the STL

The KPI prediction is also given on the Matlab GUI in Figure 50. The KPIs are calculated separately for Printing, Curing, Sintering and the whole system. The Main Usage Time and the Busy Time are also listed in Table 10. Note that on the system level, the *Availability* is always 0 for any system according to the definition in section 4.5.

Table 10: KPI Prediction by BJAM Productivity Model

Time Related KPIs				
	Printing	Curing	Sintering	System
Main Usage Time (s)	6821.04	27300	23880	58001
Busy Time (s)	7577.04	28200	24180	59957.04
Availability (%)	87.3625	52.9663	59.6711	0
Efficiency (%)	90.0225	96.8085	98.7593	93.1643
Preparation Degree (%)	1.5837	1.0638	1.2407	1.4046
Material Consumption Related KPIs				
Binder Efficiency (%)	Powder Efficiency (%)	Binder Ratio (ml/g)	Cleaner Ratio (ml/g)	Waste Ratio (ml/g)
89.4936	87.72	21.2173	24.0046	28.6634

6.2. Production by BJAM Production System

In this step, the optimized engine bracket model is being manufactured by the ExOne M-lab BJAM Production System following the printing, curing and sintering process. The final part printed is shown in Figure 51. The production parameters are set exactly as the parameters in the simulation as shown in Table 8.

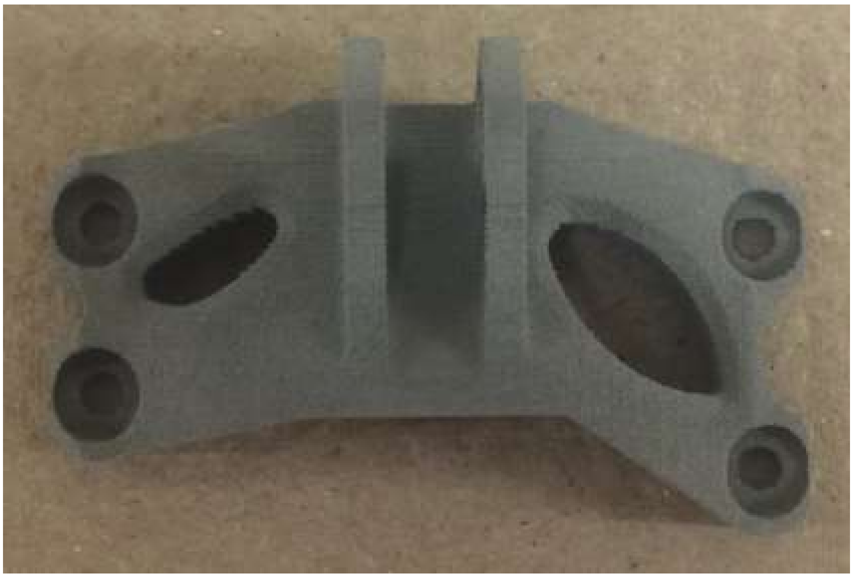

Figure 51: Engine Bracket Model manufactured by BJAM

Time of each process as well as the time in between process are recorded including the printing time, curing time, sintering time with human work time in printer preparation, transporting part from printer to curing oven, depowdering time and sintering setup time. The material consumption is measured two time before and after the production process to get the consumption during the process. Since only the difference is counted, the measurements are conducted with the container. In measuring the powder consumption, the initial filled powder is measured by weigh the powder container before and after filling the print chamber. The recycled powder is also measured by weigh the powder recycling sifter before and after recycling the powder. The final part is also weigh as the amount of value-added powder in order to calculate the waste powder. The measurement is shown in Figure 52.

Figure 52: Measurements in material consumption of practical production

The results are shown in Table 11.

Table 11: Practical Data of BJAM production

Time Consumption Recorded		Material Consumption Recorded	
Printing Time (s)	10800 (168mins)	Powder Consumption (g)	33
Curing Time (s)	30180 (8h23mins)	Cleaner Consumption (ml)	835
Sintering Time (s)	49320(13h42mins)	Binder Consumption (ml)	753
Manual Working Time (s)	2160(36mins)	Waste Generation (ml)	988
Total Time (s)/(h)	92460/25.68	Part weight (g)	24.023

Directly from the recorded data, some of the KPIs listed in Table 10 are not able to be calculated, such as the binder efficiency since no direct data can be obtained from the practical production. The only way to calculate the binder efficiency is to use the waste, assuming all the cleaner consumed is going to the waste bottle as well as the extra non-value-added binder. So the amount of non-value-added binder can be calculated by the amount of waste subtract the amount of cleaner. So the KPIs of the practical production is calculated and shown in Table 12.

Table 12: KPIs calculated from BJAM practical production

Time Related KPIs Calculated				
	Printing	Curing	Sintering	System

Preparation Time(s)	1200	180+660(depowder)	120	2160
Main Usage Time (s)	10800	30180	49320	90300
Busy Time (s)	12000	30360	49440	91800
Availability (%)	86.9281	66.9281	46.1438	0
Efficiency (%)	90	99.4071	99.7572	98.3660
Preparation Degree (%)	10	0.5929	0.2427	2.3529
Material Consumption Related KPIs				
Binder Efficiency (%)	Powder Efficiency (%)	Binder Ratio (ml/g)	Cleaner Ratio (ml/g)	Waste Ratio (ml/g)
79.68	72.79	31.34	34.76	41.13

6.3. Result Comparison

Comparing the estimation result in section 6.1 to the practical result in 6.2 as shown in Table 13, we can conclude that the estimation has a large different with the practical production. On the time aspects, the curing time prediction is accurate with only 7.55% of difference. The sintering process however bears more than 50% of difference. Through analysis, it is because the cooling down process of sintering furnace takes much longer than what ExOne given. The theoretical cooling down rate cannot be achieved. The printing time has around 30% of difference, the actual time is longer than the estimation. The difference may cause by the potential inaccuracy of layer drying time. In practical experiments, it is found that the drying process in the first couple of layers are longer than expect since the preheat process is involved to heat the powder to a desired temperature.

In the material consumption aspect, the difference about 20% for powder. And around 1% in cleaner and binder. The practical powder consumption is less than the predict value. The cause of the powder’s pack rate is less than the 60% of ExOne’s Specification. Through testing, the actually pack rate is only 52%. This difference in powder consumption leads to the difference in material consumption base KPIs.

On the time related KPIs, although there is difference between the practical time and the estimation time, the KPIs in printer’s availability and efficiency, curing oven efficiency and furnace efficiency are pretty accurate. This is because each of the processes have a much longer working time than the setup time, several hours vs. a few minutes. So the efficiency varies very little. The preparation degrees are relatively small, although there's a large different on percentage, the actual different is small. While the availability of the machines are relatively larger in the curing oven and sintering furnace because the under estimated curing and sintering time. On the system level, the predictions are pretty close to the practical data.

Table 13: Time and material consumption comparison

Time Consumption				
	Estimation	Practical	Difference	%
Printing Time (s)	7457.04	10800 (168mins)	3343	30.95%
Curing Time (s)	27300	30180 (8h23mins)	2280	7.55%
Sintering Time (s)	23880	49320(13h42mins)	25440	51.58%
Manual Working Time (s)	2400	2160(36mins)	-240	-11.11%
Total Time (s)/(h)	61037.04/ 16.95	92460/25.68	31423	33.99%
Material Consumption				
	Estimation	Practical	Difference	%
Powder Consumption (g)	39.5606	33	6.5606	19.88%
Cleaner Consumption (ml)	844	835	9	1.08%
Binder Consumption (ml)	746	753	-7	-0.93%
Waste Generation (ml)	1021	988	33	3.34%
Time Related KPIs Calculated				
	Estimation	Practical	Difference	%
Printer Availability (%)	87.3625	86.9281	-0.4344	-0.4997
Printer Efficiency (%)	90.0225	90	-0.0225	-0.025
Printer Prep Degree (%)	1.5837	10	8.4163	84.163
Curing Oven Availability (%)	52.9663	66.9281	13.9618	20.861
Curing Oven Efficiency (%)	96.8085	99.4071	2.5986	2.6141

Curing Oven Prep Degree (%)	1.0638	0.5929	-0.4709	-79.423
Furnace Availability (%)	59.6711	46.1438	-13.5273	-29.316
Furnace Efficiency (%)	98.7593	99.7572	0.9979	1.000
Furnace Prep Degree (%)	1.2407	0.2427	-0.998	-411.21
System Efficiency (%)	93.1643	98.3660	5.2017	5.28811
System Prep Degree (%)	1.4046	2.3529	0.9483	40.3035
Material Consumption Related KPIs				
Powder Efficiency (%)	87.72	72.79	14.93	20.511
Binder Efficiency (%)	89.4936	79.68	9.8136	12.316
Binder Ratio (ml/g)	21.2173	31.34	10.1227	32.2996
Cleaner Ratio (ml/g)	24.0046	34.76	10.7554	30.9419
Waste Ratio (ml/g)	28.6634	41.13	12.4666	30.3102

In summary, the Time and Material Consumption Model and the KPI Prediction Model of BJAM can provide reliable estimation to a certain extent, especially in material consumption. It is able to help the designer and production manager estimated the production cost and lead time and to coordinate and optimize the design to obtain a better production efficiency.

Chapter 7: Conclusion & Future Work

In this master research, BJAM production system is studied. A framework of AM design to production is proposed. Based on BJAM, several different modelling work have been conducted including the Time Consumption Model, the Material Consumption Model, the KPI Model and the LCA Model. Based on the previous work on STL file loading and slicing algorithm, an integrated Matlab GUI is introduced as a tool to conduct the estimation from the STL file. A case study has been performed to validate the models. Results shows an acceptable accuracy in the estimation at the same time some limitation of the models have been found. This chapter will conclude the work and discuss the future improvement of productivity model of BJAM technology.

7.1. Conclusion

Discussed in the previous chapters, the productivity model of BJAM has been developed. The idea of this research come from the prevalence of AM technologies. However, AM production system is still far from maturity. Comparing to conventional manufacturing methods, the AM bears a long leading time and instability in production quality. Even though AM is more appropriate in small scale production, the production level research is needy in order to explore the capability of AM in practical production and make real benefit of relatively new technology.

A framework of general AM modelling platform is proposed is Chapter 2. The framework defines a close loop work flow of AM modelling. It starts from the design optimization. AM enables flexible design which permits various optimization can be conducted on the parts' structure to obtain a better functionality, a better sustainability or a more efficient production. Topology optimization is introduced in order to reduce the material consumption and the weight of the parts while maintaining the functionality. According to the design, manufacturing parameters are recommended, energy, material consumption of making a single part is estimated. The estimation feeds back to the designer in order to continue the optimization. Later, a production model involves in predict the KPIs and time consumption for massive production of the part. Again, feedbacks are made to the designer for continuous optimization.

On parallel, based on this framework, a general production evaluation mechanism is proposed to generate an indexing based evaluation system of AM technologies. The evaluation mechanism is aiming at standardize various AM technologies and be able to quickly compare different AM technologies in respect of the design and manufacturing requirements. Guided by the framework and the evaluation mechanism, the structure of AM productivity model is designed. Previous work has been done on the Manufacturing Process Parameter Model. The model serves at establishing the relationship between the end-production quality and the AM process parameters. It recommends the process parameters in respect to the quality requirement as described in Chapter 3.

As a second step based on the framework proposed by Chapter 2, Time Consumption Model and Material Consumption Model are developed based on BJAM technology to predict the production time and material consumption. Algorithms are developed in estimating the consumption from the STL file. Inherent the algorithm in STL slicing developed by Xin[23], the algorithms are performed on a layer-by-layer basis. In the building of each layer, the process is decomposed into basic operations. Each operation is analyzed on time and material consumption aspects in Chapter 4. Then the algorithms are integrated into a Matlab GUI as a tool.

Based on the results of the time and material consumptions, several related KPIs are calculated. The KPIs can help production manager to better schedule the machines according to their availabilities. Machine efficiencies help identify the weak point of the whole production system. By improving the low efficient machine or reallocating the tasks helps improve the production efficiency. The material consumption KPIs help estimate the cost of the product. The material ratio help to define purchase and inventory strategies. The KPI Model is also integrated in the Matlab GUI. The KPIs, as important production indicators, are essential in the AM Production Evaluation Mechanism and the Productivity Model.

Another important aspects in AM Production Evaluation Mechanism is the production sustainability. From direct point of view, AM reduce the material wastes by adding material together rather than subtracting materials. However, due to the specialty of the material, such as powdered metal, special made binder and cleaner, the environmental impacts brought by these material and the consumption in the production of these material is unknown. So LCA is important method to verify if the production is sustainable from cradle to gate. No current LCA database has cover AM process, so analytical method is used in building up the LCA model described in Chapter 5.

Finally, a case study is performed on an optimized engine bracket model discussed in Chapter 6. The part design is firstly estimated by the developed Productivity Model. Then the part is actually made by the ExOne M-Lab BJAM production system. Practical data are recorded. Comparison has shown the accuracy of the estimation of the Productivity Model. Despite the sintering time and the powder consumption, the estimation is very accurate in both sub processes and on the system level. This BJAM Productivity Model is able to provide predictions on production consumption and evaluations on the production efficiency. It is a great progress towards the Productivity Evaluation Mechanism.

7.2. Future work

Lacking of practical data, the current LCA model is still not accurate. With the accumulation of data, the LCA model needs to be more detailed especially on the production of the raw material.

As the first step of developing a general AM evaluation platform and the mechanism, the current work is still immature and has limitations. The work is only based on the BJAM technology. In order to develop a standard AM productivity evaluation system, the method should be expanded into other AM technologies such as Select Laser Sintering technology (SLS), Stereo lithography (SLA), Electron Beam Sintering and etc.

On the vertical direction, the Model itself covers only the time consumption and material consumption and related KPIs, further work is needed to integrate the energy consumption estimation model developed by Xin[23]. Also as the framework indicated, the research on design optimization according to the feedbacks from the productivity model are still need to be fully developed to form a robust close loop system. On the quality aspects, the exploration into the end product quality such as the mechanical properties, the assembling capability, are needed too. The machine task schedule arrangement and the production optimization strategies can also be developed base on the productivity model.

Appendix

I. Experiment data

No.	Layer thickness (um)	Binder Saturation (%)	Drying Power Heat (%)	Layer Drying Time(s)	Printing Time(min)	Quality Rate	Binder Consumption (ml)	Cleaner Consumption (ml)	Waste Amount (ml)	Powder Consumption (mins)	Preparation Time (mins)	Printer Initialization Time (mins)
1.2	50	60	55	15	316	0.5	863	754	1298	451	23	2.3
1.1	50	60	55	20	175	0.5	557	368	703	194	26	2.8
2.5	50	75	70	30	393	0.2	859	703	985	497	36	3.2
2.1	50	75	70	30	375	0.2	973	689	1365	196	20	2.1
2.3	50	75	70	30	385	0.25	887	712	1171	224	20	2.1
3.1	50	90	85	45	458	1	893	697	1088	316	32	2.2
4.1	50	105	100	60	533	1	950	717	1241	168	21	2.5
7.1	100	90	100	15	226	1	484	387	640	235	30	2.2
8.1	100	105	85	30	230	1	492	363	650	370	23	2.3
5.1	100	60	70	45	256	1	503	400	671	285	27	2.5
6.1	100	75	55	60	295	1	412	363	550	167	23	3
12.1	150	105	70	15	156	0.2	300	339	456	457	20	2.2
12.2	150	105	70	15	165	0.2	292	258	395	427	24	2.2
12.4	150	105	70	15	199	0.25	288	264	410	115	35	2.1
11.1	150	90	55	30	188	1	329	265	435	107	27	3.1
10.1	150	75	100	45	180	1	332	256	430	303	28	2.2
9.1	150	60	85	60	203	1	307	288	430	383	24	2.2
14.1	200	75	85	15	136	1	252	192	322	361	23	2.4
13.5	200	60	100	30	139	0.2	234	196	308	224	28	2.6

13.1	200	690	100	30	141	0.2	234	198	309	165	37	2.4
13.2	200	60	100	30	148	0.2	246	257	370	243	23	2.5
13.3	200	60	100	30	197	0.2	315	261	410	159	26	2.2
13.4	200	60	100	30	150	0.2	227	199	310	157	23	2.2
16.1	200	105	55	45	204	1	282	165	400	91	34	2.3
15.1	200	90	70	60	175	0.33	232	201	311	176	24	3
15.3	200	90	70	60	186	0.33	221	207	304	300	29	2.9
										Average	26.38461538	2.45
										Variation	24.31360947	0.110961538

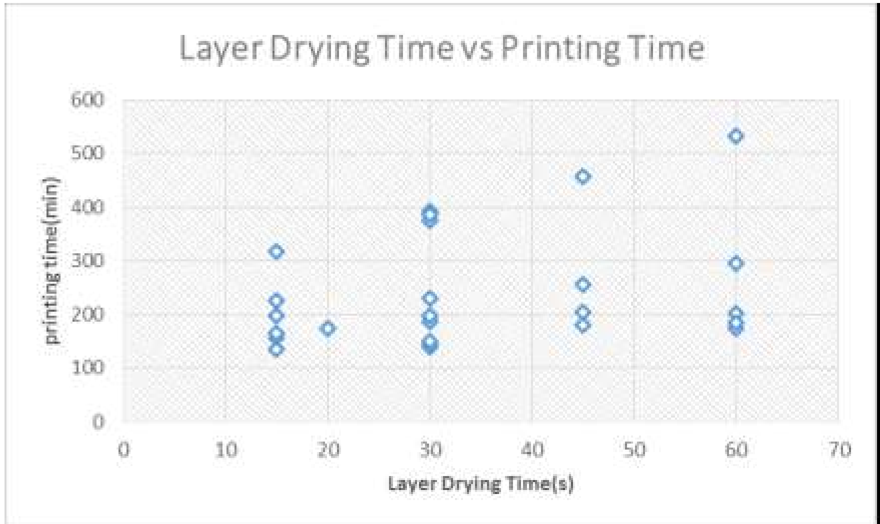

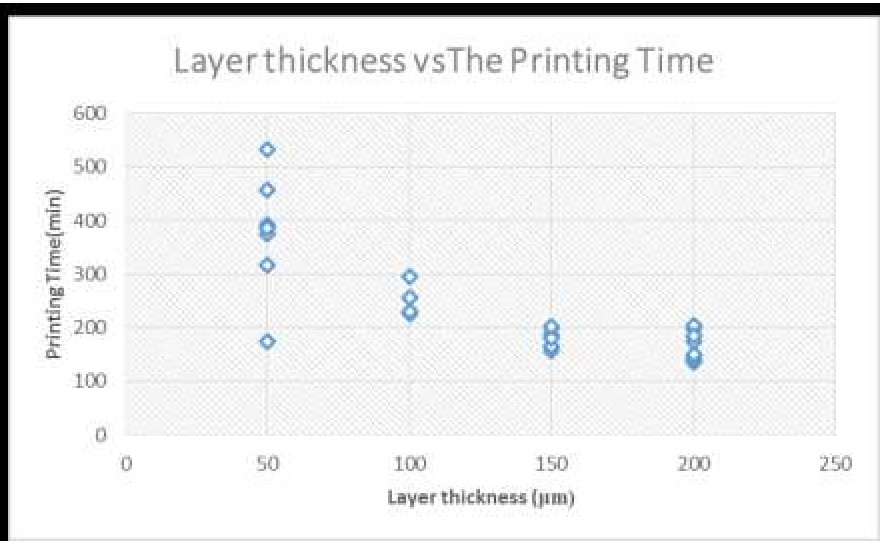

II. Umberto NXT Model

Main Net

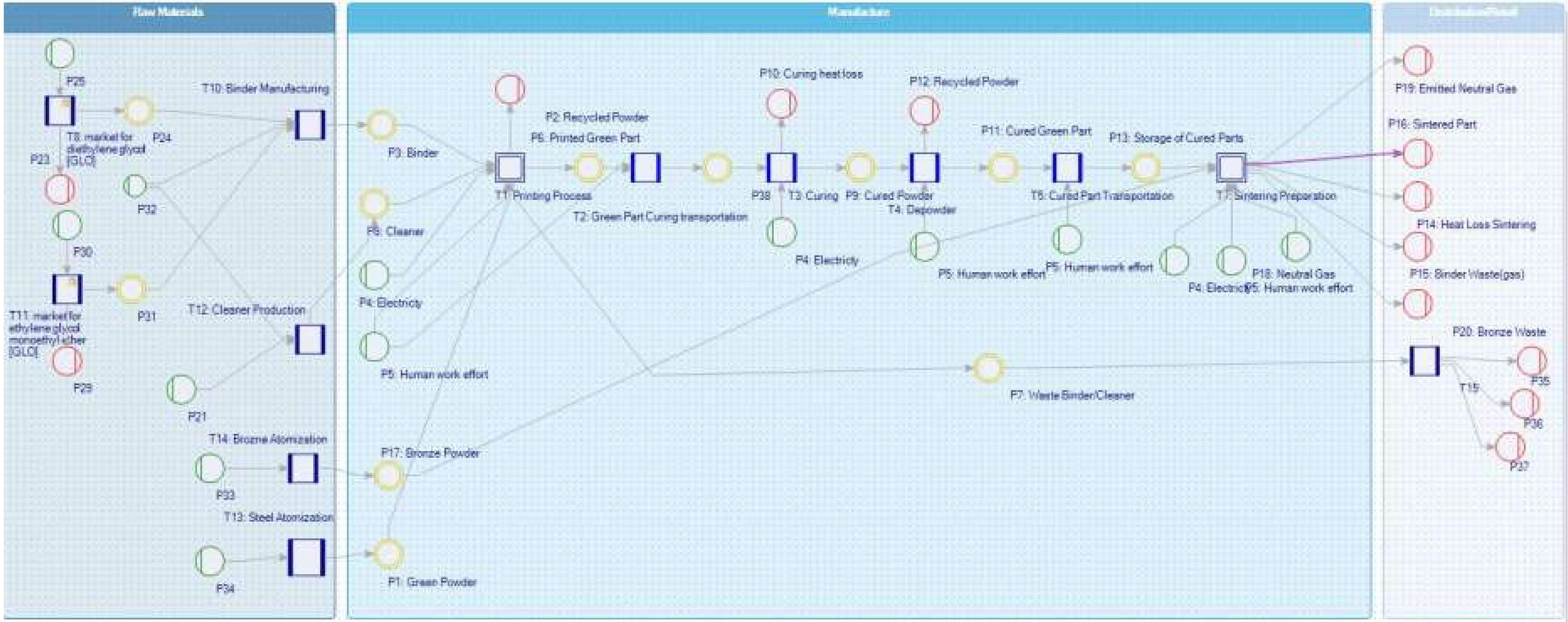

Printing Subnet

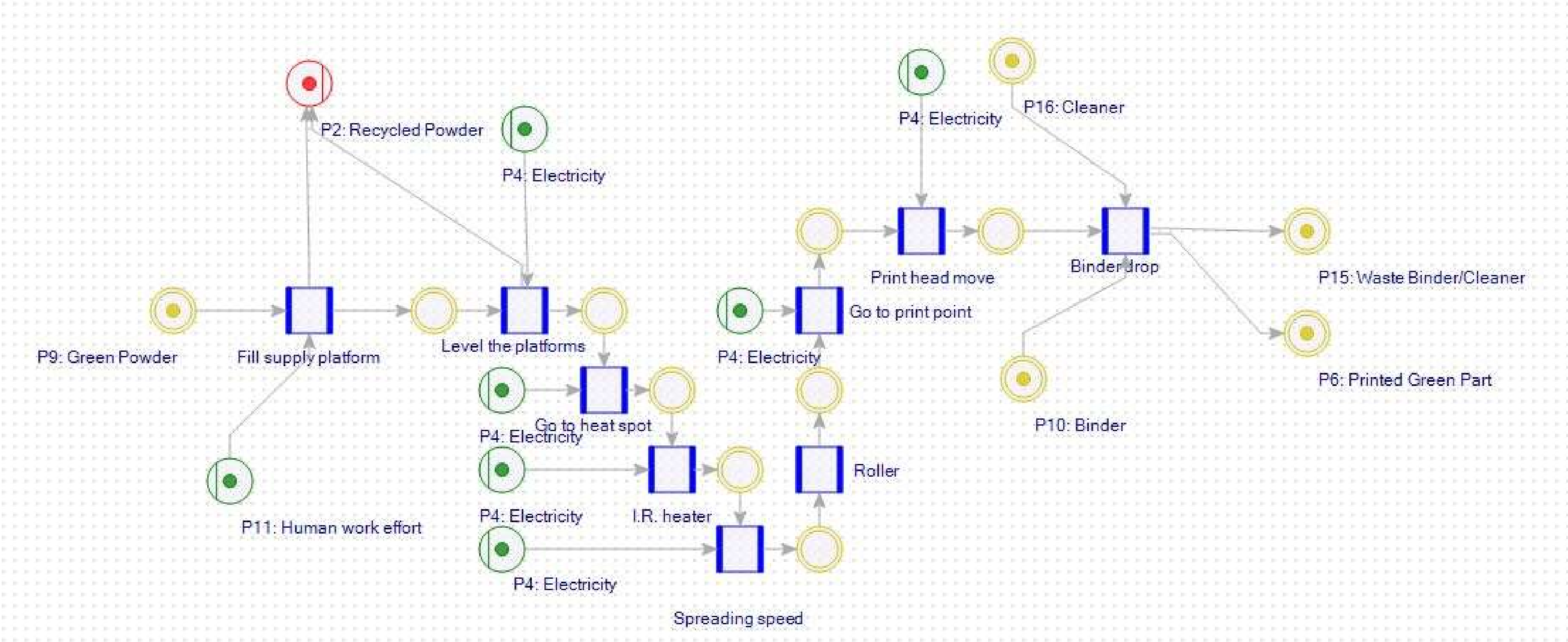

Sintering Subnet

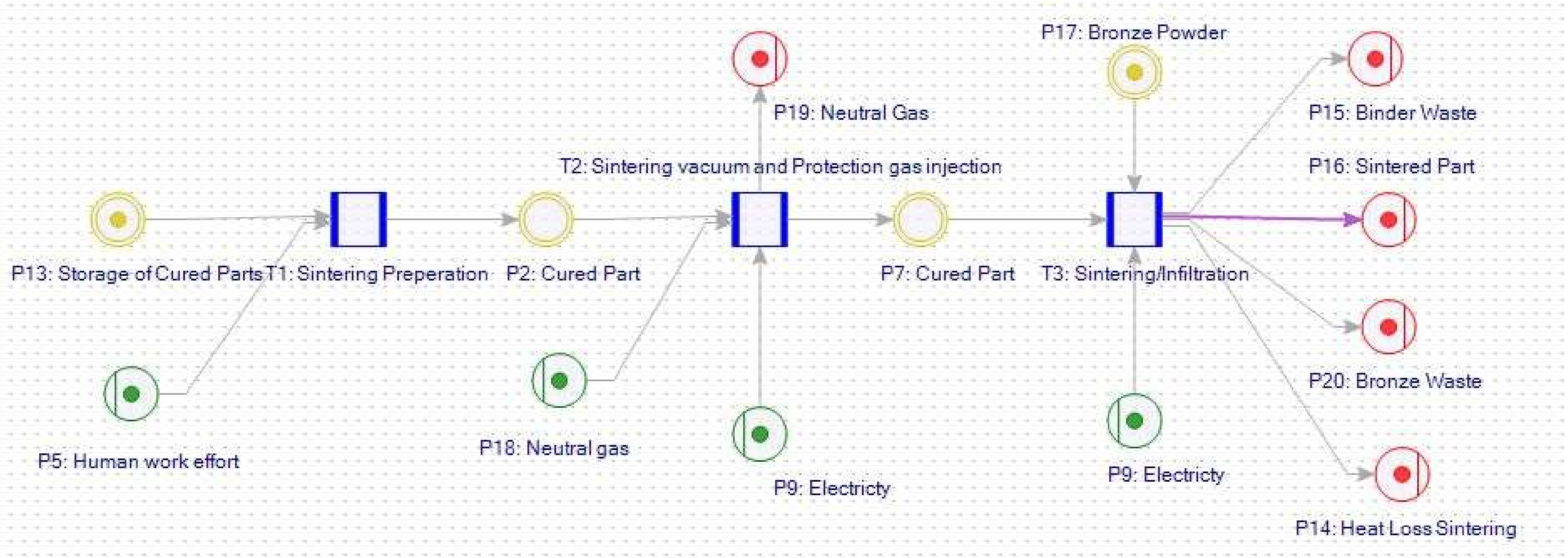

Reference

[1] B. Stucker, "Additive manufacturing technologies: technology introduction and business implications," in *Frontiers of Engineering: Reports on Leading-Edge Engineering From the 2011 Symposium, National Academies Press, Washington, DC, Sept*, 2012, pp. 19-21.

[2] V. Petrovic, *Additive layered manufacturing : sectors of industrial application shown through case studies*, 2011.

[3] Z. Yuhaowei, C. Han, T. Yunlong, S. Gopinath, X. Xin, and Y. F. Zhao, "Simulation and optimization framework for additive manufacturing processes," in *Innovative Design and Manufacturing (ICIDM), Proceedings of the 2014 International Conference on*, 2014, pp. 34-40.

[4] D. L. Bourell, M. C. Leu, and D. W. Rosen, *Roadmap for Additive Manufacturing-Identifying the Future of Freeform Processing* The University of Texas at Austin Laboratory for Freeform Fabrication Advanced Manufacturing Center, 2009.

[5] M. Schipper, "Energy-Related Carbon Dioxide Emissions in U.S. Manufacturing," DOE/EIA-0573(2005), 2006.

[6] W. R. Morrow, H. Qi, I. Kim, J. Mazumder, and S. J. Skerlos, "Environmental aspects of laser-based and conventional tool and die manufacturing," *Journal of Cleaner Production,* vol. 15, pp. 932-943, // 2007.

[7] R. Sreenivasan, A. Goel, and D. L. Bourell, "Sustainability issues in laser-based additive manufacturing," *Physics Procedia,* vol. 5, Part A, pp. 81-90, // 2010.

[8] C. Achillas, D. Aidonis, E. Iakovou, M. Thymianidis, and D. Tzetzis, "A methodological framework for the inclusion of modern additive manufacturing into the production portfolio of a focused factory," *Journal of Manufacturing Systems,* 2014.

[9] S. Cao, Y. Qiu, X. F. Wei, and H. H. Zhang, "Experimental and theoretical investigation on ultra-thin powder layering in three dimensional printing (3DP) by a novel double-smoothing mechanism," *Journal of Materials Processing Technology,* vol. 220, pp. 231-242, 2015.

[10] NIST, "Measurement Science Roadmap for Metal-based Additive Manufacturing," US Department of Commerce, National Institute of Standards and Technology2013.

[11] J. R. Duflou, J. W. Sutherland, D. Dornfeld, C. Herrmann, J. Jeswiet, S. Kara*, et al.*, "Towards energy and resource efficient manufacturing: A processes and systems approach," *CIRP Annals - Manufacturing Technology,* vol. 61, pp. 587-609, // 2012.

[12] Y. Tang, J.-Y. Hascoet, and Y. F. Zhao, "Integration of Topological and Functional Optimization in Design for Additive Manufacturing," in *ASME 2014 12th Biennial Conference on Engineering Systems Design and Analysis*, 2014, pp. V001T06A006-V001T06A006.

[13] Y. Zhou, H. Chen, Y. Tang, S. Gopinath, X. Xu, and Y. F. Zhao, "Simulation and optimization framework for additive manufacturing processes," in *Innovative Design and Manufacturing (ICIDM), Proceedings of the 2014 International Conference on*, 2014, pp. 34-40.

[14] P. Kulkarni, A. Marsan, and D. Dutta, "A review of process planning techniques in layered manufacturing," *Rapid Prototyping Journal,* vol. 6, pp. 18-35, 2000.

[15] S. Meteyer, X. Xu, N. Perry, and Y. F. Zhao, "Energy and Material Flow Analysis of Binder-jetting Additive Manufacturing Processes," *Procedia CIRP,* vol. 15, pp. 19-25, 2014.

[16] S. Haykin, *Neural Networks: A Comprehensive Foundation*: Prentice Hall PTR, 1998.

[17] Y. Ning, J. Fuh, Y. Wong, and H. Loh, "An intelligent parameter selection system for the direct metal laser sintering process," *International journal of production research,* vol. 42, pp. 183-199, 2004.

[18] A. Garg, K. Tai, and M. Savalani, "State-of-the-art in empirical modelling of rapid prototyping processes," *Rapid Prototyping Journal,* vol. 20, pp. 164-178, 2014.

[19] A. Equbal, A. K. Sood, and S. Mahapatra, "Prediction of dimensional accuracy in fused deposition modelling: a fuzzy logic approach," *International Journal of Productivity and Quality Management,* vol. 7, pp. 22-43, 2011.

[20] L. Xiao-fei, D. Jun-hui, and Z. Yong-zhi, "Modeling and Applying of RBF Neural Network Based on Fuzzy Clustering and Pseudo-Inverse Method," in *Information Engineering and Computer Science, 2009. ICIECS 2009. International Conference on*, 2009, pp. 1-4.

[21] S. Lee, W. Park, H. Cho, W. Zhang, and M.-C. Leu, "A neural network approach to the modelling and analysis of stereolithography processes," *Proceedings of the Institution of Mechanical Engineers, Part B: Journal of Engineering Manufacture,* vol. 215, pp. 1719-1733, 2001.

[22] "ISO 14040 Environmental managementd Life cycle assessmentd Principles and framework: International Organisation for Standardisation," ed. Geneva,Switzerland, 1998.

[23] X. Xu, "Energy consumption model of Binder-Jetting Additive Manufacturing Processes," Master of Engineering, Mechanical Engineering Department, McGill University, 2014.

[24] K. H. Lee and H. Woo, "Direct integration of reverse engineering and rapid prototyping," *Computers & Industrial Engineering,* vol. 38, pp. 21-38, 1/1/ 2000.

[25] Y. S. A. Inc. (2009, Instruction Manual for Gravity Convection Ovens.

[26] E. Inc., "R1 Furnace Profile," ed, 2013.

[27] European_Commission and Joint_Research_Centre, *International Reference Life Cycle Data System (ILCD) Handbook - General guide for Life Cycle Assessment - Detailed guidance*, 2010.

[28] M. F. Ashby, *Materials and the Environment, 2nd Edition*: Butterworth Heinemann, 2012.

[29] R. Steiner and R. Frischknecht, "Metals processing and compressed air supply," *Ecoinvent report,* 2007.

[30] M. Finkbeiner, A. Inaba, R. Tan, K. Christiansen, and H.-J. Klüppel, "The new international standards for life cycle assessment: ISO 14040 and ISO 14044," *The international journal of life cycle assessment,* vol. 11, pp. 80-85, 2006.

[31] B. Vigon, D. Tolle, B. Cornaby, H. Latham, C. Harrison, T. Boguski*, et al.*, "Life Cycle Assessment: Inventory Guidelines and Principles," U. E. P. A. (EPA), Ed., ed, 1993 EPA/600/R-92/245.

[32] J. Fava, R. Denison, B. Jones, M. Curran, B. Vigon, S. Selke*, et al.*, "A Technical Framework for Life-Cycle Assessment," U. SETAC, Ed., ed. Washington, 1991.

[33] F. Consoli, D. Allen, I. Boustead, J. Fava, W. Franklin, A. Jensen*, et al.*, "Guidelines for Life-Cycle Assessment: A 'Code of Practice'," SETAC, Ed., ed, 1993.

[34] S. Suh and G. Huppes, "Methods for Life Cycle Inventory of a product," *Journal of Cleaner Production,* vol. 13, pp. 687-697, 6// 2005.

[35] *Material Safety Data Sheet ProMetal R-1 Binder*, 2014.